



## ESTIMATION OF BOD IN ACTIVATED SLUDGE

MARCUS HEDEGÄRD

*Department of Signals and Systems*  
*Division of Automatic Control*  
CHALMERS UNIVERSITY OF TECHNOLOGY  
Göteborg, Sweden 2010  
*Master's Thesis EX051/2010*



# Abstract

The activated sludge process for degradation of organic matter is one of the main processes commonly used in biological wastewater treatment, and aeration in that process stands for a large part of the energy consumed in a plant. Hence, there has been many attempts to optimize the operation of the activated sludge process, which requires a model of the process. The advanced models used has in general their origin in IWA (former IAWQ) activated sludge model no 1 (ASM1). Unfortunately, feasible optimization is limited because several of the most important variables, for example bacterial biomass ( $X_{BH}$ ), readily biodegradable soluble substrate ( $S_S$ ) and slowly biodegradable particulate substrate ( $X_S$ ), cannot be reliably measured online because of their complexity hiding behind their notation. One way to resolve this problem is to estimate these concentrations using an observer and other online measurements at hand. Here we have developed an Extended Kalman Filter (EKF) that estimates the relevant concentrations in the ASM1 based on oxygen measurements and supplied air. For faster convergence, measurements of totally suspended solids in the influent flows are included in the algorithm. It is concluded that estimation does not work for one stirred tank alone, but when the activated sludge process is described by several tanks in series with oxygen measurements in each of them, the estimates converge. The filter has interesting convergence properties, and to explain these observability properties are investigated. For an implementation of the observer, it is necessary to estimate the oxygen mass transfer function and methods for this are evaluated and further developed. One of these and the EKF were evaluated for the wastewater treatment plant Ryaverket in Göteborg. The EKF is found to be divergent for this plant, which can be explained by the many uncertainties regarding the model. A more simple observer for estimation of the important measure oxygen uptake rate ( $OUR$ ) was evaluated, and this was found to be convergent for plant data. Optimization of the aeration is considered briefly and is solved for one control variable. Results based on real data are presented.

KEYWORDS: observer, extended Kalman filter, ASM1, activated sludge.

# Sammanfattning

Aktivslamprocessen för nedbrytning av organiskt material är en av de vanligaste processerna för biologisk avloppsvattenbehandling och luftningen av de aeroba zonerna i processen står för en stor del av den förbrukade energin på ett verk. Det har därför gjorts flertalet försök att optimera processen vilket kräver en modell av den. De avancerade använda modellerna har i regel sitt ursprung i IWA (tidigare IWAQ) activated sludge model no 1 (ASM1). Tyvärr, är optimering av processen begränsad eftersom flera av de mest viktiga variablerna i ASM1, tex bakteriekoncentration  $X_{BH}$ , lättillgängligt substrat  $S_S$  och partikulärt svärnedbrytbart partikulat substrat  $X_S$ , ej kan mätas förtroligt i realtid. En möjlig lösning är att använda en observatör och mätningar av andra tillgängliga processvariabler. I detta arbetet har en observatör - Extended Kalman Filter(EKF) utvecklats som estimerar de relevanta koncentrationerna i ASM1 modellen baserat på syremätningar och tillförd luft. Det visar sig att estimeringen inte fungerar för endast en tank, men om processen beskrivs av flera efterliggande tankar med syremätningar i var och en konvergerar estimaten. För en implementering av observatören är det nödvändigt att estimerar en funktion,  $K_L a$ -funktionen, vilken beskriver syreöverföringen från diffusorerna till vattnet i de aeroba zonerna. Metoder för att göra detta evalueras och vidareutvecklas. En av dessa och EKF:en har testats på data från reningsverket Ryaverket. Tyvärr, konvergerade inte filtret i detta fall vilket kan förklaras av de många osäkerheter som finns i modellen. En mer simpel observatör för den viktiga indikatorn *oxygen uptake rate (OUR)* utvärdares också, och var konvergent för datan från Ryaverket. Optimering av processen undersöks övergripande och mer ingående för en styrvariabel, och resultat baserat på riktig data presenteras.

NYCKELORD: observatör, extended Kalman filter, ASM1, aktiv slam.

# Preface

This 60 credits Master Thesis is a part of the examination of a Master's degree in Control engineering at the department of Signals and Systems Chalmers - division of. The work has been carried out in cooperation with the waste water treatment plant Ryaverket in Gothenburg, where also real experiments has been carried out. I would like to thank the following persons in my work:

- My supervisor Torsten Wik for his encouragement and help, and for interesting discussions regarding the subject.
- The personal at the plant Glen, Maria and Åsa for letting me do the work, and for a great cooperation.
- The authours of the great books I have studied during the work. I had little previous experience of biological systems and would especially like to thank the authours of books specialized in control of waste water plants.

# CONTENTS

<b>1</b>	<b>INTRODUCTION</b>	<b>1</b>
<b>2</b>	<b>NOTATION</b>	<b>4</b>
<b>3</b>	<b>THE PLANT AND MODELING</b>	<b>6</b>
3.1	Tanks	9
3.2	BOD and COD	10
3.3	The influents and the effluent	10
3.4	Measurements and data storage	10
3.5	Mathematical modeling	11
3.5.1	The activated sludge model NO.1	11
3.5.2	Parameters in the ASM1	14
3.5.3	Mass transfer of oxygen	16
3.6	Simulation platform	16
3.7	Case study	16
<b>4</b>	<b>ESTIMATION - THEORY AND SIMULATION</b>	<b>20</b>
4.1	Observers and observability conditions	20
4.1.1	Observability conditions	21
4.1.2	Observer designs	25
4.1.3	The Extended Kalman filter	26
4.1.4	Implementation of EKF:s	27
4.1.5	Random walk models	28
4.2	Estimation of sludge concentrations	28
4.3	Estimation of rate expressions, $X_{BH}$ and $S_S$	29
4.3.1	An observer model for rate expressions	30

---

4.3.2	Estimation of $NUR$ based on one reactor	32
4.3.3	Estimation of $NUR$ based on several reactors	33
4.3.4	Estimation of $OUR$ and $S_S$	34
4.4	An EKF for the aerobic compartments	36
4.4.1	Observer model	36
4.4.2	Sensitivity analysis	39
4.4.3	Simulation with one and two tanks	39
4.4.4	Simulation results for the observer based on three tanks	47
4.4.5	Additional results	51
4.5	Estimation of the $K_La$ function	51
4.5.1	DO observer	52
4.5.2	Estimation with ON/OFF control	55
4.5.3	A Kalman filter approach	58
<b>5</b>	<b>APPLIED ESTIMATION</b>	<b>65</b>
5.1	Conventions	65
5.2	Tank approximation	65
5.3	An applied model of the $K_La$ function	68
5.4	Data treatment	69
5.5	Estimation of the $K_La$ function	70
5.5.1	Experiments in Tank 7	71
5.5.2	Results from experiments in Tank 8	72
5.5.3	A new experiment	73
5.6	The aerobic EKF	73
5.7	Estimation of $OUR$	75
<b>6</b>	<b>PROCESS OPTIMIZATION</b>	<b>77</b>
6.1	Optimization based on real data	79

---

<b>7</b>	<b>REVIEW OF RESULTS ANDDISCUSSION</b>	<b>82</b>
7.1	Estimation via rate expressions . . . . .	82
7.2	An EKF for the aerobic compartments . . . . .	83
7.3	Estimation of the $K_La$ function . . . . .	85
7.4	Evaluation of the EKF based on real data . . . . .	86
7.5	Optimization of the aerobic process . . . . .	86
7.6	Possibilities for Ryaverket . . . . .	87
<b>8</b>	<b>CONCLUSIONS</b>	<b>88</b>

# 1 INTRODUCTION

The activated sludge process (ASP) is one of main processes commonly used in biological wastewater treatment. In this process, bacterial biomass grows as ammonium, phosphor and organic substances are degraded. ASP:s are costly to operate and their largest cost is for the energy required for aeration of the aerobic compartments.

To optimize the process modeling is needed. The most widely used model for modeling of the reactions in ASP:s is the Activated Sludge Model NO.1 (ASM1) (Henze *et al.* 2000), and its successors ASM2 and ASM3 (Henze *et al.* 2000). ASM1 models removal of degradable organic matter and nitrogen compounds. ASM2 includes modeling of biological phosphorus removal. ASM3 is a more comprehensive and extended version of the ASM1. Unfortunately, these models contain several concentrations that cannot reliably be measured online. This is in particular true for some of the main variables, such as dissolved and particulate organic substrate, and biomass concentration. Substrate analyzers have been available for several years but these have historically been considered unreliable (Olsson and Newell 1999), and do not differentiate between particulate and dissolved substances as in the ASM1. Totally Suspended Solids (TSS) measurements though give an indication of biomass concentration though.

A general remedy for absence of online measurements is to find an observer to estimate unmeasured variables based on a dynamic model and online measurements of other variables. In the literature, there are few examples of observers based on the ASM1 or its successors implemented at a real plant, but at the Ejby Mølle WWTP in Odense Denmark, an observer based on these models predicts the ammonium and nitrite plus nitrate concentration in real-time, based on ammonium and redox potential measurements (Cecil and Kozłowska 2009). Other implemented observers for ASP:s described in the literature are for estimation of reaction rates (Lindberg 1997). Observers to estimate biodegradable substrate based on the ASM1 have been formulated by Benazzi *et al.* (2007) and Boulkroune *et al.* (2009). Both of these are for one aerobic reactor in the COST benchmark model (Copp 2001, Alex *et al.* 1999), assuming constant and known bacterial concentration. In practice this is a highly restrictive assumption since proper measurement of the bacterial concentration is hardly feasible. Benazzi *et al.* (2007) used an extended Kalman filter but found that for the estimates to converge it was necessary that at least the influent of soluble substrate was also measured. Boulkroune *et al.* (2009) used another LMI based nonlinear observer also based on a simplified version of the ASM1. They lumped soluble and particulate degradable substrate into one variable  $X_{DCO}$ , since the presumed measurement did not make it possible to distinguish them. Further, they concluded that the system becomes unobservable if the influent concentration in  $X_{DCO}$  is unknown. This is solved by feeding the observer with the daily mean substrate level based on a presumed lab analysis. The drawbacks of these methods are that they rely on data for bacterial concentration and influent concentrations of

biodegradable substrates. Further, the latter method does not distinguish between soluble and particulate substrate, although this is very important since the effects and kinetics for the two are very different. Neither is the robustness to model errors evaluated.

As a basis for the simulation model, and to evaluate designs on, the WWTP Ryaverket in Gothenburg in Sweden is considered. The work has resulted in an EKF that estimates all relevant concentrations in the ASM1, including unknown inputs of substrate and biomass based on measurements in two or more aerobic tanks, and TSS measurements in the influents. The filter has been evaluated in simulation with good results, and it is also shown that the Runge Kutta 4 method can be used for an implementation of it. For the case with two tanks there are however restrictions on certain variations in the concentrations, and this property is analyzed based on observability conditions. The success of this filter compared to the filters by Benazzi *et al.* (2007) and Boulkroune *et al.* (2009) relies on the following features:

- Contrary to the work mentioned above, the process considered here is *predenitrifying with post nitrification*. This means that nitrification stands for a very small portion of the aerobic reactions in the ASP, which in turn leads to that fewer concentrations in the ASM1 need to be included in the observer. These are  $S_O$  (oxygen),  $S_S$  (readily biodegradable substrate),  $X_S$  (slowly biodegradable substrate) and  $X_{BH}$  (heterotrophic biomass). Among these, only oxygen is measured.
- Instead of assuming the influent concentrations known, they are considered as stochastic processes and are estimated by the observer.
- By including more than one tank additional measurements of oxygen are available and a better coupling between the states is achieved.
- The biomass concentration is modeled as a product of the sludge concentration and a variable (parameter)  $\gamma_{X_{BH}}$ , which denoted the fraction of the sludge being heterotrophic bacteria. The sludge concentration can vary fast when the operators change the flows but it can then be estimated from measured TSS in the recycled sludge flow and measured water flows. The estimated sludge concentration is thus fed to the observer and the slowly varying  $\gamma_{X_{BH}}$  is estimated.
- By describing a correlation between measured TSS in the influent to the ASP and  $X_S$  in the observer model, the convergence of the filter can be made faster.

The extension of the method to a mixed aerobic process should be straightforward. Another method for estimation of the parameter  $\gamma_{X_{BH}}$ , based on estimation of reaction rate expressions with a linear Kalman filter for the anoxic tanks has also been developed. In the anoxic compartments, rate expressions are often saturated in the soluble substrate  $S_S$ . With this knowledge, and estimated sludge concentrations,  $\gamma_{X_{BH}}$  is estimated. This can be further used for estimation of substrate in the aerobic tanks, which is evaluated for  $S_S$ , again based on estimated rate expressions.

---

The method is useful but shows to be quite sensitive to errors in the estimated parameter.

For implementation of the developed estimators, it is necessary to have an estimate of the oxygen mass transfer function, i.e. the  $K_La$  function. It describes the transfer of oxygen from diffused air to the water, and is not known for Ryaverket. There are methods to estimate it, and two of these are evaluated and further developed to be suitable for the considered plant. These includes excitation of the air flow, which is costly, which implies that although the function is known to be timevarying in a non modeled way it is not possible to estimate it on a continuous basis. On three occasions, experiments to estimate the function were performed at the plant.

Due to properties of the considered plant, only the EKF approach with measurements in two tanks for estimation of the ASM1 variables could be evaluated for real data. Unfortunately, the estimates are found to diverge. One possible reason is that concentrations vary too little in reality, and another possible reason are deviations between the real process and the internal model of it in the observer. One source of errors is the parameters in the ASM1. Another is the model of the activated sludge basin as a series of tanks, and this model is further analyzed. This also leads to errors in the estimation of the  $K_La$  function, and it is known from sensitivity analysis by simulation that the EKF is especially sensitive to such errors. The unmodeled time variation of the  $K_La$  function is another source of errors.

There are many possible control variables to optimize in an ASP, such as the air flows in the aerobic compartments, the oxygen set point, the influent flows, TSS in the return sludge flow, and the volume used for anoxic processes versus aerobic processes. In Lindberg (1997), Samuelsson *et al.* (2007) and Chachuata *et al.* (2005) these kind of problems were considered without taking substrate and biomass measurements/estimates into account. Dynamical optimization of the process is a comprehensive problem since many of the control variables need to be optimized using a model involving at least parts of the AS basin. This goes for the influent flows, TSS in the return sludge flow, and the aerobic volume. The problem of optimizing these for the aerobic compartments under the assumption that this can be done without taking into account upstream processes is considered briefly. The oxygen set point can, according to the mathematical model, be optimized independently for the aerobic compartment. The model also says that it is reasonable that a constant oxygen setpoint can be used that is identically lower than that used today, but the current value is based on properties not included in the ASM1. It is therefore concluded that it should not be varied continuously based on this model. Optimization of the individual air flows was solved and results based on real data for half a year is presented. 5 % of the total aeration cost could be saved with the developed method. The validity of the result is, however, dependent on that the tank model is valid and on the shape of the real  $K_La$  function.

## 2 NOTATION

### *Abbreviations*

AS	activated sludge
ASP	activated sludge process
BOD	biochemical oxygen demand
COD	chemical oxygen demand
CSTR	continuously stirred tank reactor
DO	dissolved oxygen
EKF	extended kalman filter
NUR	nitrate (and nitrite) uptake rate ( $mgNO_3^{-1}l^{-1}d^{-1}$ )
OUR	oxygen uptake rate ( $mgO_2l^{-1}d^{-1}$ )
S-function	state space function in Simulink
TSS	totally suspended solids
WWTP	wastewater treatment plant

### *Capital Letters*

$D$	dillution rate - $\frac{Q}{V}$ ( $d^{-1}$ )
$I$	tank index set $I = \{d1, d2, t, 1, \dots, 8\}$
$K_z$	half saturation coeffiecent in Monod expressions for the concentration $z$
$M_z$	Monod expression in the concentration $z$
$Q$	volumetric water flow rate ( $m^3d^{-1}$ )
$Q_{rec}$	water flow from the trickling filters
$Q_{in}$	influent flow to the plant ( $m^3d^{-1}$ )
$Q_X$	sludge recycle flow
$R_1$	process noise covariance matrix
$R_2$	measurment noise covariance matrix
$S$	dissolved matter
$S_S$	readily biodegradable substrate ( $mg(COD)l^{-1}$ )
$S_{NH}$	$NH_4^+ + NH_3$ nitrogen (Ammonium)
$S_{NO}$	nitrate and (nitrite) nitrogen $mgNO_3^{-1}l^{-1}$
$S_O$	dissolved oxygen concentration ( $mgO_2l^{-1}$ )
$T$	temperature ( $^{\circ}C$ ) or transformation matrix
$V$	tank volume ( $m^3$ )
$X$	particulate matter
$X_{BH}$	hetertrophic baceterial biomass $mg(COD)l^{-1}$
$X_{in}$	sludge concentration originating from $Q_{in}$ ( $mgTSSl^{-1}$ )
$X_X$	sludge concentration originating from $Q_X$ ( $mgTSSl^{-1}$ )
$X_S$	slowly (particulate) biodegradable substrate ( $mg(COD)l^{-1}$ )

*Small Letters*

$d$	day
$g$	impulse response
$h$	sampling time, or hour
$k_1$	$K_{La}$ function parameter ( $d^{-1}$ )
$k_2$	$K_{La}$ function parameter ( $m^{-3}h$ )
$q$	volumetric air flow rate ( $m^3(air)h^{-1}$ )
$t$	time
$u$	input vector in observer models
$v$	measurement noise
$x$	state vector in observer models
$y$	measurement vector in observer models

*Greek Letters*

$\gamma_{XBH}$	fraction of $X_X$ being heterotrophic biomass ( $gCOD/gTSS$ )
$\hat{\mu}_H$	maximum specific growth rate for heterotrophic biomass ( $d^{-1}$ )

*Subscripts*

$d_1, d_2$	indexes for the deox tanks
$m$	measurement of
$t$	index for the transport volume (tank)
$in$	input to an arbitrary tank, but is also used for the influent flow $Q_{in}$

*Diacritical marks*

$\sim$	sample mean
$\hat{\phantom{x}}$	approximation or estimate
$\bar{\phantom{x}}$	scaled

# 3 THE PLANT AND MODELING

Ryaverket is owned by GRYAAB who treats wastewater from its joint owners, the municipalities of Ale, Göteborg, Härryda, Kungälv, Mölndal and Partille. GRYAAB also operates a 120 km long tunnel system, which transports wastewater from within the region to the plant. There are mainly three kinds of waste that is removed in the process:

- Particles, such as sand, coffee grounds, potato peel and toilet paper.
- Organic degradable substances. When they enter natural waters, such as lakes or seas they are naturally degraded. However, the oxygen needed for the degradation is taken from the water and the result are lowered oxygen concentrations and increased bacterial biomass.
- The nutrients phosphor and ammonium. They can cause increased growth of algiers, reed and other plants in watercourses. When the algiers die, they are degraded and oxygen is consumed. This can lead to oxygen depletion resulting in dead bottoms.

The treatment process is illustrated in Figure 3.1. The water reaches the plant from a tunnel system. Before it enters the primary sedimentation step it has gone through several steps of mechanical cleaning. Different gratings are used to remove sands, gravels and other larger particles. In the primary sedimentation step the water flows through large tanks, commonly called *primary clarifiers*. The flow is low enough, to allow particles that are heavier than water to sink to the bottom and subsequently collected and pumped to further sludge treatment stages where energy is extracted from it. The water also contains grease and oils that are lighter than water and form a layer on the surface that is skimmed off. At Ryaverket, phosphor removal is not a biological- but a chemical process. Iron sulphate is added to the water, which is positively charged, while phosphor is negatively charged. The chemical reaction is that the nutrients and chemicals attract each other. In this way flocks are formed in the water that grow in size. These are bounded to the sludge in the Activated sludge process (ASP).

The ASP is centered about the activated sludge basins which contains both anoxic- (oxygen free environment) and aerobic (environment containing oxygen) processes. In this biomass grows with degradation of ammonium and mainly soluble degradable organic substances. The process at Ryaverket is *predenitrifying with post nitrification*, which means that degradation of nitrate (denitrification in the anoxic compartments) comes before the aerobic processes, and that nitrification (degradation of ammonium in trickling filters) comes after the AS basins. To make this possible, the effluent of the basins is recirculated via the trickling filters back to the influent. To sustain a high enough bacterial biomass population in the basins, there is also a

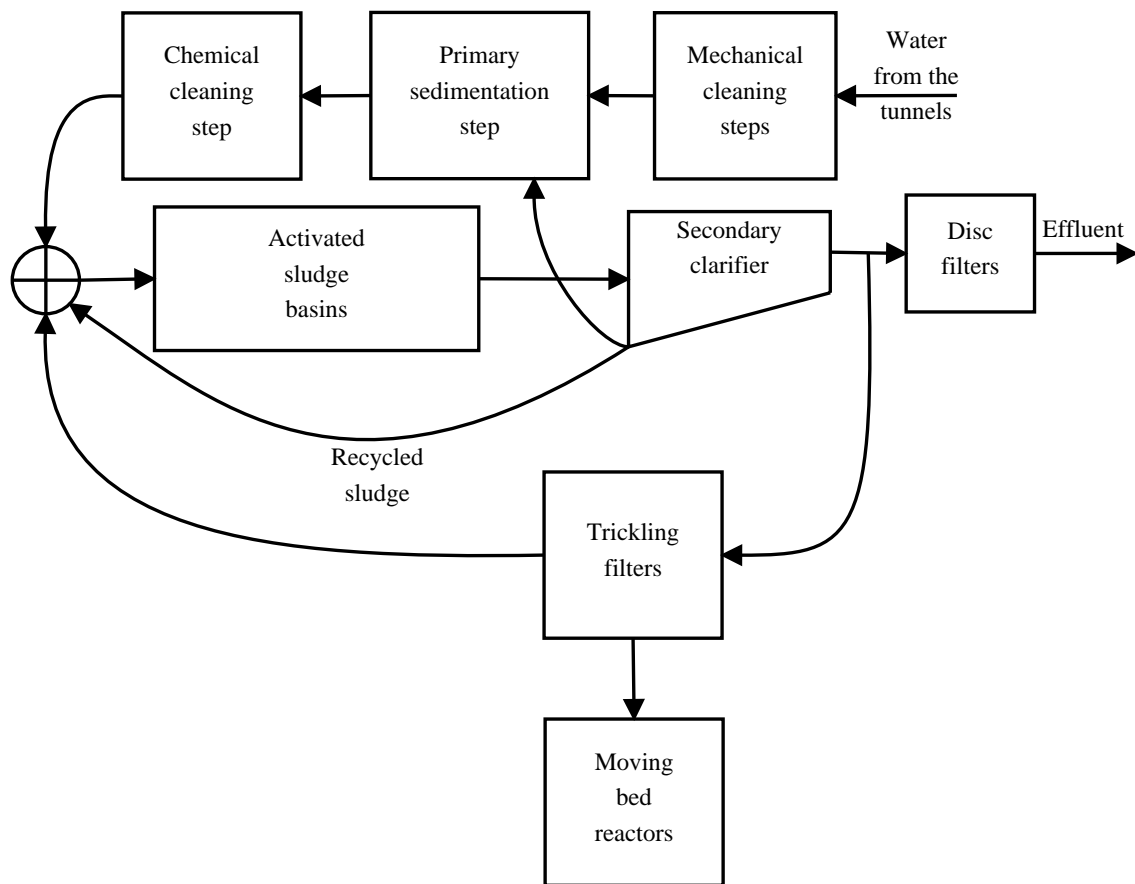


Figure 3.1. The treatment process at Ryaverket.

recirculation of the sludge containing the bacterias. Approximately half of the effluent is recirculated. There are two kinds of bacterias in the process. Heterotrophs are responsible for the main reactions in the AS basin. For growth, these need soluble carbon and a nutrient. In the anoxic compartments the nutrient is nitrate, and the rest product is nitrogen gas. In the aerobic compartments the nutrient is oxygen, and the rest product is carbon dioxide. Oxygen is here added to the water through diffusors at the bottom. Because this is costly, it is desired to degrade as much as possible of the soluble organic compounds by denitrification, since nitrate is a nutrient source formed in the process that also must be degraded. The nitrate that cannot be degraded in the basins is treated in moving bed reactors (MBR), which is a separate denitrification process in which an external carbon source is added to the water, which is also costly. Nevertheless this is necessary when the concentration of the natural carbon source in the influent to the ASP is not high enough.

The trickling filters is an aerobic process in which the second kind of bacterial biomass (autotrophs) grows with the degradation of ammonium and oxygen into nitrate. The reason why nitrification is separated from the rest of the ASP at Ryaverket is because high water flow and that heterotrophs grow much faster than autotrophs. The heterotrophs will therefore outcompete the autotrophs and, hence limit the potential nitrification in the ASP. Still, there are some nitrification in the

aerobic parts of the AS basins have been observed.

The purpose of the secondary clarifier is to allow the biological flocs and particulate compounds in the water to settle and produce sewage water containing low levels of nutrients and organic matter. A large part of the superfluous sludge is pumped back to the primary sedimentation step and treated further. To be able to handle stricter effluent standards disc filters has newly been installed. The purpose of these is to further remove particulate compounds.

Figure 3.2 gives a more detailed picture of the ASP. The focus of this work is within the dashed line, and it defines what is included in the simulation model. The water

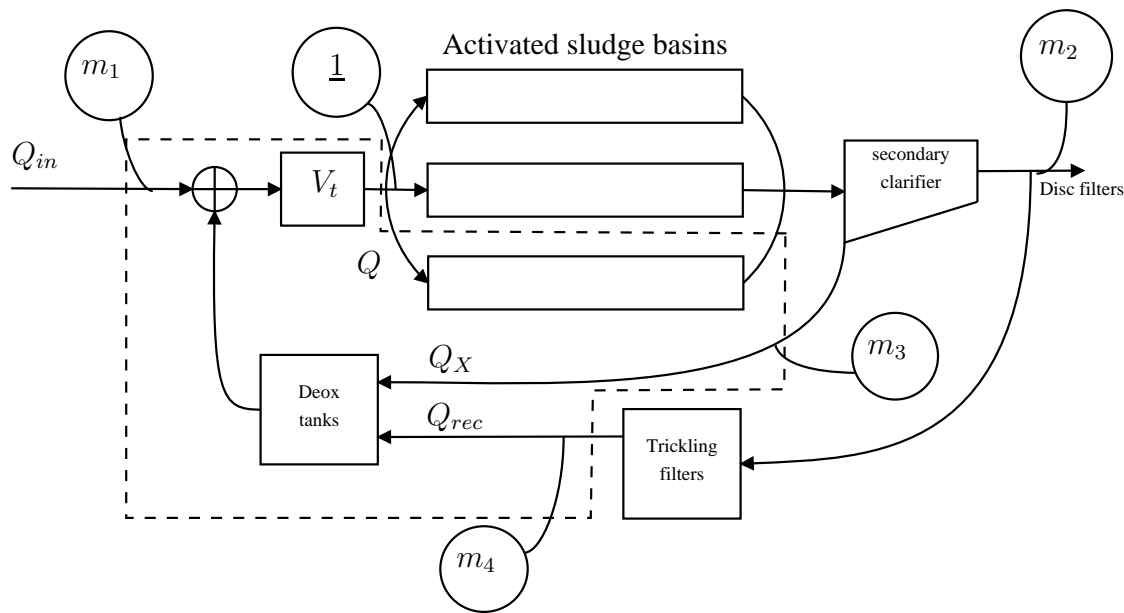


Figure 3.2. Model of the activated sludge process at Ryaverket.

from the trickling filters is saturated in oxygen, and the purpose of the deox tanks is to lower the oxygen level in the water to close to zero before it enters the anoxic compartments of the basins. In reality there are two deox tanks, recycled sludge flows and trickling filters. In simulation, the two flows  $Q_X$  and  $Q_{rec}$  are divided over two equal deox tanks.  $V_t$  is a transport volume which is non negligible. The points  $m_1$  to  $m_4$  are measurement points. The flows  $Q_{in}$  (influent wastewater),  $Q_X$  (recycled sludge flow),  $Q_{rec}$  (water from the trickling filters) are all measured. These are mixed and divided over three AS basins, or lines, that are equal and therefore only one line is included in the simulation model. The flow through one line is symbolized with  $Q$ . The AS basin is illustrated in Figure 3.3. As indicated in the upper part of the figure, the process have nine zones, where the two first ones (40 % of the process) are always anoxic, and at least the last 4 zones (also 40 % of the process) are always aerated. In the middle there are three zones, comprising 20 % of the process that can be either anoxic and mixed, or aerated. The normal case is that 40% of the basin is aerated. The dissolved oxygen (DO) concentration in the aerobic compartments is feedback controlled to  $2\text{mg l}^{-1}$  every second month and  $4\text{mg l}^{-1}$  every other. The

diffusers in the aerobic compartments are illustrated with the dashed line at the bottom of the basin. The diffusers are in reality a long chain of pipes and the total air flow through these can be controlled and measured individually per zone. The oxygen- ( $S_O$ ) and nitrate ( $S_{NO}$ ) sensors are also illustrated in the upper part of Figure 3.3. Regarding the nitrate sensors, the given positions are where there are contacts to plug in a sensor and there are not always two sensors plugged in.

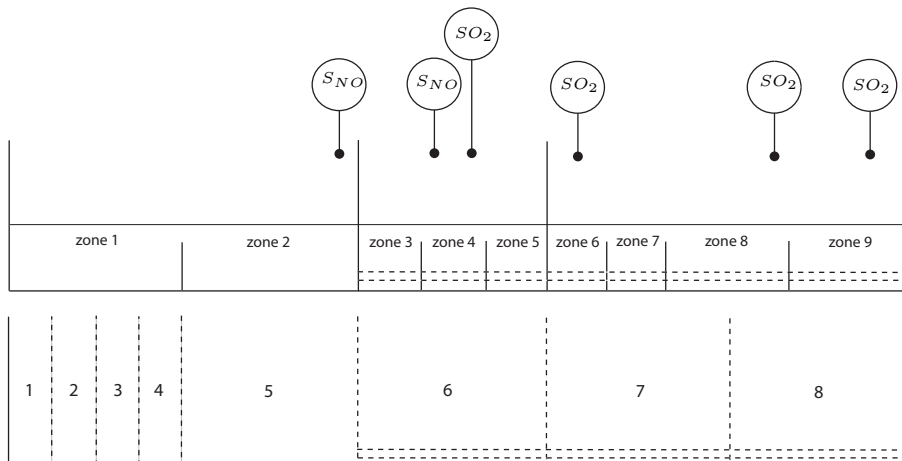


Figure 3.3. Division of the basin into zones and tanks.

## 3.1 Tanks

Lithium tracer tests carried out on the sludge basin indicated that it could be approximated by 8 ideally stirred tanks. This is illustrated in the lower part of Figure 3.3. The division into tanks is treated further in Chapter 5.2. In simulation, also the deox tanks and the transport volume  $V_t$  are assumed to be described by ideally stirred tanks. The volumes of the tanks are given in Table 3.1. Parameters, concentrations, variables, and functions are indexed based on which tank they belong to. The index set is  $I = \{d1, d2, t, 1, \dots, 8\}$ , where  $t$ ,  $d1$  and  $d2$  represents the transport volume and the deox tanks. The concentration of nitrate in the first tank in the AS basin is for example  $S_{NO:1}$ . When discussing an arbitrary tank, no index is given, and the influent concentration is indexed with  $in$ . For the simulation model, it is assumed that the air flows are controlled and measured per tank, and the same goes for nitrate and oxygen.

Table 3.1. Volumes of the bioreactors ( $m^3$ ).

$V_d$	$V_t$	$V_1 - V_4$	$V_5 - V_8$
3960	1700	11930/12	3310

## 3.2 BOD and COD

Describing the organic content of waste water is not trivial, since we are not dealing with one certain substance. One usually measures it as *chemical oxygen demand (COD)* or *biochemical oxygen demand (BOD)*. *COD* expresses how much oxygen that is needed to chemically oxidize all organic substances. Chemical degradation of a substance means degradation by burning it. *BOD* expresses how much oxygen that is needed to biologically degrade all biodegradable organic substances in a compound biologically. In laboratory, *BOD* in a water sample can be analyzed by measuring the amount oxygen that the sample consumes in a specified time period. There are different *BOD* measurements depending on the time of analysis. The two most common are the *BOD*<sub>5</sub>(5-day BOD), and the one used in Sweden *BOD*<sub>7</sub>(7-day BOD).

## 3.3 The influents and the effluent

In the cleaning steps preceding the ASP, as much as possible of the particulate compounds in the water are removed. All can, however, not be removed and the flow  $Q_{in}$  contains particulate compounds in the form of heterotrophic biomass, biodegradable organic matter and inert (non biodegradable) organic matter, where the latter ones are dominant. Relevant dissolved compounds in  $Q_{in}$  are ammonium, biodegradable- and inert organic matter. During rainy periods, due to nitrification in the tunnels, the concentration of nitrate in this flow is also significant.  $Q_{rec}$ , the effluent from the trickling filters is very clear and contains little particulate matter. Except for nitrate,  $Q_{rec}$  holds a small concentration of autotrophs, and the water is saturated in oxygen. The particulate concentration in  $Q_X$  is large, and consists in addition to heterotrophs of biodegradable- and inert organic matter. The exact composition of the sludge is not well known, but approximately 70 % are organic compounds. It is also reasonable that this flow holds concentrations of dissolved organic matter but the biodegradable part should be small (because of the high bacterial concentration).

## 3.4 Measurements and data storage

The measurements in the measurement points in Figure 3.2 are listed in Table 3.2. Daily samples of COD are taken in measurement point  $m_1$  ( $Q_{in}$ ) and in the effluent in measurement point  $m_4$ . Totally suspended solids is a measurement of the concentration of particles in the water. Weakly samples from the effluent are also analyzed for BOD. The restriction on the effluent in mean organic content over a year is  $10mg(BOD)l^{-1}$ . If the plant cannot live up to this GRYAAB must pay a penalty fee. For a less noisy signal, the output of the oxygen sensors are means of measurements for the last 60 seconds. In addition to this, the data of all measurements in the central data storage system are means of the signals for the last 30

seconds. According to the plant staff the nitrate sensors may be drifting, i.e. the measurement error may be biased. Water temperature is also measured online.

Table 3.2. Measurements in the measurement points

Measurement	Measurement point in Figure 3.2	$m_1$	$m_2$	$m_3$	$m_4$
Daily measurement of COD		*	*		
Suspended solids		*	*	*	*
Ammonium		*			*
Nitrate				*	

## 3.5 Mathematical modeling

The basic block in the simulation model is the model of one single tank. For a full model, the tank models are linked by massbalances. Below, the model of Tank  $i$  is given.

$$\frac{d}{dt}Z_i = D_i(Q)(Z_{i-1} - Z_i) + \xi(q, Z_i), \quad i \in I \quad (3.1)$$

$Z_i$  is the concentration vector and  $D_i = \frac{Q}{V_i}$  is the dilution rate ( $day^{-1}$ ).  $\xi$  describes the mass transfer of oxygen from the diffusers and the reactions in the tank.  $q_i$  is the air flow of the diffusers in the tank.  $Z_{i-1}$  is the concentrations in the previous upstream tank or in the influents. In the complete model the mixing of the three influent flows in Figure (3.1) is included.

### 3.5.1 The activated sludge model NO.1

To describe the reactions occurring in the tanks, the activated sludge model NO.1 (ASM1) is chosen. It was described by Henze *et al.* (2000). It is physically based and is a good compromise between simplicity and accuracy. The concentrations in the model are listed in Table 3.3. Eight of these describe organic compounds measured in  $mg(COD)l^{-1}$ . This includes readily- (dissolved) and slowly (particulate) biodegradable substrate, inert organic matter, and heterotrophic- and autotrophic biomass. The rest of the variables in the model are nitrogen compounds and Alkalinity. The concentrations denoted by an  $S$  are soluble, and the ones denoted by an  $X$  are particulate. The reactions in the ASM1 are described by process rates and stoichiometry. The stoichiometry describes the quantitative relations between the compounds in the reactions. It describes for example how much oxygen ( $S_O$ ), and readily biodegradable substrate ( $S_S$ ) that is needed for the growth of 1g heterotrophic biomass. The reactions in the ASM1 are given with a matrix notation, the ASM1 matrix. This matrix is given in Table 3.4.

Table 3.3. Concentration variables in the ASM1

Symbol	Name	Dimension
$S_O$	Oxygen	$M(-COD)L^{-3}$ (negative COD)
$S_S$	Readily biodegradable substrate	$M(COD)L^{-3}$
$X_S$	Slowly biodegradable substrate	$M(COD)L^{-3}$
$X_{BH}$	Active heterotrophic biomass	$M(COD)L^{-3}$
$S_{NO}$	Nitrate and nitrite nitrogen	$M(N)L^{-3}$
$X_{BA}$	Active autotrophic biomass	$M(COD)L^{-3}$
$S_{NH}$	Ammonium	$M(N)L^{-3}$
$S_I$	Soluble inert organic matter	$M(COD)L^{-3}$
$X_I$	Particulate inert organic matter	$M(COD)L^{-3}$
$X_P$	Particulate products arising from biomass decay	$M(COD)L^{-3}$
$S_{ND}$	Soluble biodegradable organic nitrogen	$M(N)L^{-3}$
$X_{ND}$	Particulate biodegradable organic nitrogen	$M(N)L^{-3}$
$S_{ALK}$	Alkalinity	Molar units

Table 3.4. Process kinetics and stoichiometry

Component $i$ Process $j$	1 $S_I$	2 $S_S$	3 $X_I$	4 $X_S$	5 $X_{BH}$	6 $X_{BA}$	7 $X_p$	8 $S_O$	9 $S_{NO}$	10 $S_{NH}$	11 $S_{ND}$	12 $X_{ND}$	13 $S_{Aik}$	Process Rate $\rho_j$
1 Aerobic growth of heterotrophs		$-\frac{1}{Y_H}$			1			$-\frac{1-Y_H}{Y_H}$		$-i_{XB}$			$\frac{i_{XB}}{14}$	$\mu_H \frac{S_S}{K_S+S_S} \frac{S_O}{K_{O,H}+S_O}$
2 Anoxic growth of heterotrophs		$-\frac{1}{Y_H}$			1			$-\frac{1-Y_H}{2.86Y_H}$		$-i_{XB}$			$\frac{1-Y_H}{14 \cdot 2.86Y_H}$ $-\frac{i_{XB}}{14}$	$\mu_H \frac{S_S}{K_S+S_S} \frac{K_{O,H}}{K_{O,H}+S_O}$ $\times \frac{S_{NO}}{K_{NO}+S_{NO}} \eta_9 X_{BH}$
3 Aerobic growth of autotrophs						1		$\frac{Y_A-4.57}{Y_A}$	$\frac{1}{Y_A}$	$-i_{XB} - \frac{1}{Y_A}$			$-\frac{i_{XB}}{14}$	$\mu_A \frac{S_{NH}}{K_{NH}+S_{NH}} \frac{S_O}{K_{O,A}+S_O}$
4 'Decay' of heterotrophs				$1 - f_p$	-1		$f_p$					$i_{XB} - f_p i_{XB}$		$b_H X_{BH}$
5 'Decay' of autotrophs				$1 - f_p$		-1	$f_p$					$i_{XB} - f_p i_{XB}$		$b_A X_{BA}$
6 Ammonification of soluble organic nitrogen										1	-1		$\frac{1}{14}$	$k_a S_{ND} X_{BH}$
7 'Hydrolysis' of entrapped organics		1		-1										$k_h \frac{X_S/X_{BH}}{K_X+X_S/X_{BH}} \left( \frac{S_O}{K_{O,H}+S_O} \right)$ $+ \eta_h \frac{K_{O,H}}{K_{O,H}+S_O} \frac{S_{NO}}{K_{NO}+S_{NO}} X_{BH}$
8 'Hydrolysis' of entrapped organic nitrogen											1	-1		$\rho_7 X_{ND}/X_S$

Observed Conversion Rates ( $\text{g}/\text{m}^3\text{d}$ ):  $r_i = \sum_{j=1}^8 \nu_{ij} \rho_j$

In the upper part of the matrix, the concentrations are listed. The mid part describes the stoichiometry while the right hand column gives the process rates. The name of the processes is given in the left column. To get the reaction rate of a concentration, we should multiply each stoichiometric coefficient in its column with the process rate on the same row and sum them up. The reaction rate of oxygen is for example

$$-\frac{1 - Y_H}{Y_H}\rho_1 - \frac{4.57 - Y_A}{Y_A}\rho_3.$$

Concentrations enter the reactions in the ASM1 mainly in Monod expressions. A Monod expression in a concentration  $z$  is either  $\frac{z}{K_z+z}$  or  $\frac{K_z}{K_z+z}$ . The first one models that a process rate is strictly monotonically increasing with  $z$ , but is bounded. The other kind models the same for  $\frac{1}{z}$ . The parameter  $K_z$  is called the half saturation coefficient for  $z$  and defines the value of  $z$  for which the Monod expression equals 0.5. The concentrations in the upper part of Table 3.3 stands for the dominating part of the reactions in this kind of ASP. The variables in the mid of the table,  $X_{BA}$  and  $S_{NH}$  are included in the simulation model but stands for only a small portion of the reactions. Mathematically, this follows from that they enter the reactions as  $\frac{S_{NH}}{K_{NH}+S_{NH}}X_{BA}$ , and the concentration of autotrophs is small. These will be considered as disturbances in observer models derived later and it is therefore uninteresting how they are formed. The variables in the lower part of the table only affects the variables in the upper part via  $X_{BA}$  and  $S_{NH}$  or not at all. These are thus excluded from the simulation model by setting them to zero in the influent. As seen in Table 3.3,  $S_{NO}$  is used to refer to both nitrate and nitrite in the ASM1. There is no measurement of nitrite at the plant, but the concentration can be assumed to be small and is not considered in the model.  $S_{NO}$ , thus further on refers to Nitrate. The degradation of  $S_O$  and  $S_S$ , and the growth of heterotrophic biomass  $X_{BH}$  in an aerobic tank is described by the process rate *Aerobic growth of heterotrophs* ( $\rho_1$ ), and is limited by the same variables. Degradation of slowly biodegradable (particulate) substrate ( $X_S$ ) into  $S_S$  is described by the process rate *'Hydrolysis' of entrapped organics* ( $\rho_7$ ), and is limited by  $S_O$ ,  $X_S$ , and  $X_{BH}$ . It is also limited by  $S_{NO}$ , but this applies mainly to the anoxic compartments. Biomass not only grows, but of course also dies. This is described by the process rate *'Decay' of heterotrophs* ( $\rho_4$ ). It is also described that part of the heterotrophs is degraded into  $X_S$  when they die. For the anoxic compartments we have the process rate *Anoxic growth of heterotrophs*, which is limited by  $S_{NO}$ ,  $X_{BH}$  and inversely limited by the oxygen concentration.

### 3.5.2 Parameters in the ASM1

The parameters in the ASM1 are specific for each plant. At Ryaverket, one has been tuning many of the parameters for their simulation model, but some are kept at default values. The parameters vary with temperature, but may also vary with other conditions. In Table 3.5 those ASM1-parameters that are important in this project are given for the plant at 20 °C.

Table 3.5. ASM1 parameters for Ryaverket.

Symbol	name	value	unit
$Y_H$	Yield for heterotrophic biomass.	0.666	$\text{g cell COD formed} / (\text{g COD oxidized})^{-1}$
$\hat{\mu}_H$	Maximum specific growth rate for heterotrophic biomass.	3	$\text{day}^{-1}$
$\eta_g$	Correction factor for $\mu_H$ under anoxic conditions.	1	dimensionless
$\eta_h$	Correction factor for hydrolysis under anoxic conditions.	0.8	dimensionless
$k_h$	Maximum specific hydrolysis rate.	2.81	$\text{g slowly biodegradable COD} / (\text{g cell COD} \cdot \text{day})^{-1}$
$K_X$	Half saturation coefficient of slowly biodegradable substrate.	0.15	$\text{g slowly biodegradable COD} / (\text{g cell COD})^{-1}$
$K_S$	Half saturation coefficient for heterotrophic biomass.	5	$\text{gCOD} \text{m}^{-3}$
$K_{NO}$	Nitrate half saturation coefficient for denitrifying heterotrophic biomass.	1	$\text{gNO}_3 - \text{Nm}^{-3}$
$K_{OH}$	Oxygen half saturation coefficient.	0.2	$\text{gO}_2 \text{m}^{-3}$
$b_H$	Decay coefficient for heterotrophic biomass.	0.62	$\text{day}^{-1}$
$f_p$	Fraction of biomass leading to particular products	0.08	dimensionless
$Y_A$	Yield for autotrophic biomass	0.15	$\text{g cell N formed} / (\text{g COD oxidized})^{-1}$
$b_A$	Decay coefficient for autotrophic biomass.	0.04	$\text{day}^{-1}$
$K_{NH}$	Ammonia half-saturation coefficient for autotrophic biomass	1	$\text{g NH}_3 - \text{Nm}^{-3}$
$\hat{\mu}_A$	Maximum specific growth rate for autotrophic biomass	0.1	$\text{day}^{-1}$
$i_{XB}$	Mass of nitrogen per mass of COD in biomass	0.068	$\text{gN} / (\text{g(COD)})^{-1}$
$i_{XP}$	Mass of nitrogen per mass of COD in biomass	0.068	$\text{gN} / (\text{g(COD)})^{-1}$
$K_{OA}$	Oxygen half-saturation half saturation coefficient for autotrophic biomass	0.2	$\text{gO}_2 \text{m}^{-3}$

### 3.5.3 Mass transfer of oxygen

Mass transfer of oxygen is described by

$$K_L a(q)(S_{O_{sat}} - S_O)$$

(Olsson and Newell 1999). This concerns only the oxygen equation in  $\xi$ , and enters this in a sum with the reactions in the ASM1. The oxygen mass transfer function  $K_L a$  ( $day^{-1}$ ) is not known for Ryaverket, but it is often assumed to be exponential w.r.t. the air flow:

$$K_L a(q) = k_1(1 - e^{-k_2 q}), \quad (3.2)$$

with parameters  $k_1$  and  $k_2$  (Olsson and Newell 1999).  $S_{O_{sat}}$  is the oxygen saturation concentration and defines the maximum oxygen concentration in the water. Wik (1999) gave a temperature model for  $S_{O_{sat}}$ :

$$S_{O_{sat}} = 14.53 - 0.411T + 9.6 \cdot 10^{-3}T^2 - 1.2 \cdot 10^{-4}T^3.$$

This claims to work well for both fresh and waste water, but there is a common used conversion between  $S_{O_{sat}}$  for the two kind of waters:

$$S_{O_{sat}}(wastewater) = \beta S_{O_{sat}}(freshwater).$$

According to Stenstrom and Gilbert (1981)  $\beta$  for domestic wastewater is generally about 0.95 but it can vary over a much broader range for industrial wastewater. 0.95 is used here.

## 3.6 Simulation platform

The simulation and programming language used in this work is Matlab/Simulink. A part of the model is illustrated in Figure 3.4. The tanks are modeled using an S-function (state space function) block together with a C-file implementing the ASM1 model together with inputs and outputs. This file was developed in the COST benchmark project (Copp 2001, Alex *et al.* 1999). The full model also includes the creating and mixing of the three influents and oxygen PI controllers for the aerobic tanks. Depending on the application, discrete or continuous controllers are used.

## 3.7 Case study

Compared to linear systems, analytic verification of a nonlinear system may be difficult because equations may be very complicated. Another possibility would be to verify it for every possible condition but this is of course not realistic. To evaluate designs, a specific simulation case is therefore used in this work. The use for an observer with unknown inputs implies that high resolution data on all concentrations in the model is not available. Still, daily mean samples are analyzed for COD at the

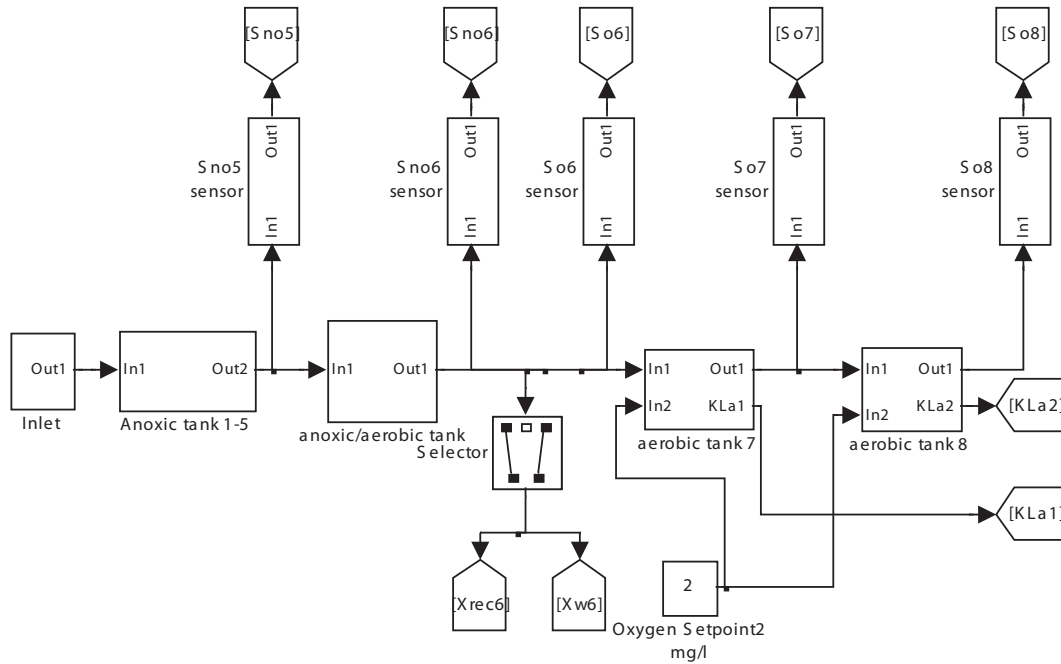


Figure 3.4. Simulink model

plant. Using a scheme, this is divided over the organic compounds in the ASM1. This is however only for the influent  $Q_{in}$  and not for the other flows. The plant simulation model is more complex and takes among others recirculation and the trickling filters into account. For a reasonable case, the simulation data presented here are based on data from the Ryaverket plant simulation model. Simulation conditions for waste water plants are commonly categorized based on weather conditions. The simulation files at the plant are divided into "dry summer", "rainy summer", "dry winter" and "rainy winter". The chosen conditions here are a "dry summer" with the temperature 20 °C. Parameter values in the model for these conditions are defined in Section 3.5. The concentrations in the influents are chosen such that mean concentrations in the simulation model coincide with the plants simulation data at point 1 in Figure 3.2. The choice of the concentrations in the individual flows are based on measurements, lab analysis and knowledge of the process (refer to Section 3.3). The variations in the concentrations about their means are chosen to have a reasonable effluent and an interesting simulation case. The shape of the variations in  $S_S$  and  $X_S$  in  $Q_{in}$  are based on the weather files from the COST benchmark project (Copp 2001, Alex *et al.* 1999). The simulation case is for a 14 days period. The mean values of the considered concentrations in the ASM1 for this period, for the three influents and in the point 1 in Figure 3.2 are listed in Table 3.6. To simplify simulation of some of the estimators developed in the next chapter, the water flows  $Q_{in}$ ,  $Q_{rec}$  and  $Q_X$  are chosen to be constantly 4, 4 and  $3 \text{ m}^3 \text{ s}^{-1}$  which corresponds to normal conditions at the plant. Noises in the water flow measurements are assumed to be negligible. For later purposes it will be convenient to model  $X_{BH}$  in  $Q_X$  as a

Table 3.6. Mean concentrations in the influents and the point  $\underline{1}$  in Figure 3.2

Concentration	Unit	$Q_{in}$	$Q_{rec}$	$Q_X$	$\underline{1}$
$S_O$	$mg(-COD)l^{-1}$	0	8.7	0	0.05
$S_S$	$mg(COD)l^{-1}$	127	0	2.5	42.5
$X_S$	$mg(COD)l^{-1}$	376	0	280	210
$X_{BH}$	$mg(COD)l^{-1}$	52	0	3670	1020
$S_{NO}$	$mg(N)l^{-1}$	0	12	0	3.5
$X_{BA}$	$mg(COD)l^{-1}$	0	70	0	25
$S_{NH}$	$mg(N)l^{-1}$	11	0	2	3.9

fraction of TSS in the same flow:

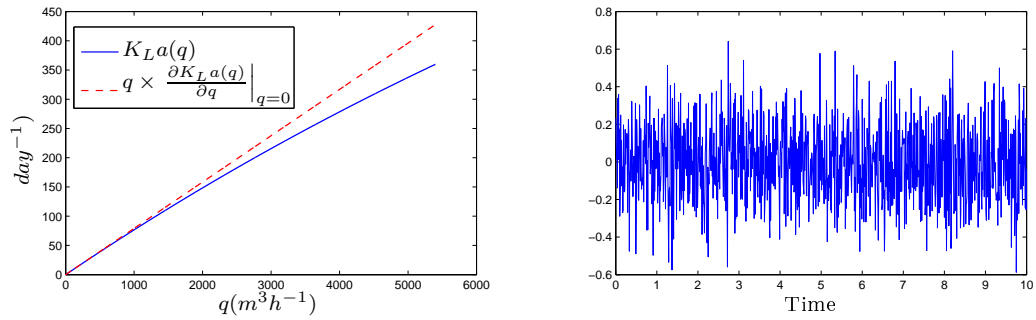
$$X_{BH} \text{ in } Q_X = (TSS \text{ in } Q_X) \cdot \gamma_{X_{BH}},$$

where  $\gamma_{X_{BH}}$  is a slowly time varying parameter.  $X_{BH}$  in the AS basin may vary fast with changes in the relation between the three influent flows, while the TSS concentration in  $Q_X$  is controlled to a constant value. The influent flows are set to be constant, so to simulate fast changes in  $X_{BH}$ , instead the TSS concentration in  $Q_X$  is varied. The shape of this variation is a sinus with the period two days. The parameter  $\gamma_{X_{BH}}$  is also simulated as a sinus with the period 20 days. The TSS concentration in  $Q_{in}$  is formed by multiplying the time varying part of  $X_S$  in the same flow with sinus signals of different frequencies and amplitudes, and adjusting its mean. For purposes that will become evident later on,  $X_S$  is then delayed 30 minutes. TSS measurements are assumed to have negligible noise.

Only the last 2 tanks (40 % of the basin) are aerated and the oxygen reference of the PI controllers are set to  $2mgO_2l^{-1}$ . In reality the maximum air flow in the aerated part of the AS basin is  $2160 m^3h^{-1}$  per zone. In the model it is assumed that the maximum air flow is  $q_{max} = 2.5 \cdot 2160m^3h^{-1}$  in each of the aerated tanks. As stated in Section 3.5, the  $K_La$  functions of the tanks are unknown and assumed parameter values are used here. The function is chosen to be the same for both of the aerated tanks and the choice of the parameters  $k_1$  and  $k_2$  in the Model (3.2) is based on the following two made up criteria

- $\left. \frac{\partial K_La(q)}{\partial q} \right|_{q=q_{max}} = 0.7 \left. \frac{\partial K_La(q)}{\partial q} \right|_{q=0}$ .
- $K_La(q_{max})$  should equal the maximally needed  $K_La$  function during simulation with the case study when the DO-reference is set to be  $4mgO_2l^{-1}$  in Tank 7.

The explicit values of  $k_1$  and  $k_2$  are given in Table 3.7 and the function is illustrated in Figure 3.5(a) It is assumed that air flow measurements have negligible measurement noise. Although, the properties of the real sensors stated in Section 3.4, noises in the nitrate and oxygen sensors are chosen to be Gaussian white noise to be more general. The standard deviation is assumed to be 0.2 which is 10 % of the oxygen reference. To illustrate the variance of the noise, a series is shown in Figure 3.5(b).

(a)  $K_L a$  function in the simulation case.

(b) Illustration of the variance of the measurement noise of oxygen and nitrate sensors.

Figure 3.5.

Table 3.7.  $K_L a$  parameters.

$k_1 (d^{-1})$	$k_2 (m^{-3}h)$
$6.6 \cdot 10^{-5}$	1200

# 4 ESTIMATION - THEORY AND SIMULATION

If other conditions are not stated, the simulation data used in this chapter is the same as in the case study in Section 3.7. The focus here is on estimation of  $S_S$ ,  $X_S$  and  $X_{BH}$  in the ASM1. For optimization of several of the control variables in ASP:s it is necessary with estimates for the whole AS basin. It is, however, concluded that it would not be possible to estimate all the considered concentrations in the anoxic compartments separately. This must include measurements in the aerobic compartments or estimates from an observer for these. It is much worth with estimates only for the aerobic compartments, and an extension is much simplified once this is available. Mainly two categories of solutions are considered here:

- Separate estimation of the heterotrophic biomass in the anoxic tanks and  $S_S$  in the aerobic compartments via estimation of rate expressions. This is based on that we may know that the Monod expression in  $S_S$  is saturated in the early upstream tanks and we can assume a value for the Monod expression.
- Estimation of all concentrations of interest with an extended Kalman filter for the aerobic compartments.

Methods to estimate the for an implementation necessary  $K_L a$  function are finally evaluated and further developed.

## 4.1 Observers and observability conditions

*If not stated explicitly, the theory in this section is taken from Besançon (2007) or Lewis (1986).*

The purpose of an observer is to recover the state vector  $x$  of a system based on measurements of inputs  $y$  and outputs  $u$  up to the current time  $t$ , and an internal model of the system. The theory is here presented for continuous time systems of dimension  $n$  ( $dim(x) = n$ ) on the form

$$\begin{cases} \dot{x} = a(x, u, t) + w & \text{state equation} \\ y = c(x, u, t) + v & \text{measurement equation} \end{cases}, \quad (4.1)$$

where  $w$  is process noise (white Gaussian) with covariance  $R_1 = E[ww^T]$ , and  $v$  is measurement noise (white Gaussian) with covariance  $R_2 = E[vv^T]$ . This system formulation is quite general and includes the following generalizations:

- LTI systems for which  $a(x, u, t) = Ax + Bu$  and  $c(x, u, t) = Cx + Du$ .

- LTV systems for which  $a(x, u, t) = A(t)x + B(t)u$  and  $c(x, u, t) = C(t)x + D(t)u$ .
- State affine systems for which  $a(x, u, t) = A(u)x + B(u)$  and  $c(x, u, t) = C(u)x + D(u)$ .

If  $R_1$  and  $R_2$  are zero matrices, the System (4.1) is deterministic, otherwise it is stochastic.

**Definition 1 (Observer for deterministic systems)** *An observer for a deterministic system (4.1) with  $R_1$  and  $R_2$  equal to zero is an auxiliary system*

$$\begin{aligned}\dot{X} &= F(X, u, y, t) \\ \hat{x} &= H(X, u, y, t),\end{aligned}$$

such that

$$\begin{aligned}(i) \quad & \hat{x}(0) = x(0) \Rightarrow \hat{x} = x, \forall t \geq 0 \\ (ii) \quad & \|\hat{x} - x\| \rightarrow 0 \quad \text{as } t \rightarrow \infty.\end{aligned}$$

If (ii) holds for any pair  $x(0)$ ,  $\hat{x}(0)$ , the observer is global.

If (ii) holds with exponential convergence, the observer is exponential.

If (ii) holds with a convergence rate which can be tuned, the observer is tunable.

A definition of an observer for a stochastic system can be formulated by loosening the conditions (i) and (ii), since these cannot hold strictly for such a system.

### 4.1.1 Observability conditions

Observability conditions should express that there indeed is a possibility that the purpose of the observer can be achieved, namely that it might be possible to recover  $x$  from the only knowledge of  $u$  and  $y$  up to time  $t$ . At first glance this will be possible only if  $y$  bears the information on the full state vector when considered over some time interval. This roughly corresponds to the notion of observability. However when restricting the definition of an observer strictly to items (i)-(ii), it is possible to construct observers even in cases when  $y$  does not bear the full information on the state vector. This corresponds to detectable systems. Observability conditions for a stochastic system are investigated for the corresponding deterministic system. We start with a very general definition of observability. Let  $\chi_u(t, x_{t_0})$  denote the solution to the state equation in the System (4.1) for a given input  $u$  on  $[t_0, t]$  and initial condition  $\chi_u(t_0, x_{t_0}) = x_{t_0}$ .

**Definition 2 (Indistinguishability)** *A pair  $(x_0, x'_0)$  is indistinguishable for the system (4.1) if*

$$\forall u \in U, \forall t \geq 0, c(\chi_u(t, x_0), u, t) = c(\chi_u(t, x'_0), u, t).$$

From this, observability can be defined.

**Definition 3 (Observability)** *The System (4.1) is observable if it does not admit any indistinguishable pair.*

#### 4.1.1.1 Observability of linear systems

An observer for the deterministic LTI version of the system (4.1) is

$$\dot{\hat{x}} = A\hat{x} + Bu + K(C\hat{x} - y), \quad (4.2)$$

where  $K$  is the observer gain, here assumed to be constant. Define the observer error  $e = \hat{x} - x$ . The differential equation describing  $e$  is

$$\dot{e} = (A - KC)e,$$

which is asymptotically stable if  $(A - KC)$  is stable, or equivalently, if the eigenvalues of  $(A - KC)$  are strictly negative. If the eigenvalues of  $(A - KC)$  can be placed arbitrarily by choosing  $K$ , the system is observable. If this does not hold but  $(A - KC)$  is stabilizable (can be made stable) the system is detectable. In other words, this means that the unobservable modes of the system are stable. Observability can be checked in several ways:

- By direct investigation of the eigenvalues of  $(A - KC)$ , by which we also can investigate detectability.
- By confirming that the rank of the observability matrix equals the dimension of the system, see Åstrom and Wittenmark (1997). This condition is referred to as the Kalman rank condition.
- In Matlab, observability of an LTI system can be investigated by a linear transformation into a staircase form. By this, the observable states of the transformed system are found. The eigenvalues of the unobservable states are also displayed, from which one can conclude if the system is detectable. By an inverse transformation, observability/detectability of the original systems states can be investigated.

The last method is to prefer if the dimension of the system is large. The transformation of the state  $x$  is described by  $x' = Tx$ , where  $T$  is the transformation matrix. Consider the case with one undetectable mode. In the transformed system, this is the first element  $x'_1$  of  $x'$ . Let  $T'$  be the inverse transformation matrix -  $T^{-1}$ . The relative dependency for the  $i$ :th state in  $x$  of the undetectable mode can be calculated by

$$\frac{T'(i, 1)x'_1}{\sum_{k=1}^n |T'(i, k)x'_k|}.$$

Yet another method to investigate detectability is presented in Section 4.1.2.1.

### 4.1.1.2 Observability of nonlinear systems

For a nonlinear systems, Definition (3) of observability might be too general for practical use since one might mainly be interested in distinguishing states from their neighbors. Consider for instance the system

$$\begin{cases} \dot{x} = u \\ y = \sin(x) \end{cases} .$$

Clearly  $y$  cannot help distinguish between  $x_0$  and  $x_0 + 2k\pi$ . However,  $y$  allows to distinguish states in  $] -\frac{\pi}{2}, \frac{\pi}{2}[$ . A general notion of observability which includes this case is weak observability.

**Definition 4 (Weak observability (resp. at  $x_0$ ))** *The System (4.1) is weakly observable (resp. at  $x_0$ ) if there exists a neighborhood  $U$  of any  $x$  (resp. at  $x_0$ ) such that there is no indistinguishable state from  $x$  (resp.  $x_0$ ) in  $U$ .*

Notice that it is allowed that trajectories may go far from  $U$  before one can distinguish two states of  $U$ . The system

$$\begin{cases} \dot{x} = u \\ y = \begin{cases} x, & |x| \geq 1 \\ 0, & |x| < 1 \end{cases} \end{cases}$$

is weakly observable since any state is distinguishable from any other one by applying some nonzero input, but distinguishing two points of  $[-1, 1]$  needs to wait for  $y$  to move away from 0. Hence, to prevent from this situation, an even more local definition of observability can be given.

**Definition 5 (Local weak observability (resp. at  $x_0$ ))** *The System (4.1) is locally weakly observable (resp. at  $x_0$ ) if there exists a neighborhood  $U$  of any  $x$  (resp. of  $x_0$ ) such that for any neighborhood  $V$  of  $x$  (resp.  $x_0$ ) contained in  $U$ , there are no indistinguishable state from  $x$  (resp.  $x_0$ ) in  $V$  when considering time intervals for which trajectories remain in  $V$ .*

This roughly means that one can distinguish every state from its neighbors without "going too far". Local weak observability can be checked with the observability rank condition. Note that this property does not say anything about global properties. Let

$$Y = \begin{bmatrix} y \\ \frac{dy}{dt} \\ \vdots \\ \frac{dy^m}{dt^m} \end{bmatrix}, \quad O(x) = \begin{bmatrix} c(x, u, t) \\ L_{f_u} c(x, u, t) \\ \vdots \\ L_{f_u}^m c(x, u, t) \end{bmatrix},$$

where  $L_{f_u}^k c(x, u, t)$  are Lie derivatives of for any constant input  $u$ , and  $m$  is an arbitrary positive integer.  $Y$  is what we can see from measurements and if the

system is deterministic we have that  $Y = O(x)$ . From a theorem in multivariable calculus it follows that  $O(x)$  as a function of  $x$  is bijective about a point  $x_0$  if the rank of  $\frac{\partial O(x)}{\partial x}$  at this point equals  $n$ , see Persson and Böiers (1988). From this follows the observability rank condition.

**Theorem 1 (The observability rank condition)** *The System (4.1) is weakly locally observable if  $\text{rank}\left(\frac{\partial O(x)}{\partial x}\right) = n$  for any  $x$ , and is locally weakly observable at  $x_0$  if*

$$\text{rank}\left(\frac{\partial O(x)}{\partial x}\Big|_{x=x_0}\right) = n.$$

This theorem is somewhat simplified compared to the presentation in Besançon (2007). If the system is locally weakly observable, we can confirm this by choosing  $m$  large enough and using the theorem. It might however be difficult to confirm the contrary since we are free to chose  $m$  infinitely large. Still, it is reasonable to assume that the condition does not hold if increasing  $m$  over some value does not seem to increase the rank of the jacobian. For LTI systems, the observability rank condition simplifies to the Kalman rank condition. For nonlinear systems, local weak observability is not enough for a possible observer design since the observability may depend on the inputs. We want to differentiate between systems for which observability is a property of the inputs and not. For that, the notion of *uniform observability* is introduced.

**Definition 6 (Universal inputs)** *An input is universal for the system (4.1) if  $\forall x_0 \neq x'_0, \exists \tau \geq 0$  such that  $c(\chi_{u(\tau, x_0)}, u, \tau) \neq c(\chi_{u(\tau, x'_0)}, u, \tau)$ . An input is singular if it is not universal.*

**Definition 7 (Uniformly observable systems)** *The system (4.1) is uniformly observable if every input is universal.*

The system

$$\begin{cases} \dot{x} = \begin{bmatrix} 0 & 1 & 0 & \cdots & 0 \\ & & \ddots & \ddots & \\ & & & & 0 \\ \vdots & & & & 1 \\ 0 & \cdots & & & 0 \end{bmatrix} x + \begin{bmatrix} \phi_1(x_1) \\ \phi_2(x_1, x_2) \\ \dots \\ \phi_{n-1}(x_1, \dots, x_{n-1}) \\ \phi_{n-1}(x_1, \dots, x_n) \end{bmatrix} u \\ y = x_1 \end{cases} \quad (4.3)$$

with nonlinear functions  $\phi_i$  is uniformly observable. This can be checked by considering any pair of distinct states  $x \neq x'$ : assuming indeed that their respective components  $x_k$  and  $x'_k$  coincide up to order  $i$  and that  $x_{i+1} = x'_{i+1}$ , then it is clear that  $\dot{x}_{i-1} - \dot{x}'_{i-1} \neq 0$  and thus there exist a  $t_0$  such that  $x_i(t) \neq x'_i(t)$  for  $0 < t < t_0$ , which is true for any  $u$ .

## 4.1.2 Observer designs

For linear time invariant- (LTI) and linear time variant (LTV) systems, the theory and design of observers are general concepts, while for nonlinear systems these concepts are system dependent. Special kinds of observers are filters in which properties of disturbances acting on the system are taken into account in the observer synthesis.

### 4.1.2.1 Observers for linear systems

A general form of an observer for a linear system is given by Equation (4.2) with the addition that  $K$  might be time varying. The deterministic case is not treated further but it is stated that given that the system is observable, the convergence rate can be made arbitrarily fast. In the design of observers for stochastic systems, there is a compromise between noise dampening and fastness. A Kalman filter for an LTI system is optimal in the sense that that it minimizes the expectation of the quadratic error (covariance)  $P = E[ee^T]$ . The continuous time version for the LTI system (4.1) is presented below.

#### Algorithm 1 (Continuous time Kalman filter.)

$$\begin{aligned}
 P(0) = P_0, \quad \hat{x}(0) = \hat{x}_0 & \quad \textit{Initialization} \\
 \dot{\hat{x}} = A\hat{x} + K[y - C\hat{x}] & \quad \textit{Estimate update} \\
 \dot{P} = AP + P^T A + R_1 - PC^T R_2^{-1} CP & \quad \textit{Error covariance update} \\
 K = PC^T R_2^{-1} & \quad \textit{Kalman gain}
 \end{aligned} \tag{4.4}$$

$P(0)$  is the covariance of the initial error:  $P(0) = E[(\hat{x}(0) - x(0))(\hat{x}(0) - x(0))^T]$ , which never is known exactly but should reflect the "quality" of the initial guess  $\hat{x}(0)$  of  $x(0)$ . The algorithm is taken from Lewis (1986), in which the corresponding one for discrete LTI systems also is given. Equation (4.4) is the Ricatti equation. There is a connection between the Ricatti equation and detectability:

**Theorem 2 (Detectability and the Ricatti equation)** *Let  $R_1 = \sqrt{R_1} \sqrt{R_1^T}$ , and  $R_2 > 0$ . Suppose  $(A, \sqrt{R_1})$  is reachable. Then  $(A, C)$  is detectable if and only if:*

- *There is a unique positive definite limiting solution  $P$  to Equation (4.4), which is independent of  $P(0)$ . Furthermore,  $P$  is the unique positive definite solution to this.*
- *The error  $e = (\hat{x} - x)(\hat{x} - x)^T$  is asymptotically stable.*

The Algorithm 1 also works and is optimal for LTV- and state affine systems.

### 4.1.2.2 Observers for nonlinear systems

In systematic design of observers for nonlinear systems, one differentiates between uniformly- and non-uniformly observable systems. Uniformly observable systems can (at least locally) be transformed into an observable canonical form. For a system on this form, it is possible to design tunable observers and there exists general design methods. The System (4.3) is on this form and admits an observer on the form

$$\dot{\hat{x}} = A\hat{x} + \phi(\hat{x}, u) - \begin{bmatrix} \lambda & 0 & \cdots & 0 \\ 0 & \lambda^2 & \ddots & \vdots \\ \vdots & \cdots & \ddots & 0 \\ 0 & \cdots & \cdots & \lambda^n \end{bmatrix} K(C\hat{x} - y),$$

with  $K$  such that  $(A - KC)$  is stable, and  $\lambda$  large enough. This design is known as a *high gain observer* since it relies on the choice of some sufficiently large tuning parameter  $\lambda$ . There are much more general *observability canonical forms*, for a full treatment, see Besançon (2007).

### 4.1.3 The Extended Kalman filter

The optimal filter problem for nonlinear systems is in general very complicated, and only in a few cases do algorithms exist which are easy to implement or understand. In applications, it is common to design a Kalman filter for the linearization of the nonlinear system around a point  $x_0$ . This is useful, if for example  $x_0$  is a reference state, which the system is stabilized to by feedback control. An extension to this, is to let the linearization in the Kalman filter be continuously time varying and be that around the current estimate  $\hat{x}$ . This is the algorithm of the extended Kalman filter (EKF). In Lewis (1986) one derives the conditional probability density function of the state given measurement data. This is then used to find optimal update equations for the estimate and error covariance which are in general not computationally realizable. To obtain a computationally viable algorithm for general nonlinear systems, one makes approximations that result in the EKF. The algorithm is stated below for the System (4.1).

#### Algorithm 2 (Continuous time Extended Kalman filter.)

$$P(0) = P_0, \quad \hat{x}(0) = \hat{x}_0 \quad \textit{Initialization}$$

$$\dot{\hat{x}} = a(\hat{x}, u, t)x + K[y - c(\hat{x}, u, t)] \quad \textit{Estimate update} \quad (4.5)$$

$$\dot{P} = A(\hat{x})P + P^T A(\hat{x}) + R_1 \quad \textit{Error covariance update} \quad (4.6)$$

$$-PC(\hat{x})^T R_2^{-1} C(\hat{x})P$$

$$K = PC(\hat{x})^T R_2^{-1} \quad \textit{Kalman gain}$$

$$A(x) = \frac{\partial a(x, u, t)}{\partial x}, \quad C(x) = \frac{\partial c(x, u, t)}{\partial x} \quad \textit{Jacobians}$$

The filter is a good - almost optimal if the variances are small - local observer but it is in general not a globally converging observer. Intuitively, if the initial guess is far from the actual state, the linearization around the estimate has no sense. Theorems regarding convergence of EKF:s has not been found in the litterature, but it is reasonable that observability of linerizations of the nonlinear model in the observation space is an important property. For systems that can be transformed into an observability canonical form there are special variants of EKF:s that are globally converging. The high gain extended Kalman filter (HG-EKF) is an extension of the extended Kalman filter in which the covariance matrix  $R_1$  is chosen in a special way. The idea is to "kill" the nonlinear part of the model. The drawback is that it is very sensitive to noise, i.e. the estimates get very noisy. An interesting extension of the HG-EKF is the adaptive gain extended Kalman (AG-EKF). This behaves as a HG-EKF at startup but the observer itself converges in time to an ordinary EKF. Also if large perbutations occur, the high gain part takes over again.

#### 4.1.4 Implementation of EKF:s

The equations in the Algorithm 2 are continuous and cannot directly be solved on a computer. In Lewis (1986) it was suggested to implement EKF:s using the Runge Kutta 4 method. This is a common method to solve ordinary differential equations (ODE:s). The method is presented for a system on the form

$$\frac{dx}{dt} = f(x, t). \quad (4.7)$$

in the algorithm below.

**Algorithm 3 (The Runge Kutta 4 method)** *Let  $(x_k, t_k)$  be the solution to Equation (4.7) at time  $kh$ . The solution at time  $kh+h$  can be approximated by sequentially calculating*

$$\begin{aligned} a &= hf(x_k, t_k) \\ b &= hf(x_k + a/2, t_k + h/2) \\ c &= hf(x_k + b/2, t_k + h) \\ d &= hf(x_k + c, t_k + h) \\ x_{n+1} &= x_k + \frac{a + 2(b + c) + d}{6}. \end{aligned}$$

The algorithm has been taken from Xin-She (2008). Note that when using it to solve the equations in the EKF in Algorithm (2), the Equations (4.5) and (4.6) for  $[\hat{x}, P]$  should be treated as one system of equations.

### 4.1.5 Random walk models

A random walk process  $x$  is a variable which is modeled as being completely driven by noise. In its simplest form, a model for  $x$  is

$$\dot{x} = w_x. \quad (4.8)$$

Here,  $w_x$  is white noise, with variance  $R_x$ . This is useful to model variables/parameters without known dynamical equation. In a Kalman filter  $R_x$  is used to relate the variation of  $x$  compared to other variables and noises in the model. In the discrete case, the Model (4.8) translates to

$$x(k+1) = x(k) + w_x(k)$$

## 4.2 Estimation of sludge concentrations

The experience at the plant is that the substrate concentration is correlated with the TSS measurement in the influent  $Q_{in}$ .  $S_S$  is too much affected by upstream processes for this information to be useful in an observer for the aerobic process.  $X_S$ , however, is little affected by reactions in the basin and is mainly driven by massbalances. It consists mainly of particulate compounds, and a correlation with the TSS measurement intuitively seems reasonable. This motivates an introduction of the variable  $X_{in}$  (*gTSS*):

*The sludge concentration originating from the flow  $Q_{in}$ .*

This can be estimated for the tanks by simulating the *TSS* measurement in  $Q_{in}$  with massbalances

$$\begin{aligned} \dot{\hat{X}}_{in:t} &= \frac{3Q}{V_t} \left( \frac{Q_{in}}{3Q} ((\text{measured TSS in } Q_{in}) - \hat{X}_{in:t}) \right) & (4.9) \\ \dot{\hat{X}}_{in:1} &= D_1(Q)(\hat{X}_{in:t} - \hat{X}_{in:1}) \\ &\vdots \\ \dot{\hat{X}}_{in:8} &= D_8(Q)(\hat{X}_{in:7} - \hat{X}_{in:8}). \end{aligned}$$

Because of the physical distance between the TSS sensor and the later tanks, we can predict the future concentration, which can be used to make an observer react faster to changes. To make this easily implementable,  $X_S$  was delayed 30 minutes compared to the TSS concentration in the the simulation case in Section 3.7.

The dominating source of heterotrophs  $X_{BH}$  in the AS basin is the recycled sludge flow  $Q_X$ . There is also a relatively small concentration in the influent flow  $Q_{in}$  and we also have growth and decay in the tanks. The composition of the sludge varies slowly, but  $X_{BH}$  may vary fast due to changes in the relation between the influent flows to the ASP. Therefore the sludge concentration  $X_X$  (*gTSS*) is introduced which is

The concentration of TSS in a tank originating from the recycled sludge flow.

This can be estimated with the same method as was used for  $X_{in}$  and with the TSS measurement in  $Q_X$ . In the simulation case, the slow variation has been modeled with the parameter  $\gamma_{X_{BH}}$ . We therefore assume that there is a slowly time varying parameter  $\bar{\gamma}_{X_{BH}}$  with

$$E[\bar{\gamma}_{X_{BH}} \hat{X}_{X:i}] = X_{BH:i}, \quad i \in I,$$

and that  $\bar{\gamma}_{X_{BH}} \approx \gamma_{X_{BH}}$ . The index set  $I$  was defined in Section 3.1. We can thus model  $X_{BH}$  as  $\bar{\gamma}_{X_{BH}} \hat{X}$ , and the parameter can be estimated. In the coming designs we will neglect the two parameters differences and use  $\gamma_{X_{BH}}$  for  $\bar{\gamma}_{X_{BH}}$ . We thus have the model

$$X_{BH:i} = \gamma_{X_{BH}} \hat{X}_{X:i}, \quad i \in I. \quad (4.10)$$

The C-file implementing the tank model described in Section 3.6 have been altered to include estimation of  $X_X$  and  $X_{in}$ .

### 4.3 Estimation of rate expressions, $X_{BH}$ and $S_S$

The rate expressions *oxygen uptake rate OUR* and *nitrate uptake rate (NUR)* describes the reaction rate of oxygen, and Nitrate respectively. Let  $z$  be either the oxygen ( $S_O$ ) or nitrate ( $S_{NO}$ ) concentration and  $N_z$  the corresponding rate expression. A general model for  $z$  in a tank is

$$\dot{z} = D_i(Q)(S_{z_{in}} - z) + K_L a(q)(S_{O_{sat}} - z) - N_z, \quad (4.11)$$

where  $K_L a$  is identically zero in an anoxic tank, since the air flow is zero. Nitrification has small effect in an anoxic tank, and in this kind of ASP also in an aerobic one (refer to Section 3.5). If nitrification is neglected, the two rate expressions can be identified from Table 3.4 as

$$\begin{aligned} NUR &= \eta_g \hat{\mu}_H \frac{1 - Y_H}{2.86 Y_H} \frac{S_S}{K_S + S_S} \frac{S_{NO}}{K_{NO} + S_{NO}} X_{BH} \\ OUR &= \hat{\mu}_H \frac{1 - Y_H}{Y_H} \frac{S_S}{K_S + S_S} \frac{S_O}{K_{OH} + S_O} X_{BH}. \end{aligned} \quad (4.12)$$

in the ASM1. Estimated rate expressions can be used for reference control, see for instance Olsson and Newell (1999). From the stoichiometry in the ASM1, it follows that we from  $N_z$  also gets an approximation of the degradation rate of soluble substrate  $S_S$ . This can, for example, be used to express the total amount of substrate degraded over period of time. It is here considered to base the estimation of  $S_S$  and  $X_{BH}$  on estimated rate expressions. The Monod expression  $M_{S_S} = \frac{S_S}{K_S + S_S}$  is shown in Figure 4.1(a). In the early upstream anoxic tanks,  $S_S$  is probably above  $30 \text{mg(COD)} l^{-1}$  for most of the day. For these concentrations,  $M_{S_S}$  is saturated, and we can assume a value of around 0.9 for it. By applying this, an estimate of  $NUR$ , and measured/estimated nitrate concentration to Equation (4.12) we get an estimate of  $X_{BH}$ , or rather  $\gamma_{X_{BH}}$  by applying Equation (4.10). It follows that  $\hat{\gamma}_{X_{BH}}$

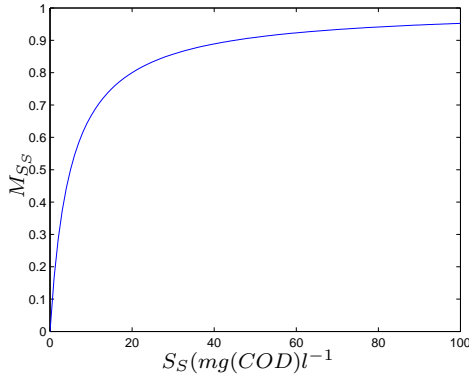
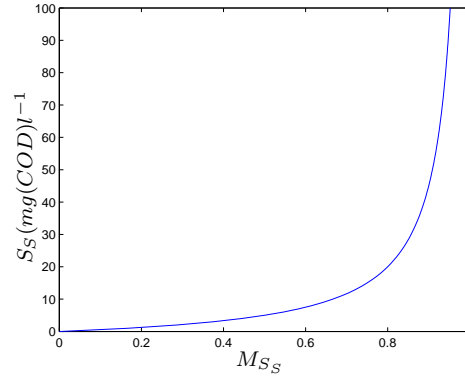
(a) The Monod expression  $M_{S_S}$ (b) The inverse of the Monod expression  $M_{S_S}$ 

Figure 4.1.

with these calculations is increasing with  $S_S$ , and only reasonable when  $S_S$  is large, since it is assumed that the Monod expression is saturated. This thus implies that  $\hat{\gamma}_{X_{BH}}$  makes sense only when it is relatively large. The method used to estimate  $X_{BH}$  and the parameter implies that the estimated value cannot be used to estimate  $S_S$  in the same tanks. This since the inverse of  $M_{S_S}$  is here very sensitive to noise and model errors. The inverse is illustrated in Figure 4.1(b), and it should be clear that independently of choice of method, it is unreasonable to estimate  $S_S$  in anoxic tanks based only on a model of these. On the other hand, in the last aerobic tank  $S_S$  is much smaller, and can be approximated from an estimate of  $OUR$  by using the estimated value of  $\gamma_{X_{BH}}$  and measured/estimated DO concentration.

### 4.3.1 An observer model for rate expressions

A continuous observer model for  $z$  ( $S_O$  or  $S_{NO}$ ) and  $N_z$  ( $OUR$  if  $z = S_O$  and  $NUR$  if  $z = S_{NO}$ ) if derived from Equation (4.11) is

$$\left\{ \begin{array}{l} \frac{d}{dt} \underbrace{\begin{bmatrix} z \\ N_z \end{bmatrix}}_x = \underbrace{\begin{bmatrix} -D(Q) - K_L a(q) & -1 \\ 0 & 0 \end{bmatrix}}_{A(t)} x + \underbrace{\begin{bmatrix} D(Q)z_{in} + K_L a(q)S_{O_{sat}} \\ 0 \end{bmatrix}}_{B(t)} \\ + \begin{bmatrix} D_i(Q)w_{z_{in}} \\ 0 \end{bmatrix} + \begin{bmatrix} 0 \\ w_N \end{bmatrix} \\ y = \underbrace{\begin{bmatrix} 1 & 0 \end{bmatrix}}_C x + v \end{array} \right. \quad (4.13)$$

Time indices have been used for the matrices to emphasize that they vary with time due to the variation in the inputs.  $w_{z_{in}}$  describes measurement noise in the input concentration  $z_{in}$ . The variance equals the variance of the measurement noise  $v$ , which is  $R_2$ . The rate expression  $N_z$  is here modeled as a random walk process

with variance  $R_N = E[w_N w_N^T]$ , which is a design parameter. To make it simpler to implement the observer on a computer, the observer model (4.13) is discretized. The sampling time is symbolized with  $h$  and the discrete time instants are indexed by  $k$ . The discretized observer model becomes

$$\begin{cases} x(k+1) = A_d(k)x(k) + B_d(k) + w_d(k) \\ y(k) = C_d x(k) + v_d(k) \end{cases} . \quad (4.14)$$

With the small approximation that the inputs are constant during the sampling periods, most of the matrices and covariances in this model can be calculated using the standard formulas found in Lewis (1986). Initially we have

$$\begin{aligned} A_d(k) &= e^{A(k)h} \\ B_d(k) &= \int_0^h e^{A(k)s} ds B(k) \\ C_d(k) &= C \\ R_{2d}(k) &= \frac{R_2}{h} \quad \text{variance of the measurement noise } v_d(k). \end{aligned} \quad (4.15)$$

The variance of the discrete process noise  $w_d(k)$ ,  $R_{1d}(k)$ , can be calculated as a sum of the contributions from  $w_N$  and  $w_{zin}$ , since these are independent. The measured oxygen input concentration is sampled, and the corresponding discrete measurement noise is  $w_{zind}(k)$ , with variance  $\frac{R_2}{h}$ . According to Equation (4.15), this has the following effect on the states during one sampling period

$$\int_0^h e^{A(k)s} ds \begin{bmatrix} D(Q(k))w_{zind}(k) \\ 0 \end{bmatrix}.$$

The variance of this expression is

$$R_{11d}(k) = \int_0^h e^{A(k)s} ds \begin{bmatrix} \frac{R_2 D(Q(k))^2}{h} & 0 \\ 0 & 0 \end{bmatrix} \int_0^h e^{A(k)^T s} ds, \quad (4.16)$$

which is the contribution of  $w_{zin}$  to  $R_{1d}(k)$ . The way  $N_z$  is modeled,  $w_N$  varies continuously within the sampling periods, and its contribution to  $R_{1d}(k)$  is

$$R_{12d}(k) = \int_0^h e^{A(k)s} \begin{bmatrix} 0 & 0 \\ 0 & R_N \end{bmatrix} e^{A(k)^T s} ds,$$

which follows from the formulas in Lewis (1986). Finally, we have

$$R_{1d}(k) = R_{11d}(k) + R_{12d}(k).$$

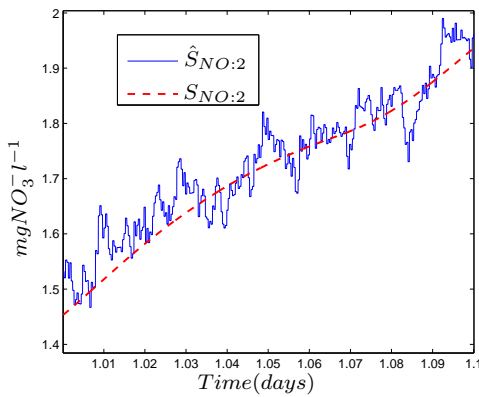
It is trivial to check that the model (4.14) is observable using the Kalman rank condition, and it is not shown here.

### 4.3.2 Estimation of $NUR$ based on one reactor

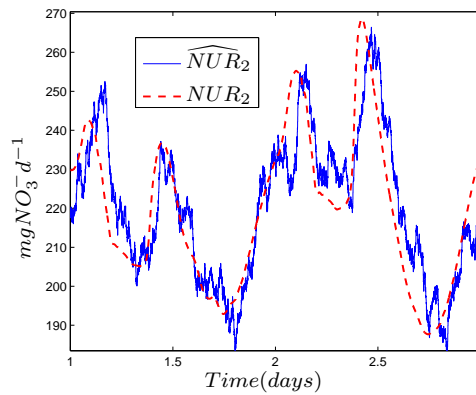
It is here assumed that there is one nitrate sensor in the second anoxic tank, and also one in the inlet to the same - the first anoxic tank. A stationary Kalman filter given in Åstrom and Wittenmark (1997) is used, since with the water flow constant, the System (4.14) is LTI, and convergence is not an issue. This was implemented in Simulink. According to Section 3.7,  $R_2$  is  $0.2^2$ . The sample time  $h$  is chosen to be  $0.5 \text{ min}$ . The method described in the beginning of this section to estimate  $X_{BH}$  and  $\gamma_{X_{BH}}$  is evaluated using the constant value  $0.89 \approx M_S|_{S_S=40}$  for the Monod expression  $M_S$ . Instead of the measured nitrate concentration, the concentration estimated by the Kalman filter is used in this calculation.

#### 4.3.2.1 Simulation result

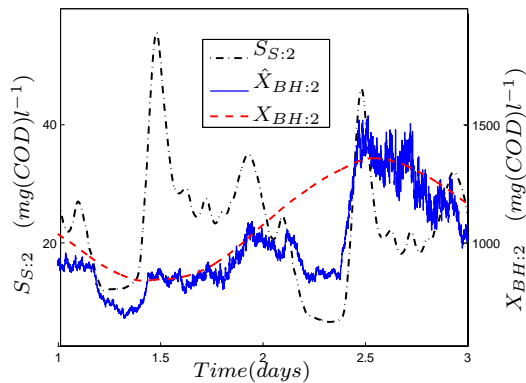
The estimate of the nitrate concentration is illustrated in Figure 4.2(a), refer to Figure 3.5(b) for a picture of the measurement noise.  $\widehat{NUR}_2$  is shown in Figure



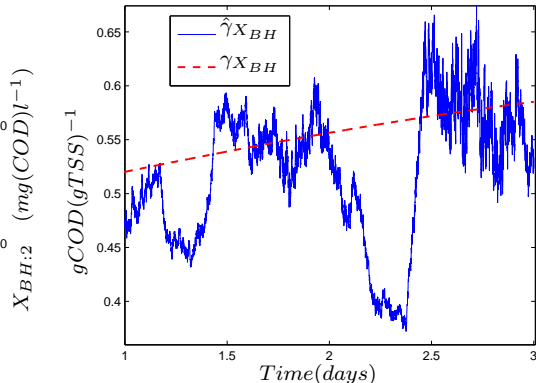
(a) Estimation of  $S_{NO}$ .



(b) Estimation of  $NUR$ .



(c) Estimation of  $X_{BH:2}$ .



(d) Estimation of  $\gamma_{X_{BH}}$ .

Figure 4.2. Estimates with a Kalman filter for the first anoxic tank.

4.2(b). The result is not very impressive, the convergence rate is quite is slow.

There is a compromise between convergence rate and noise dampening, and in this case there are disturbances in both the measurement of the input and the output to the filter. Noise in the input has particularly large effect since the input variance is proportional to  $(\frac{Q}{V})^2$ , and the tank volume is small.  $\hat{X}_{BH:2}$  is illustrated in Figure 4.2(c) together with  $S_{S:2}$ . The estimate only makes sense when  $S_S$  is large because of the assumption that  $M_{S_S}$  is saturated. In Figure 4.2(d),  $\hat{\gamma}_{X_{BH}}$  is shown. This is strictly increasing with  $S_S$ , and as stated earlier; when  $\hat{\gamma}_{X_{BH}}$  is large it is also quite good. It might be a good idea to form a mean value of  $\hat{\gamma}_{X_{BH}}$  for a period of time when this holds. The relatively large noise is due to the calculations after the filtering which amplifies the noise. It may therefore be better to use an EKF to directly estimate the parameter.

### 4.3.3 Estimation of $NUR$ based on several reactors

One would like to estimate  $NUR$  based on a model of more than one tank. The reason is twofold:

- As stated earlier, the variance of the noise caused by the measurement of the input concentration is proportional to  $(\frac{Q}{V})^2$ . If the sensors were more separated in distance, this variance would be reduced.
- The assumption about the sensors placement in the process is not valid, at least not for now.

A possible solution would be to extend the observer with more tanks and with rate expressions for each, modeled as random walk processes. There are nitrate sensors in the outlets of the trickling filters that could be used as the measured input, and the sensor in either Tank 5 or 6 could be used as output measurement. One could also use that the rate expressions are correlated and express this in the process noise covariance matrix. This solution was considered and tested for a series of two tanks. The result was a non convergent filter with estimates that stationary depended on the initial conditions. This also follows from the non detectability of such an observer model. Another possible solution that could help to reduce the noise is to approximate two tanks as one. This was considered for the two first anoxic tanks in the process with one nitrate measurement in the inlet to the first and one in the second. Approximating two tanks as one means that a second order system is approximated as a first order system. It is not obvious that the volume  $V_{tot}$  in the approximated model should be the total volume of the two tanks, there might be a value that is more optimal. Let  $g_1$  be the impulse response for the original system with the two tanks, and  $g_2$  the impulse response of the first order approximation. The volumes of the tanks in the original system are in this case equal and we have that

$$\begin{aligned} g_1(t) &= \left(\frac{Q}{V_1}\right)^2 t e^{-\frac{Q}{V_1}t} \\ g_2(t) &= \frac{Q}{V_{tot}} e^{-\frac{Q}{V_{tot}}t}, \end{aligned}$$

for the flow  $Q$  constant (Lennartson 2002). A candidate for an optimal  $V_{tot}$  is that which minimizes the integrated quadratic difference between the step responses:

$$\int_0^{\infty} (g_1(t) - g_2(t))^2 dt. \quad (4.17)$$

The solution is then  $V_{tot} \approx 2.74V_1$ .

#### 4.3.3.1 Simulation result

A stationary Kalman filter for the observer model (4.14) for the approximated system was implemented in Simulink. The sampling time  $h$  was set to 0.5 min. Both when the value  $2.74V_1$  which minimizes the Criterion (4.17) and when the tanks total volume was used for  $V_{tot}$ , the filter estimates of  $NUR$  was biased. By trial and error it was found that the value  $2.2V_1$  gave quite a good result. This is illustrated in Figure 4.3. The optimal choice of  $V_2$  is however dependent on the concentrations

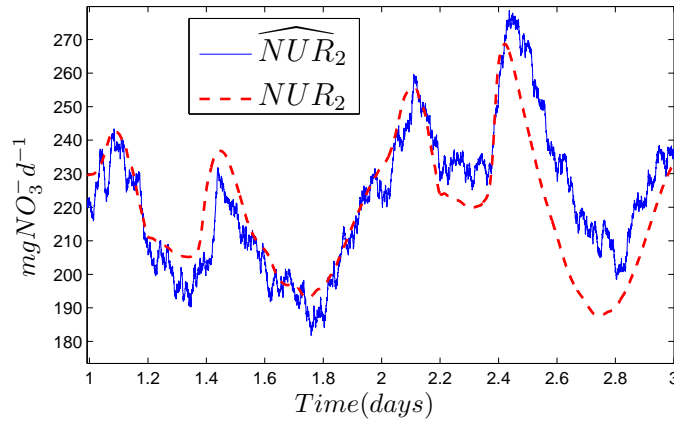


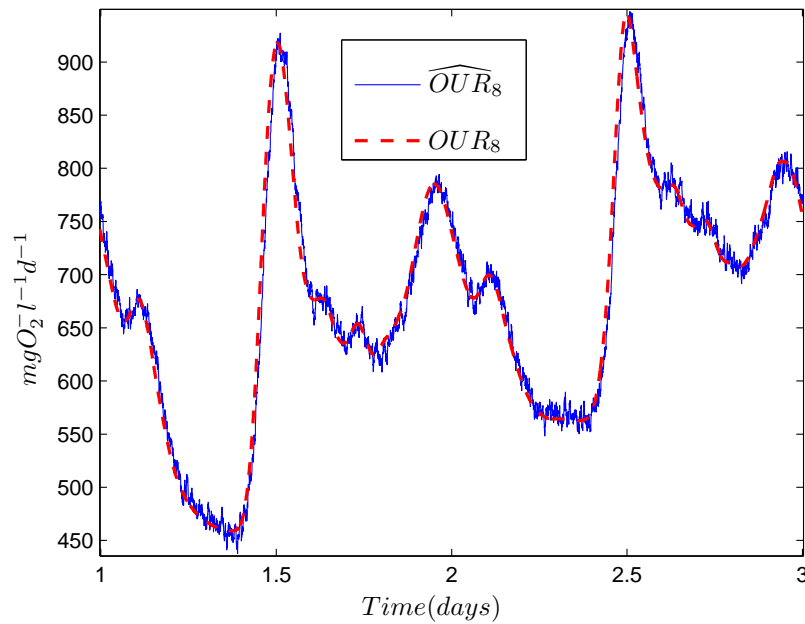
Figure 4.3. Estimation of  $NUR$  based on a one-tank model of two tanks.

in the tank, which can be seen in the figure as the estimate becomes more biased with time. Any improvement of convergence rate and noise dampening is at least not significant.

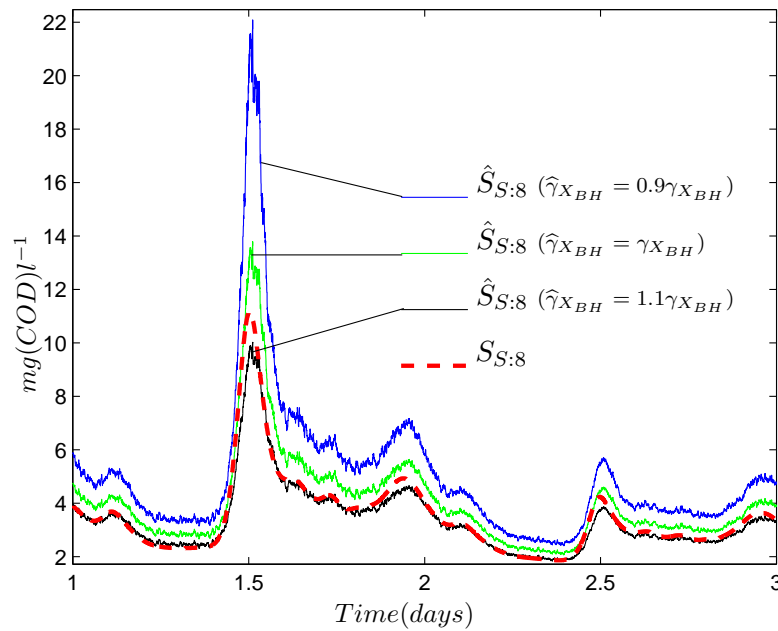
#### 4.3.4 Estimation of $OUR$ and $S_S$

In the aerobic tanks there are measurements of oxygen in all of them. These tanks are also larger than the early anoxic tanks, which makes the variance of the measured input concentration have a relatively smaller effect. What contributes more is that oxygen mass transfer have a relatively large effect in the equations. A non stationary discrete Kalman filter (Lewis 1986), based on the Model (4.14) was implemented for the last reactor.  $\widehat{OUR}_8$  is shown in Figure 4.4(a). Estimates of  $S_{S:8}$  based on the method described in the introduction to this section using the estimated DO concentration, and with different values of  $\widehat{\gamma}_{XBH}$  are illustrated in Figure

4.4(b). The bias for the case with  $\hat{\gamma}_{X_{BH}} = \gamma_{X_{BH}}$  is mainly due to the neglect



(a) Estimation of  $OUR$  in the last aerobic tank.



(b)  $S_{S:8}$  (smooth) and its estimate  $\hat{S}_{S:8}$

Figure 4.4.

of nitrification/denitrification in the calculations. For  $\hat{\gamma}_{X_{BH}} = 1.1\gamma_{X_{BH}}$  this error is evened out. We can conclude that estimation errors may become large, especially if  $S_{S:8}$  is relatively large. There are also more possible model errors that has not been considered here, such as an erroneous  $K_L a$  function.

## 4.4 An EKF for the aerobic compartments

We are interested in estimating  $S_S$  and  $X_S$  in all the aerobic tanks. In the previous section, a method to estimate  $X_{BH}$  and  $\gamma_{X_{BH}}$  in the anoxic compartments, and  $S_S$  in one aerobic tank was presented. From the results we learn that the model is sensitive to errors in the parameter. Therefore, it is here considered to let also  $X_{BH}$  be an unknown concentration in the observer model. Examples of earlier developed extensive observers based on the ASM1 have been formulated by Benazzi *et al.* (2007) and Boulkroune *et al.* (2009). These are based on measurements in one aerobic tank, and although the bacterial biomass concentrations was assumed to be known, estimation of substrate from unknown inputs was not possible. The lesson of this is that more online measurements are necessary. Therefore an EKF based on several aerobic tanks in series is developed, which takes into account the estimated sludge concentrations from Section 4.2. The possibility of an HG-EKF or AG-EKF was considered, but was abandoned due to the difficulty to transform a model based on the complex ASM1 equations into an observable canonical form (this may not be possible at all). The performance of the filter based on two tanks is dependent of the real concentrations, and therefore a redefined model in which the last 40 % of the process contains three aerated tanks for one more measurement of oxygen is considered.

### 4.4.1 Observer model

First, a simplified tank model corresponding to the one in Section 3.5 is derived. The first simplification made is to exclude  $X_{BA}$ ,  $S_{NH}$  and  $S_{NO}$  from the state vector  $Z$ , and also the corresponding expressions in the function  $\xi$  involving these. Exclusion of the first two is motivated in Section 3.5. Exclusion of the last one is motivated by that  $S_{NO}$  enters the reactions as  $\frac{S_{NO}}{K_{NO}+S_{NO}} \frac{S_O}{K_{OH}+S_O}$ , and that  $S_{NO}$  is relatively small and  $S_O$  is relatively large. In the next step  $X_{BH}$  is removed from the state vector and substituted with  $\hat{X}_X \gamma_{X_{BH}}$  in the remaining equations (see Section 4.2). Note that these approximations are observer model errors.

The simplified state space model for aerobic reactor number  $i$  then becomes

$$\dot{\bar{Z}}_i = D_i(Q)(\bar{Z}_{i-1} - \bar{Z}_i) + \bar{\xi}(q_i, \bar{Z}_i, \hat{X}_{X:i}, \gamma_{X_{BH}}),$$

where

$$\bar{Z} = \begin{bmatrix} S_O \\ S_S \\ X_S \end{bmatrix}, \text{ and } \bar{\xi}(q, \bar{Z}, \hat{X}_X, \gamma_{X_{BH}}) = \begin{bmatrix} K_L a(q)(S_{O_{sat}} - S_O) - \frac{1-Y_H}{Y_H} \hat{\mu}_H \frac{S_S}{K_S+S_S} \frac{S_O}{K_{OH}+S_O} \hat{X}_X \gamma_{X_{BH}} \\ -\frac{1}{Y_H} \hat{\mu}_H \frac{S_S}{K_S+S_S} \frac{S_O}{K_{OH}+S_O} \hat{X}_X \gamma_{X_{BH}} + k_h \frac{X_S / \hat{X}_X \gamma_{X_{BH}}}{K_X + X_S / \hat{X}_X \gamma_{X_{BH}}} \frac{S_O}{K_{OH}+S_O} \hat{X}_X \gamma_{X_{BH}} \\ (1 - f_p) b_h \hat{X}_X \gamma_{X_{BH}} - k_h \frac{X_S / \hat{X}_X \gamma_{X_{BH}}}{K_X + X_S / \hat{X}_X \gamma_{X_{BH}}} \frac{S_O}{K_{OH}+S_O} \hat{X}_X \gamma_{X_{BH}} \end{bmatrix}.$$

A redefinition of the tank index set is made to simplify the extension to a model with more tanks. The new index set is  $I = \{d1, d2, t, 1, \dots, m\}$ , where  $m = 8$  in the original simulation model. A simplified model of the last  $n$  aerobic tanks in the ASP is formed by connecting the corresponding simplified tank models via the mass balance part. We say that the model is for  $n$  tanks, but it also involves inputs from Tank  $(m - n)$ . The input concentrations in  $S_S$ ,  $X_S$  and the parameter  $\gamma_{XBH}$  are unmeasurable. These cannot be modeled based on physical relationships, and are instead modeled as random walk processes. The state vector  $x$ , the input vector  $u$  and the process noise vector  $w$  for the observer model then become.

$$x = \begin{bmatrix} S_{S:m-n} \\ X_{S:m-n} \\ \gamma_{XBH} \\ \bar{Z}_{m+1-n} \\ \dots \\ \bar{Z}_m \end{bmatrix}, \quad u = \begin{bmatrix} Q \\ q_{m+1-n} \\ \dots \\ q_m \\ \hat{X}_{X:m+1-n} \\ \dots \\ \hat{X}_{X:m} \\ S_{O:m-n} \end{bmatrix}, \quad w = \begin{bmatrix} w_{X_S} \\ w_{S_S} \\ w_\gamma \\ w_{S_O} \\ 0 \\ \vdots \\ 0 \end{bmatrix} \quad (4.18)$$

The state equation in the observer model becomes

$$\dot{x} = \underbrace{\begin{bmatrix} 0 \\ 0 \\ 0 \\ D_{m+1-n}(Q)(\bar{Z}_{m-n} - \bar{Z}_{m+1-n}) + \bar{\xi}(q_{m+1-n}, \hat{X}_X, \bar{Z}_{m+1-n}, \gamma_{XBH}) \\ \dots \\ D_9(Q)(\bar{Z}_{m-1} - \bar{Z}_m) + \bar{\xi}(q_m, \hat{X}_X, \bar{Z}_m, \gamma_{XBH}) \end{bmatrix}}_{a(x,u,t)} + w.$$

Note, that  $S_{O:m-n}$  is a measured input and enters via  $\bar{Z}_{m-n}$ . The process noise covariance matrix  $R_1$  is chosen to be diagonal, and the upper first three elements on the diagonal belongs to the random walk processes and are design parameters. One could argue that the unknown inputs in  $S_S$  and  $X_S$  are correlated, and express this in  $R_1$ . This would work well for the data of the simulation case, but to be more general this have not been included. The value of the entry in  $R_1$  corresponding to the state  $S_{O:m+1-n}$  originates from noise in the measurement of  $S_{O:m-n}$ . If Tank  $(m - n)$  is aerated, this entry is  $D_{m+1-n}^2(Q)R_{S_O}$ , where  $R_{S_O}$  is the variance of the oxygen measurements, otherwise it is zero since the oxygen concentration in that tank then is identically zero, and this knowledge can be used instead of the measurement. The measurement equation becomes

$$y = \underbrace{\begin{bmatrix} S_{O:10-n} \\ \vdots \\ S_{O:9} \end{bmatrix}}_{c(x,u,t)} + v$$

The covariance of the measurement noise  $v$  is  $R_2 = I_{n \times n} R_{S_O}$ . The total observer

model becomes

$$\begin{cases} \dot{x} = a(x, u, t) + w \\ y = c(x, u, t) + v \end{cases}, \quad (4.19)$$

which is on the form (4.1) and the EKF given by Algorithm (2) can be applied directly to it.

#### 4.4.1.1 An extension of the observer model

According to Section 4.2, it is reasonable to assume that there is a correlation between the unknown input concentration  $X_S$  and  $TSS$  in the flow  $Q_{in}$ . The estimated variable  $\hat{X}_{in:m-n}$  introduced Section 4.2 is included as a state in the observer model and is considered as measurable. In the observer it is modeled as

$$\dot{\hat{X}}_{in:9-n} = w_{in},$$

where  $w_{in}$  is white noise with variance  $R_{1:in}$ . The new observer model becomes

$$\begin{cases} \dot{\bar{x}} = \bar{a}(\bar{x}, u, t) + \bar{w} \\ \bar{y} = \bar{c}(\bar{x}, u, t) + \bar{v} \end{cases} \quad (4.20)$$

, with

$$\bar{x} = \begin{bmatrix} x \\ \hat{X}_{in:m-n} \end{bmatrix}, \quad \bar{a}(\bar{x}, u, t) = \begin{bmatrix} a(x, u, t) \\ 0 \end{bmatrix}, \quad \bar{w} = \begin{bmatrix} w \\ w_{in} \end{bmatrix},$$

$$\bar{c}(\bar{x}, u, t) = \begin{bmatrix} c(x, u, t) \\ \hat{X}_{in:m-n} \end{bmatrix}, \quad \text{and } \bar{v} = \begin{bmatrix} v \\ v_{in} \end{bmatrix}.$$

The variance of  $v_{in}$  is  $R_{2:in}$  and the new measurement covariance matrix  $\bar{R}_2$  is diagonal and is defined implicitly. The correlation between  $X_{S:m-n}$  is included by choosing the entries in  $\bar{R}_1$  corresponding to  $E[w_{X_S} w_{in}^T]$  to a positive nonzero number. All the additional introduced variances are design variables.

#### 4.4.1.2 Inclusion of measurement noise in the air flow rates

The observers performance for noise disturbances in the measurements of the air flows will be investigated. The measurements of one of the flows -  $q$  are assumed to be described by  $q_m = q + w_m(q)$ , where  $w_m(q)$  is Gaussian white noise with variance  $R_m(q) = (0.1q)^2$ . The error introduced by the noise on the oxygen equation in the observer model is

$$e(w_m(q)) = (K_L a(q + w_m(q)) - K_L a(q))(S_{O_{sat}} - S_O).$$

The mean of  $e$  is

$$\mu_e(q) = E[e(w_m(q))] = \int_{-\infty}^{\infty} \frac{1}{\sqrt{2\pi R_m(q)}} e^{-\frac{w_m^2}{2R_m(q)}} e(q) dw_m = \quad (4.21)$$

$$k_1 e^{-k_2 q} (S_{O_{sat}} - S_O) (1 - e^{k_2^2 (0.1q)^2 / 2}).$$

The variance of  $e$  is

$$\sigma(q)^2 = E[(e(w_m(q)) - \mu_e(q))^2] = \int_{-\infty}^{\infty} \frac{1}{\sqrt{2\pi R_m(q)}} e^{-\frac{w_m^2}{2R_m(q)}} (e(w_m(q)) - \mu_e(q))^2 dw_m = (k_1(S_{O_{sat}} - S_O)e^{-k_2q})^2 e^{k_2^2(0.1q)^2} (e^{k_2^2(0.1q)^2} - 1).$$

Here, rules for expectation of random variables and the distribution of a normal random variable has been used (Miller and Childers 2004). For Tank  $i$ ,  $\delta_i(q_i)$  and  $\sigma_i(q_i)$  can be approximated by substituting  $q$  and  $S_O$  in Equations (4.21) and (4.22) with the measurement  $q_{m:i}$  and the DO setpoint. The approximated variance  $\hat{\mu}_{e:i}$  should be added to the diagonal entry in  $R_1$  in the observer model (4.19) corresponding to the oxygen concentration  $S_{O:i}$ . The approximated mean  $\hat{\mu}_{e:i}$  should be subtracted from corresponding oxygen equation in the state equation in the observers model.

## 4.4.2 Sensitivity analysis

Sensitivity of the estimated variables to parameter errors will be investigated. Let  $\theta_0$  be the vector of parameters in the simulation model and  $\theta$  the corresponding for the observer model. Let  $J$  be the vector of the actual values of the concentrations that are estimated by the EKF. Let  $\hat{J}$  be the estimate of  $J$  when  $\theta = \theta_0$ . Let  $\hat{J}_{i,j}(\theta_j)$  be the estimation of  $J_i$  as a function of the  $j$ :th parameter in  $\theta$ ,  $\theta_j$  with all other parameters in the observer fixed at  $\theta_0$ . The mean relative error in the estimation of concentration number  $i$  as a function of the relative error  $\Delta_j = (\theta_j - \theta_{0:j})/\theta_j$  in  $\theta_j$  is

$$e_{EKF,i,j}(\Delta_j) = \frac{\int_2^{14} \hat{J}_{i,j}((\Delta_j + 1)\theta_{0:j}) - \hat{J}_i dt}{\int_2^{14} \hat{J}_i dt}.$$

The integration is started 2 days after the startup of the filter to let it settle. A linear approximation of the function is  $k_{i,j} \cdot \Delta_j$ , where

$$\begin{aligned} k_{i,j} &= \frac{\partial e_{EKF,i,j}}{\partial \Delta_j} \Big|_{\Delta_j=0} = 1 / \left( \frac{d\Delta_j}{d\theta_j} \right) \frac{\partial e_{EKF,i,j}}{\partial \theta_j} \Big|_{\theta_j=\theta_{0:j}} = \\ &\theta_{0:j} \cdot \frac{\partial}{\partial \theta_j} \left( \frac{\int_2^{14} \hat{J}_{i,j}((\theta_j) - \hat{J}_i dt)}{\int_2^{14} \hat{J}_i dt} \right) \Big|_{\theta_j=\theta_{0:j}} \approx \\ &\frac{\int_2^{14} \hat{J}_{i,j}(1.1\theta_{0:j}) - \hat{J}_i + \hat{J}_{i,j}(0.9\theta_{0:j}) - \hat{J}_i dt}{0.2 \int_2^{14} \hat{J}_i dt} = \hat{k}_{i,j}. \end{aligned}$$

We have the approximate error function

$$\hat{e}_{EKF,i,j}(\Delta_j) = \hat{k}_{i,j} \cdot \Delta_j.$$

## 4.4.3 Simulation with one and two tanks

Here, the division of the AS basin is that described in Section 3.1. The EKF was implemented as a continuous S-function in Simulink. In the case study in Section

3.7, the correlation between variations in  $\hat{X}_{in}$  and  $X_S$  is strong, but how strong this is in reality is more hypothetical, and therefore in simulation, the extension of the observer model described in Section 4.4.1.1 is evaluated separately. The possibility to implement the observer with the Runge Kutta 4 method, and to include noise in the air flow rate measurements is also investigated separately. In all simulations, the initial guess  $\hat{x}_0$  is 1.6 times the true initial state  $x_0$  and the initial error covariance is chosen in accordance with this. The values  $1.4 \cdot 10^7$ ,  $5 \cdot 10^5$  and 0.3 are chosen for the variances of the noises  $w_{S_S}$ ,  $w_{X_S}$  and  $w_\gamma$  respectively.

#### 4.4.3.1 Simulation with the basic observer model

In the case with one reactor, the observer diverges. Simulation results of the observer with two tanks is presented in Figure 4.5 together with the corresponding variables in the simulation model. For  $X_S$  and  $X_{BH}$  the estimates are only shown for one tank - Tank 7, since  $X_S$  and  $X_{BH}$  are mainly affected by massbalances.  $\hat{X}_{BH:7}$  is calculated using the Model (4.10).  $X_{BH:7}$  and  $\gamma_{X_{BH}}$  are shown for a longer period due to their slower variation. The estimated  $S_S$  states are close to unbiased, and  $\hat{X}_{S:7}$  is good but a bit slow.  $\hat{\gamma}_{X_{BH:7}}$  is quite biased. The biases in the estimates are due to the errors introduced when neglecting nitrification and denitrification in the derivation of the observer model. The observer model performs well for the simulation case, but there are choices of simulation data for which the quality of the estimates is poor. The performance of the filter is namely dependent on large enough variations in the actual input concentrations, both in frequency and in amplitude. It is especially sensitive to variations in the input  $S_S$  concentration, though one large peak a day seem to be enough for good estimates. If the variation is not large enough, the estimate errors may become large, at least for periods of time. One extreme case is when all concentrations in the simulation model are set to constants and the only real variable that varies is the noise in the oxygen measurements. Simulation result for  $S_{S:6}$  for this case is illustrated in Figure 4.6. The quality of the estimates is also somewhat dependent on the phase between the input in  $S_S$  and  $X_S$ .

#### 4.4.3.2 Observability

To explain some of the properties of the observer, observability was investigated for the system. The variables in the simulation model were sampled once an hour during the second day and observability of the observer model (4.19) was investigated for each sample point. For none of the points could locally weakly observability be confirmed for the model based on one tank, while this was confirmed for all of the sampled points for the model based on two tanks. This is not in contradiction with the restriction on concentration variations, the EKF is not an optimal filter.

Stationary, close to a point, we would expect the EKF to behave as a Kalman filter based on the linearization of the observer model around that point. Therefore, intuitively observability or detectability of linearizations of the observer model should

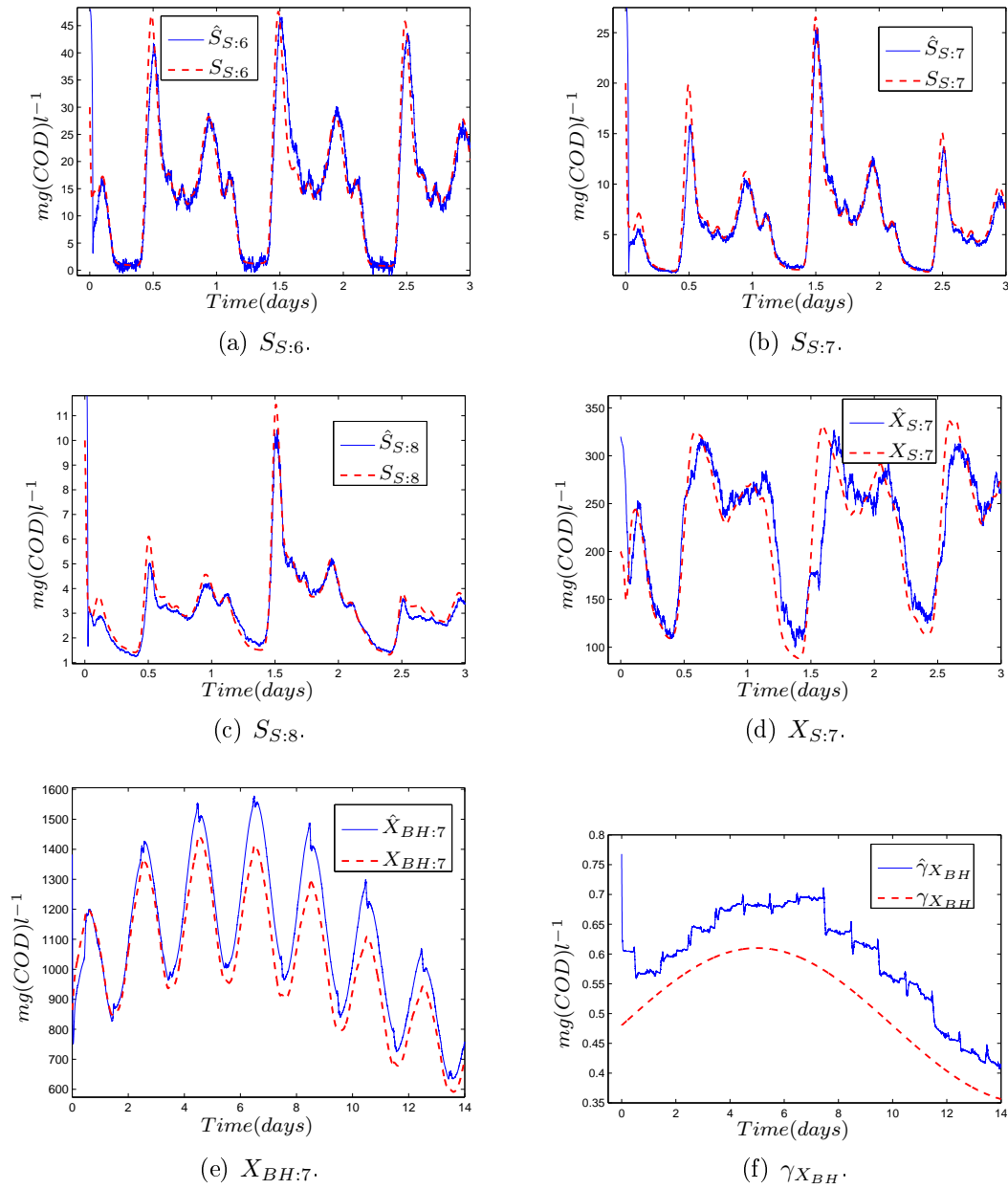


Figure 4.5. Estimates of the EKF for two tanks.

be an important property for the performance of the filter. This was investigated for the sampled points by solving the Riccati equation together with Theorem (2). Neither the linearizations of the observer model for one or that for two tanks were observable, and not even detectable. The results for the observer model based on one tank is in accordance with the corresponding filter being divergent.

The case with two tanks is now considered in more detail. A transformation of the linearized systems into a staircase form yielded that the eigenvalue of nondetectable mode was zero. The relative dependency defined in Section 4.1.1.1 to the undetectable mode of the concentrations as a function of time (the sampled points)

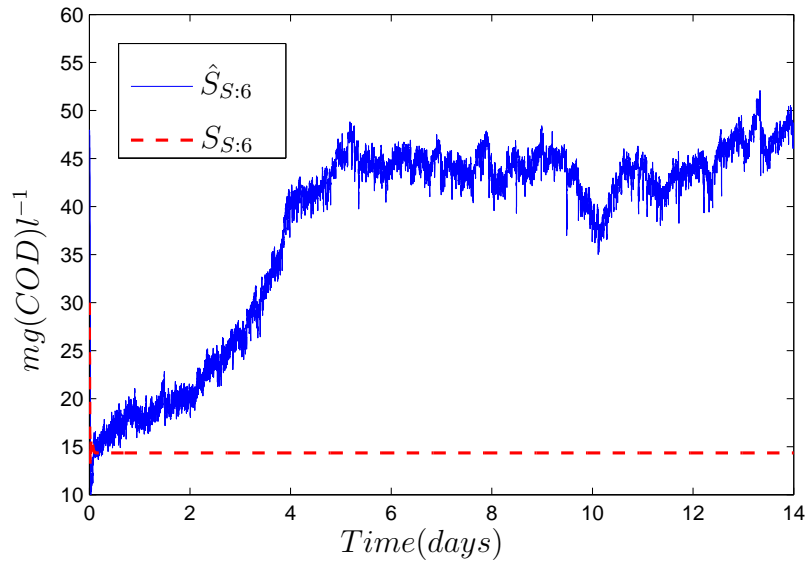


Figure 4.6. Estimation of  $S_{S:6}$  when all concentrations are set to constants.

is illustrated in Figure 4.7. As seen the dependency of this is relatively large, es-

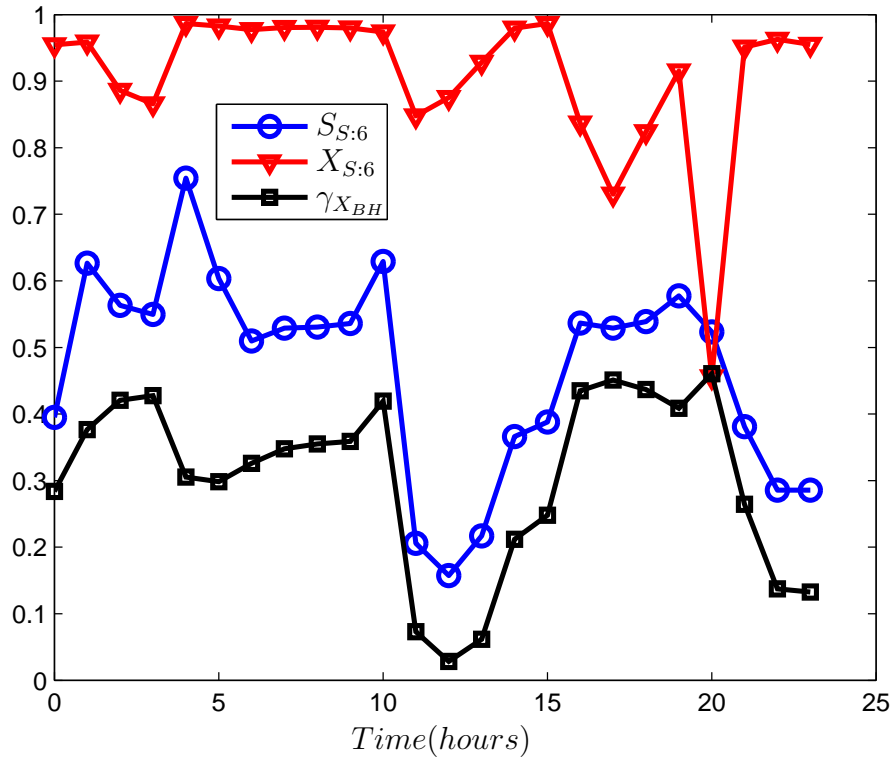


Figure 4.7. Relative dependency of the non detectable mode in linearizations of the observer model around the true states.

pecially for  $X_S$ , and it is surprising that the filter is convergent even for the data

in the simulation case. In Figure 4.8 the same dependency is illustrated, but for when the linearizations are around the estimates of the EKF instead of the real variables. Interesting enough, the relative dependencies of the undetectable mode

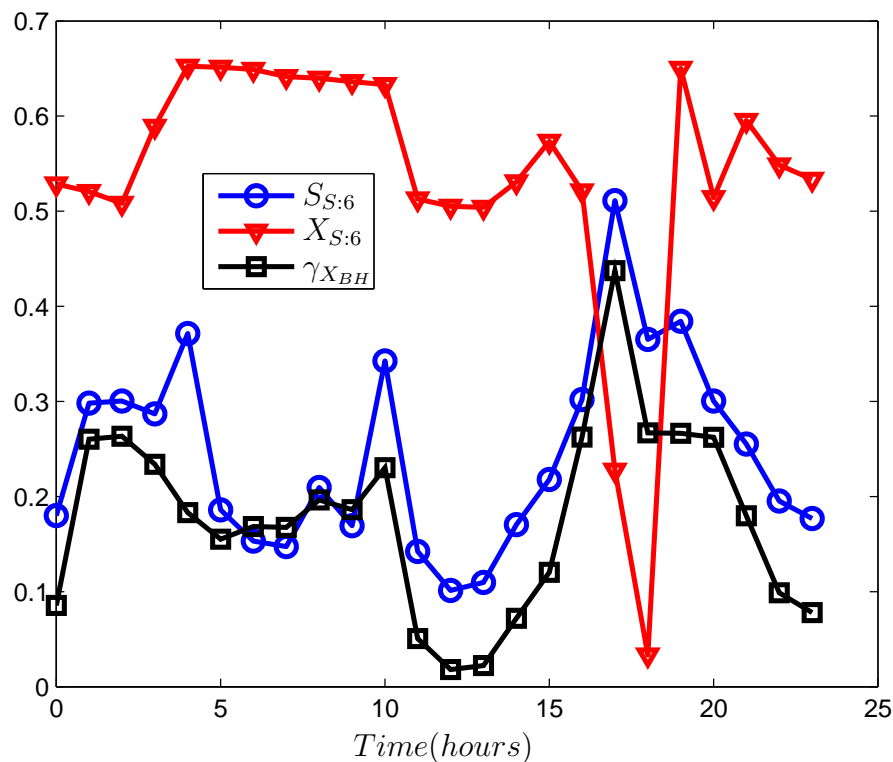


Figure 4.8. Relative dependency of the non detectable mode in linearizations of the observer model around the estimates of the EKF.

are smaller then. The aim of this investigation was really to show that each state in the observer model is little dependent of the undetectable mode in the linearization for some period of each day in the case study. This to further suggest that as long the concentrations varies with a large enough amplitude and frequency, all states are close to observable often enough in the linearizations to make the estimates non divergent. Clearly, none of this holds, and the reason for the variation dependency of the filter cannot be explained in this way.  $X_{S:s}$  larger relative dependency to the undetectable mode can possibly explain its slower convergence.

#### 4.4.3.3 Correlation included

In Figure 4.9  $X_{S_6}$  and  $\hat{X}_{in}$  are illustrated. In Figure 4.10, the estimation of  $X_{S:6}$  for the EKF for two tanks with the extension described in Section 4.4.1.1 is illustrated. Also shown is the corresponding estimate of the original EKF and the real concentration. As seen, the estimate of the first one is faster. The estimation of this is however sensitive to a reasonable choice of the covariance  $E[w_{X_S}w_{in}]$ . If this is

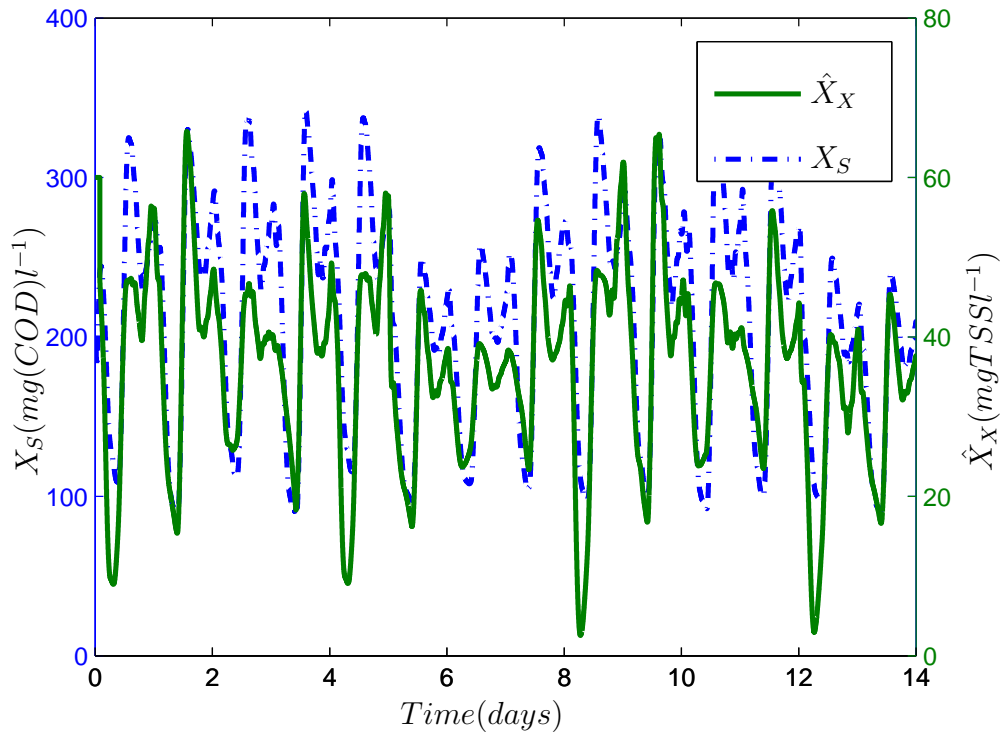


Figure 4.9.

chosen too large, the estimation error of all estimates may become large. The value used here is 500. The variance of the "measured"  $\hat{X}_{in}$  is very small, and the choice of  $E[v_{in}^2]$  can be chosen as an arbitrarily small value, but  $\hat{R}_1$  needs to be invertible.

#### 4.4.3.4 Additional process noise and implementation of the EKF

Here, the addition of measurement noise in the air flows described in Section 4.4.1.2 is included. The possibility to implement the EKF with the Runge Kutta 4 method described in Section 4.1.4 is also investigated. In Simulink, this is solved by using an S-function with discrete states, that in the beginning of each sampling period goes through the Algorithm 3. Discrete PI controllers are here used for oxygen reference control with the same sampling time. The performance of the filter is illustrated in Figure 4.11 for some of the concentrations. The sampling time used here is 0.5 minutes. As seen, the result is equivalent to that in Section 4.4.3.1 for the original observer model.

#### 4.4.3.5 Sensitivity to parameter errors

When investigating the sensitivity of the EKF to parameter errors we only consider those parameters that may be of significant importance. The  $X_S$  concentrations

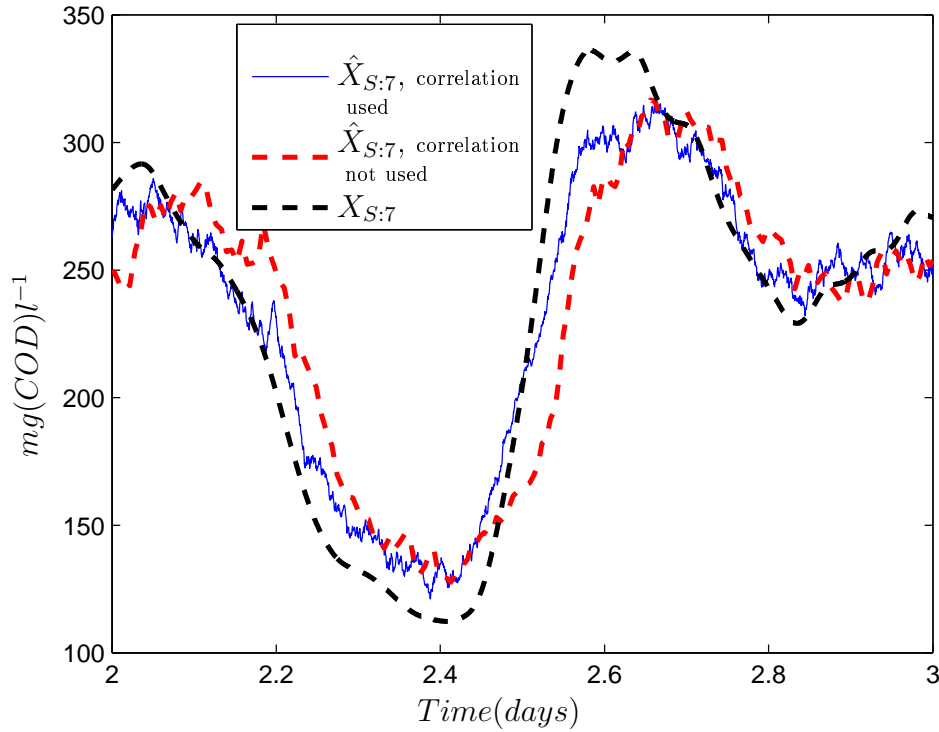


Figure 4.10. Inclusion of a correllation between  $\hat{X}_{in}$  and  $X_S$  in the observer model.

are mainly driven by mass balances, and since  $f_P$  and  $b_h$  only have minor affect in the equations describing these, they are excluded from the simulation. Nor is the parameter  $K_{OH}$  considered, this since the Monod expression in oxygen is saturated for the setpoint oxygen concentration in this simulation case. For the  $K_{La}$  function we only consider errors in the  $k_1$  - parameters since results for errors in the  $k_2$  - parameters are difficult to interpret. The vector of investigated parameters is defined by

$$\theta_0 = [ k_{1:7} \quad k_{1:8} \quad V_7 \quad V_8 \quad S_{O_{sat}} \quad k_h \quad K_S \quad K_X \quad \hat{\mu}_H \quad Y_H ] .$$

The EKF was simulated for the different parameter errors and the approximation of the defined sensitivity measure  $\hat{k}_{i,j}$  is shown in Table 4.1 for some of the estimated concentrations. As an example on how to interpret the sensitivity measure, the error in  $\hat{S}_{S:6}$  due a 20% error in  $S_{O_{sat}}$  is approximately  $20 \cdot 0.14$  %. The  $X_S$  and  $X_{BH}$  concentrations are so dominantly driven by mass balances that we can expect the error to be the same for all tanks. The result is therefore presented simply for  $X_S$  and  $X_{BH}$ , but was calculated for Tank 7.

*During this simulation autotrophs and nitrate was precluded from the aerobic tanks in the simulation model. It was later decided to change this, but this simulation is very time consuming and have not been repeated.*

Errors in the volumes and  $K_S$  seem to have minor affect, which is a little surprising

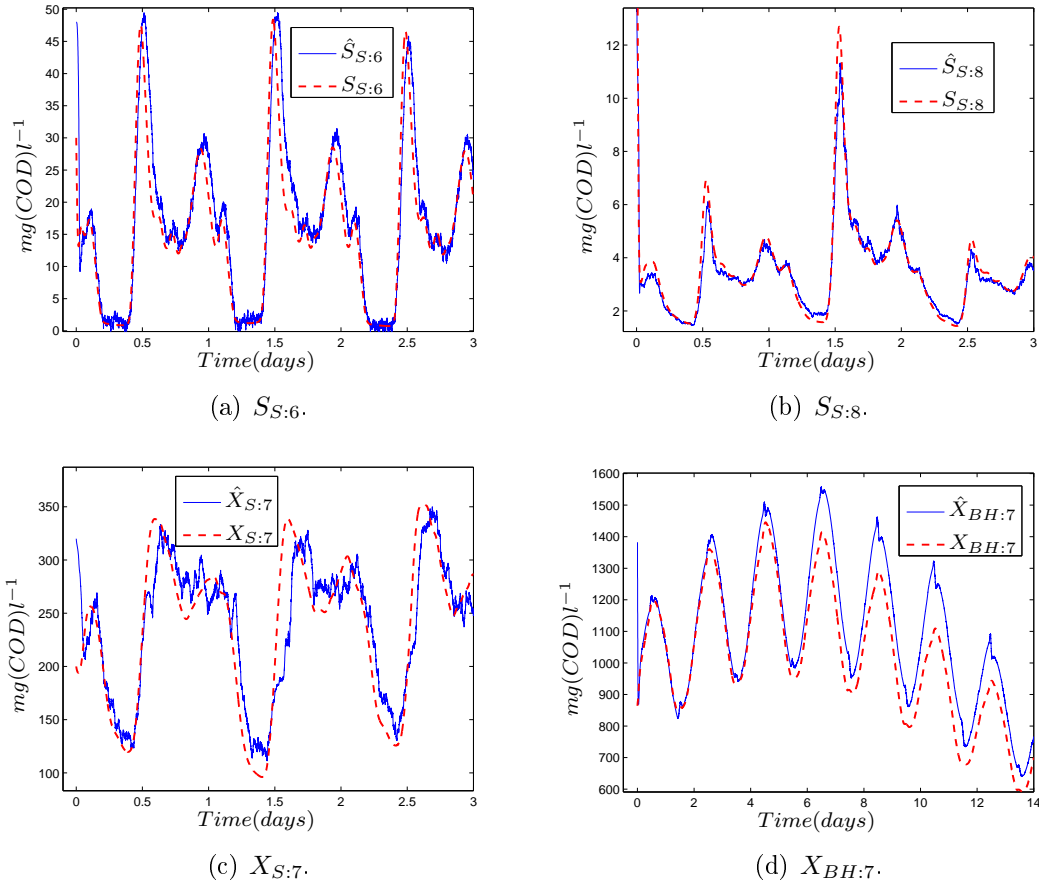


Figure 4.11. The EKF implemented with the Runge Kutta 4 method and with additional process noise.

Table 4.1. Sensitivity ( $\hat{k}_{i,j}$ ) of the estimates w.r.t the parameters in the observer.

	$\hat{S}_{S:6}$	$\hat{S}_{S:7}$	$\hat{S}_{S:8}$	$\hat{X}_S$	$\hat{X}_{BH}$
$k_{17}$	0.1342	-0.1028	-0.2756	-0.2614	0.1332
$k_{18}$	-0.0305	0.1424	0.2520	0.2979	-0.0513
$V_7$	0.0855	-0.0038	-0.0377	-0.0421	0.0195
$V_8$	0.0160	0.0466	0.0308	0.0340	-0.0200
$S_{O_{sat}}$	0.1391	0.0626	-0.0049	0.0926	0.1042
$k_h$	-0.0265	-0.0289	-0.0201	-0.1798	0.0119
$K_S$	0.0139	0.0291	0.0450	-0.0304	0.0217
$K_X$	0.0089	0.0100	0.0069	0.0773	-0.0041
$\mu_H$	0.0215	0.0253	0.0163	0.0946	-0.0962
$Y_H$	0.1112	0.0674	0.0416	0.1370	0.2321

for the latter one.  $\hat{X}_S$  is quite sensitive to all other parameters.  $\hat{S}_{S:6}$  and  $\hat{X}_{BH}$  are quite sensitive to  $Y_H$ , but this is a stoichiometric parameter, and these are often quite well known. All estimates are especially sensitive to errors in the  $K_{La}$  function, but  $X_{BH}$  less than the others. The estimation result for an error only in  $K_{1:8}$  of 10% is given in Figure 4.12 for some of the concentrations. As seen, the

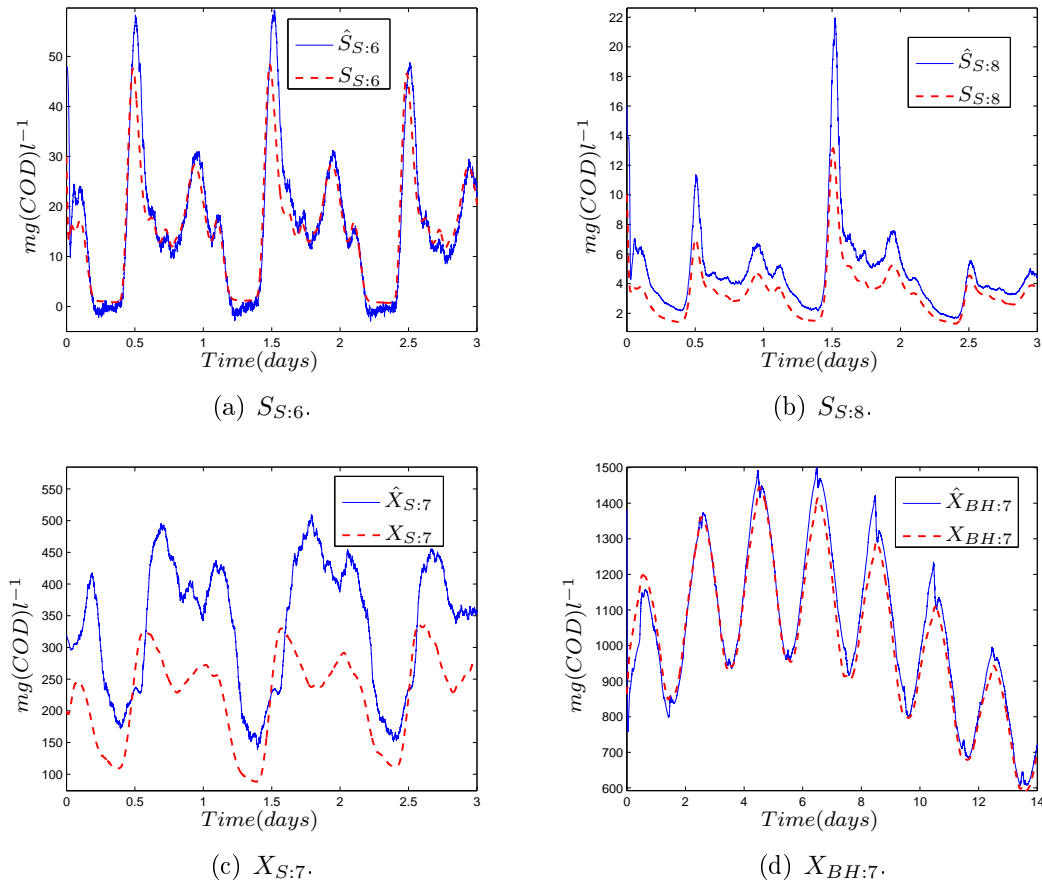


Figure 4.12. Result for the EKF for a 10% error in  $k_{1,8}$ .

error in the estimates increases nonlinearly with the amplitude of the corresponding concentrations, which has its origin in the nonlinear Monod expressions. This error in the parameter happens to have a positive effect on  $X_{BH}$ , compare to Figure 4.5. The reason is that it evens out the effect of neglecting nitrification and denitrification in the observer model. The difference between errors in the  $K_La$  function and other parameter errors is that the latter are the same in the two tank models. It is actually the case that as long as the error in the  $k_1$  parameters are the same for both tanks, then  $X_S$  and the  $S_S$  states are not much affected.  $X_{BH}$ , however, seem to be somewhat more sensitive to this condition. The result for a 10 % error in both these parameters is illustrated in Figure 4.13. This is fortunate since the real  $K_La$  function might be the same for all the tanks or at least related by their physical description. Unfortunately, this does not hold if we consider errors in the  $k_2$  parameters, since the error in  $K_La$  is then nonlinear w.r.t. the air flows.

#### 4.4.4 Simulation results for the observer based on three tanks

The EKF based on two tanks has some undesirable properties. Even though, the input concentrations to a WWTP often follows a daily rhythm, and often with a

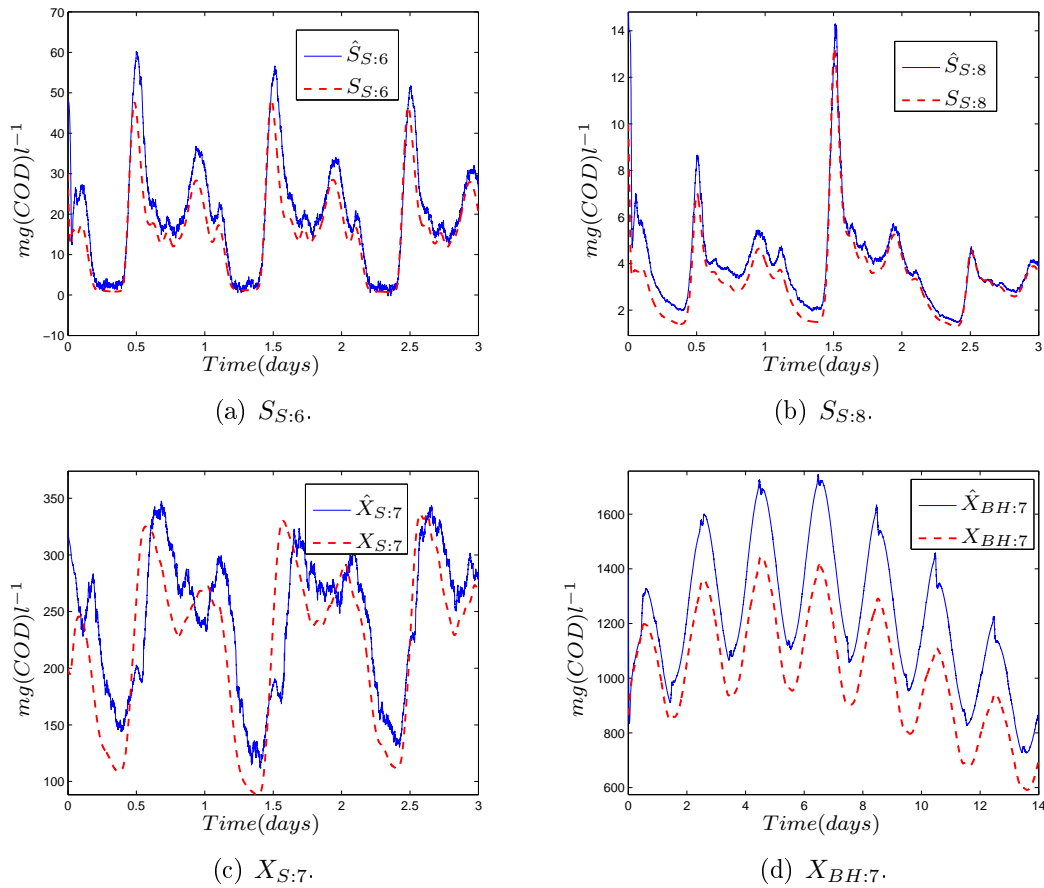


Figure 4.13. Result for the EKF for a 10% error in both  $k_1$  parameters.

large peak each day, the property that the quality of the estimates depends on variations in the actual concentrations is severe. A filter which is less sensitive to errors in the  $K_L a$  parameters is also desirable. For that reason an altered model is introduced including 9 tanks of whom the last three are aerated. The hypothesis is that an additional measurement, will lead to better observability properties and less sensitivity to variations in concentrations, and parameter errors. The volume of the AS basin corresponding to the last two tanks is redefined to be described by three tanks of equal size. To show the power of the way  $X_{BH}$  is modeled, we also make a small redefinition of the simulation case. The TSS concentration in  $Q_X$  is set to a constant value while the flows  $Q_{in}$  and  $Q_{rec}$  are set to vary stepwise, periodically and synchronically, both between  $3m^3s^{-1}$  to  $4m^3s^{-1}$ . The flow  $Q_X$  is set to  $3m^3s^{-1}$ . It is also more natural with variations in the influent flows than in TSS in  $Q_X$ . The other concentrations in the influents are unchanged while they may differ somewhat in the point 1 in Figure 3.2 and in the rest of the AS basin because of the variation in  $X_{BH}$ . The same initial condions and variances as in the previous section are used here.

#### 4.4.4.1 Simulation of the basic observer model

In Figure 4.14(a) the estimated  $X_{BH:7}$  is illustrated. As seen, the way it is modeled, it is possible to handle stepwise changes in it. To clarify this result even more, in Figure 4.14(b)  $\hat{X}_{BH:7}$  is shown again for when nitrification and denitrification are precluded from the aerobic tanks. The result for the rest of the concentrations is

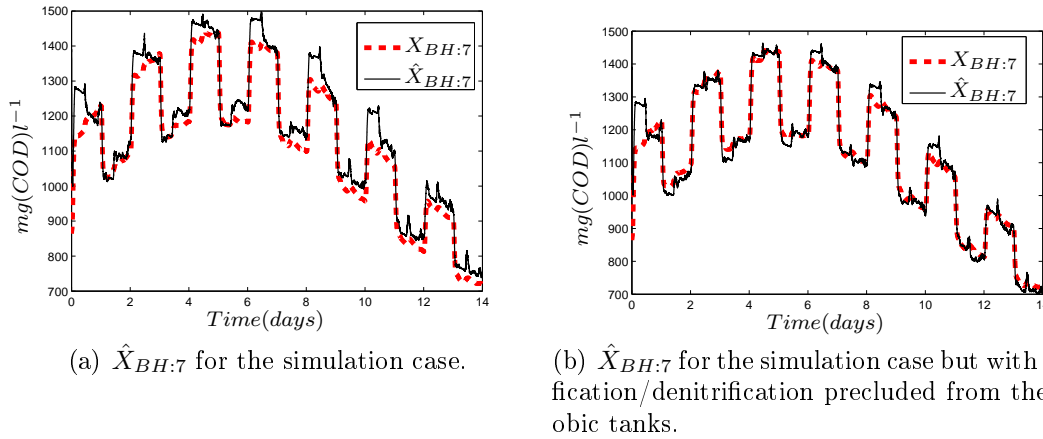


Figure 4.14. Estimation  $X_{BH:7}$ .

equivalent to that with 2 tanks regarding the case study, but the estimation of  $X_S$  is somewhat faster. The main advantage of this filter shows when different simulation data is considered. There are now no restrictions on variations in the concentrations. This is illustrated in Figure 4.15 for when the concentrations in the influents are set to constants (compare to Section 4.4.3.1 and Figure 4.6).

#### 4.4.4.2 Observability

As with the case with two tanks, the concentrations in the simulation model were sampled once an hour during the second day, and observability of the system was investigated. Because of a high dimension of the observer model, it was not possible to directly confirm locally weak observability. But both the model of Tank 7 and 8, and the model of Tank 8 and 9 are locally weakly observable, and from this it follows that the total model of the three tanks must be locally weakly observable. Regarding observability, the advantage of introducing an additional tank in the model is that it could be confirmed for the linearizations of the observer around the sampled points. This helps to explain why this filter don not need variations in the concentrations as was the case with two tanks.

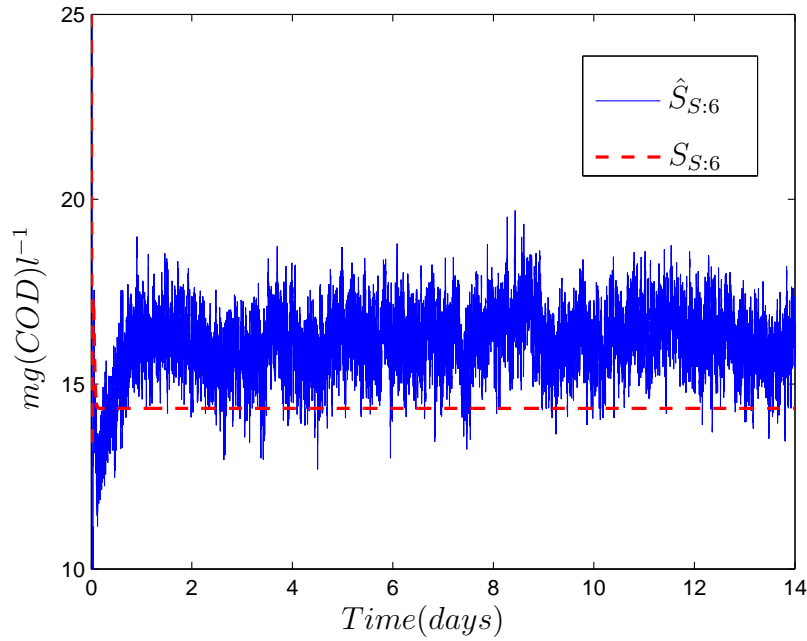


Figure 4.15. Estimation of  $S_{S:6}$  when all concentrations are set to constant.

#### 4.4.4.3 Sensitivity to parameter errors

Sensitivity to parameters was investigated for the corresponding set of parameters and concentrations as in Section 4.4.3.5. The parameter vector is

$$\theta_0 = [ k_{1:7} \quad k_{1:8} \quad k_{1:9} \quad V_7 \quad V_8 \quad V_9 \quad S_{O_{sat}} \quad k_h \quad K_S \quad K_X \quad \hat{\mu}_H \quad Y_H ],$$

and the sensitivity measure  $\hat{k}_{i,j}$  is illustrated for some of the concentrations in Table 4.2. Compared to the result in Section 4.4.3.5, in this case nitrification and denitri-

Table 4.2. Sensitivity ( $\hat{k}_{i,j}$ ) of the estimates w.r.t the parameters in the observer.

	$\hat{S}_{S:6}$	$\hat{S}_{S:7}$	$\hat{S}_{S:8}$	$\hat{S}_{S:9}$	$\hat{X}_{S:7}$	$\hat{X}_{BH:7}$
$k_{1:7}$	0.0596	-0.1338	-0.2567	-0.2764	-0.1962	0.1428
$k_{1:8}$	0.2479	0.4145	0.3991	0.3048	0.1275	-0.2632
$k_{1:9}$	-0.1454	-0.1304	-0.0402	0.0395	0.1562	0.0600
$V_7$	0.0609	-0.0214	-0.0481	-0.0530	-0.0360	0.0261
$V_8$	0.0268	0.0514	0.0278	0.0294	0.0245	-0.0183
$V_9$	-0.0075	-0.0044	0.0046	-0.0033	0.0124	0.0023
$S_{O_{sat}}$	-0.0169	-0.0171	-0.0125	-0.0069	-0.0026	0.0002
$k_h$	-0.0202	-0.0205	-0.0148	-0.0085	-0.1977	0.0045
$K_S$	0.0191	0.0338	0.0500	0.0570	-0.0329	0.0171
$K_X$	0.0073	0.0082	0.0069	0.0044	0.0768	-0.0017
$\mu_H$	0.0140	0.0160	0.0126	0.0068	0.1127	-0.0870
$Y_H$	0.1134	0.0772	0.0483	0.0418	0.1226	0.2326

fication was included in the aerobic tanks. That is the reason why the  $S_S$  estimates here shows even more sensitivity to errors in the  $K_La$  parameters than for the case with two tanks. Also in this case all the estimates except for  $\hat{X}_{BH}$  are little affected by errors in the  $k_1$  parameters as long as these are the same.  $\hat{X}_S$  is also in general less sensitive to errors in  $K_La$ . To conclude, the total benefit regarding sensitivity of introducing an additional tank was at most minor.

#### 4.4.5 Additional results

Several EKF:s based on predecessors to the observer model (4.19) has been investigated. Initially it was considered to model  $X_{BH}$  just as  $S_S$  and  $X_S$  with an unknown input, modeled as a random walk process, and with separate states for each reactor, i.e. the parameter  $\gamma_{X_{BH}}$  was not included in the model. This was not suitable for the case with two tanks, since only very slow variations in the concentration could be assumed. It may work better with three tanks. In the next development,  $X_{BH}$  was only described with  $\gamma_{X_{BH}}$  and  $\hat{X}_X$  in the input to the first tank in the observer model, and with separate states for the rest of the tanks. This solution is somewhat more accurate since growth and decay of biomass in the tanks in the observer is included. The reason for the different modeling in the observer model (4.19) was to decrease the dimension of it, since problems with a high dimension of the predecessor made it difficult to analyze observability/detectability properties.

In the choice of the process covariance matrix in Section 4.4.1 model errors were not considered. The reason for this is that such errors leads to disturbances that are non white, but rather constant for periods of time, and are not well described by white noise. However, such disturbances can be described by a random walk process in an observer model. Introducing such models will give worse observability properties of the system though. For the case with an observer model with two tanks this possibility was investigated. The result was a diverging filter.

### 4.5 Estimation of the $K_La$ function

In the observers described in Sections 4.3 and 4.4 the  $K_La$  function was assumed to be known. Here methods to estimate it are evaluated and further developed. The oxygen equation including  $K_La$  model (3.2) is repeated below.

$$\dot{S}_O = \frac{Q}{V}(S_{O_{in}} - S_O) + \underbrace{k_1(1 - e^{-k_2q})}_{K_La(q)}(S_{O_{sat}} - S_O) - OUR \quad (4.22)$$

The parameters describing the  $K_La$  function are known to be time varying, and therefore, ideally these should be estimated on a continuous basis. When estimating it with only oxygen measurements at hand, it is however necessary to excite the air flow (Lindberg 1997), which is costly. One example of an estimation method in which this is not necessary has been found in the literature (Soons *et al.* 2008). This

is for an application to biopharmaceutical production, and offline measurements of bacterial biomass concentration is taken into account in the estimation algorithm. Measurements of bacterial biomass are not available at WWTP:s and it would most likely be necessary to also include offline measurements of substrate concentration for this to be useful.

If it is necessary to estimate the function on a continuous basis, one would like to vary the air flow with as small amplitude as possible for low cost. Olsson and Newell (1999) described a dual controller with two purposes: to control the oxygen concentration and to make it oscillate. The estimation algorithm was not stated, but has been evaluated on a real plant with success. The DO concentration was held within  $reference \pm 0.2 mg O_2 l^{-1}$ . With larger excitation, better accuracy could be achieved. This small excitation of the oxygen concentration does not make sense for Ryaverket since the concentration normally vary way more even within the tanks. Also, a small variation in the DO concentration does not really imply a small amplitude of the variation in the air flow.

Methods described in the literature, that are reasonable consider for the Ryaverket are:

- ON/OFF control in which the air flow is changed stepwise to change the number of unknowns in Equation (4.22) (Suescun *et al.* 1998).
- Excitation of the air flow with different frequencies and estimation with either an EKF or some system identification method (Lindberg 1997).

In both of these methods quite large excitation is necessary.

The parameters in the  $K_L a$  function have shown to not be very unique, i.e. the estimated parameters may deviate much from the true ones, while the corresponding estimated function still is a good approximation. For that reason the following error criteria is used to describe the quality of the estimates

$$e_{K_L a} = \frac{\int_0^{q_{max}} (K_L a(q) - \widehat{K_L a}(q)) dq}{\int_0^{q_{max}} (K_L a(q)) dq}. \quad (4.23)$$

$\widehat{K_L a}(q)$  is the Function (3.2) with estimated parameters  $\hat{k}_1$  and  $\hat{k}_2$  inserted.

### 4.5.1 DO observer

Industrial DO-sensors traditionally have had dynamics which cannot be neglected in an estimation problem since they are slow to be robust (Lindberg 1997). Lindberg (1997) used a filter to compensate for the dynamics before estimating the  $K_L a$  function. The DO-sensors at Ryaverket are quite new and does not have the kind of dynamics as traditional, but to reduce noise it is possible to let the sensor output be

the mean of the last  $T$  seconds. At Ryaverket the time span  $T$  is set to 60 seconds. A mean for the last 30 seconds is also taken when the data reaches the central data system. Neglecting measurement noise, the mean value formed DO -  $y_m$  is described by the filter

$$y_m(t) = \frac{1}{30} \int_{t-30}^t \left( \frac{1}{60} \int_{\tau-60}^{\tau} y(\rho) d\rho \right) d\tau,$$

where  $y$  is the true DO. For a constant slope  $k_0$  starting at time  $t_0$ , and after 90 seconds we have

$$y_m(t) = y(t_0) + k_0(t - 45). \quad (4.24)$$

For infrequent and small changes, the filter is thus mainly a time delay. Therefore this has not been considered in the designs in Section 4.3 and 4.4. When exciting the air flow heavily this might however not be negligible. A discrete model for  $y_m$  with sampling time  $h$  is given below

$$y_m(n) = \frac{1}{n_1 n_2} \sum_{i=n-n_2+1}^n \left( \sum_{k=i-n_1+1}^i y(k) \right) + \underbrace{\frac{1}{n_1 n_2} \sum_{i=n-n_2+1}^n \left( \sum_{k=i-n_1+1}^i v(k) \right)}_{V(n)}, \quad (4.25)$$

where  $n_2 h = 30$  and  $n_1 h = 60$  and  $v$  is (presumably) white noise with variance  $r_2$ . When designing a Kalman filter one usually makes the assumption that the measurement noise is white.  $V$  is certainly not white but we know its function of  $v$ . There are two alternatives

- Use a Kalman filter including a whitening filter, i.e. include the model of  $V$  in the Kalman filter, and introduce states for the noise terms  $v(k)$ .
- Neglect the non whiteness of  $V$ , and design a Kalman filter without a whitening filter.

To estimate  $y$  a drifting model of it is needed. Here the random walk model

$$y(n+1) = y(n) + w(n)$$

is used.  $w$  is white noise with variance  $R_1$  (a design parameter). To avoid a large filter it can be designed with a longer sampling time  $h^*$  with corresponding  $n_1^*$  and  $n_2^*$ . For the case without a whitening filter, a suitable observer model is

$$\left\{ \begin{array}{l} x(n+1) = \begin{bmatrix} 1 & 0 & \dots & 0 \\ & \dots & & \dots \\ & I_{(n_1^*+n_2^*-1)} & & 0 \end{bmatrix} x(n) + \begin{bmatrix} 1 \\ 0 \\ \dots \\ 0 \end{bmatrix} w(n) \\ y_m(n) = \frac{1}{n_1^* n_2^*} \begin{bmatrix} 1 & \dots & n_2^* - 1 & \underbrace{n_2^* \dots n_2^*}_{n_1^* - n_2^* + 1 \text{ elements}} & n_2^* - 1 & \dots & 1 \end{bmatrix} x(n) + V(n) \end{array} \right. , \quad (4.26)$$

where the state vector is

$$x(n) = [y(n), \dots, y(n - n_1^* - n_2^* + 1)]^T. \quad (4.27)$$

It is possible to derive an exact expression of the autocovariance of  $V - R_2 = E[V(k)^2]$  as a function of  $r_2$ , the variance of  $v$ . This is however unnecessary since we can assume a value for it and relate  $R_1$  to this. The Kalman filter gives an estimate  $\hat{x}(n|n)$ , which is the optimal estimate of  $x$  at time  $nh^*$  based on measurements up to the same time. The  $i$ :th value in  $\hat{x}(n|n)$  is then  $\hat{y}(n - i + 1|n)$ , which is the best estimate of  $y$  at time  $(n - i + 1)h^*$  given measurements up to time  $nh^*$ . With larger  $i$ , the better the estimate is, but choosing  $i \geq 2$  for the filter output of course gives a delay of  $ih^*$  seconds.

#### 4.5.1.1 Simulation

It is assumed that the sampling time of the sensor system is  $h = 1s$ . The sampling time  $h^*$  was chosen to be  $5s$ , which gives  $n_1^* = 12$ , and  $n_2^* = 6$ .  $r_2$  is assumed to have the same variance as for the sensors in the simulation case  $\frac{0.2^2}{h^*}$  (discrete time). A stationary Kalman filter is used here. The response to a step in  $y$  for  $y_m(n)$  and  $\hat{y}(n - i + 1|n)$  for  $i = 1$  and  $i = 18$  (the last element in  $\hat{x}(n|n)$ ) are shown in Figure 4.16. The time delay in the second case has been removed. The designed filter can reconstruct the step response well but the coloured noise in  $y_m$  is amplified. A Kalman filter including a whitening filter has been evaluated, but it did not improve the performance.

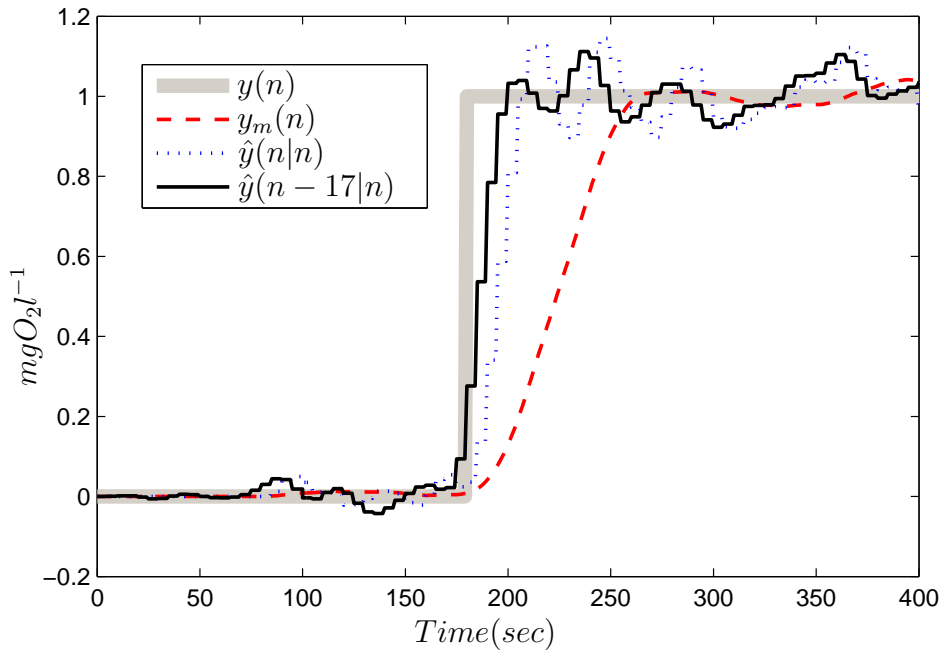


Figure 4.16. Estimation of the DO concentration from corrupted measurements.

## 4.5.2 Estimation with ON/OFF control

(Suescun *et al.* 1998) estimated  $OUR$  and  $K_La$  for a specific constant air flow by neglecting mass balances and turning the aeration between ON (constant air flow:  $q_0$ ) and OFF (zero air flow) stepwise. This variation of the air flow is here called ON/OFF control. When the aeration is turned to OFF, the only unknown in Equation (4.22) is  $OUR$  and can then be estimated from the slope of oxygen measurements. When the aeration is turned to ON, it is assumed that  $OUR$  is known and  $K_La(q_0)$  can be estimated as with  $OUR$ .

At Ryaverket, the water flow is relatively large, and it is therefore not reasonable to neglect mass balances in the estimation algorithm, and the above method should not be applied directly. Instead, they are estimated by minimizing the error between the measured DO concentration and the one in a model. The method is also extended to estimation of the parameters in the  $K_La$  function.

### 4.5.2.1 Estimation of $K_La$ for a specific air flow $\tilde{q}_0$

Here,  $K_La(\tilde{q}_0)$  is estimated with only one ON, and one OFF period, where  $\tilde{q}_0$  is the sample mean of the measured air flow. The experiment starts with an OFF period. Discrete time with sampling time  $h$  is used here. The time  $kh$  is shortened with the time index  $k$ .  $k \in [0, m]$  during the OFF period and  $k \in [m + 1, n]$  during the ON period. The measured DO is symbolized with  $S_{O_m}$ . Sample means of measurements are given with a tilde ( $\sim$ ) above, for example  $\tilde{S}_O$ .

**Estimation of  $OUR$**  Solving Equation (4.22) with the aeration turned off, and assuming that all variables except  $S_O$  in the considered tank are constant gives

$$S_O(k) = Ce^{-\frac{Q}{V}kh} + S_{O:in} - \frac{V}{Q}OUR, \quad k \in [0, m],$$

where  $C$  is an integration constant. Substituting  $S_O(k)$  with  $S_{O_m}(k)$ , and the variables in the right hand side of the equation with sample means we get

$$v(k) = f_1(k) = Ce^{-\frac{\tilde{Q}}{V}kh} + \tilde{S}_{O:in} - \frac{V}{\tilde{Q}}OUR - S_{O_m}(k),$$

where  $v(k)$  is measurement noise. If the mean is approximately zero, it follows that it is reasonable solve the following optimization problem for  $OUR$ :

$$\text{minimize} \quad \left( O_1 = \sum_{k=0}^m f_1(k)^2 \right) \quad \text{w.r.t.} \quad OUR, \quad C. \quad (4.28)$$

The value of  $OUR$  that minimizes the objective function  $O_1$  is taken as the estimate  $\widehat{OUR}$ . An important property of an optimization problem is convexity of the objective function, and is the criterion for convergence to the optimal value in many

optimization algorithms. See Andréasson *et al.* (2005) for a definition of convexity and related theorems. The optimization problem (4.28) is convex, since it is quadratic in  $OUR$  and  $C$ .

**Estimation of  $K_La(\tilde{q}_0)$**  At time  $k = m + 1$ , the aeration is turned to ON ( $q = q_0$ ). Note that  $q_0$  is the ordered air flow, while  $\tilde{q}_0$  is the estimate of the true air flow based on a mean value of measurements.  $OUR$  is assumed to be constant from the OFF period and the estimated value  $\widehat{OUR}$  is used here. With a derivation similar to that for  $OUR$ , an estimate  $\widehat{K_La_0}$  of  $K_La(\tilde{q}_0)$  is found by solving the following optimization problem

$$\text{minimize} \quad \left( O_2 = \sum_{k=0}^m f_2(k)^2 \right) \quad \text{w.r.t.} \quad K_La(\tilde{q}_0), \quad (4.29)$$

where

$$f_2(k) = C e^{-(K_La(\tilde{q}_0) + \frac{\tilde{Q}}{V})kh} + \frac{\frac{\tilde{Q}}{V} \tilde{S}_{O:in} + S_{O:sat} K_La(\tilde{q}_0) - \widehat{OUR}}{\frac{\tilde{Q}}{V} + K_La(\tilde{q}_0)} - S_{O_m}(k).$$

Convexity of this problem has not been confirmed.

#### 4.5.2.2 Estimation of the $K_La$ function

By successively turning the aeration between ON and OFF several times, and solving the problems (4.28) and (4.29), we get a series of estimated values of the  $K_La$  function for different air flows:

$$(\widehat{K_La_i}, q_i), \quad i \in [0, p]. \quad (4.30)$$

To extract as much as possible of the measurement data, the problem (4.29) should be solved twice for each ON period. One time with  $\widehat{OUR}$  from the previous OFF period, and one time with  $\widehat{OUR}$  from the following OFF period. To estimate the parameters in the function (3.2), the following optimization problem is solved

$$\text{minimize} \quad \left( O_2 = \sum_{i=0}^p f_3(i)^2 \right) \quad \text{w.r.t.} \quad k_1, k_2, \quad (4.31)$$

where

$$f_3(i) = k_1(1 - e^{k_2 q_i}) - \widehat{K_La_i}$$

This problem is convex. For a good estimate,  $p$  should be large, and as large difference between the smallest and the largest value in the series is desirable.

#### 4.5.2.3 Simulation

The experiment was carried out on Tank 8. In simulation, the DO concentration was varied between  $DO_{max} = 4mgO_2l^{-1}$  and  $DO_{min} = 2mgO_2l^{-1}$ . The  $DO_{min}$

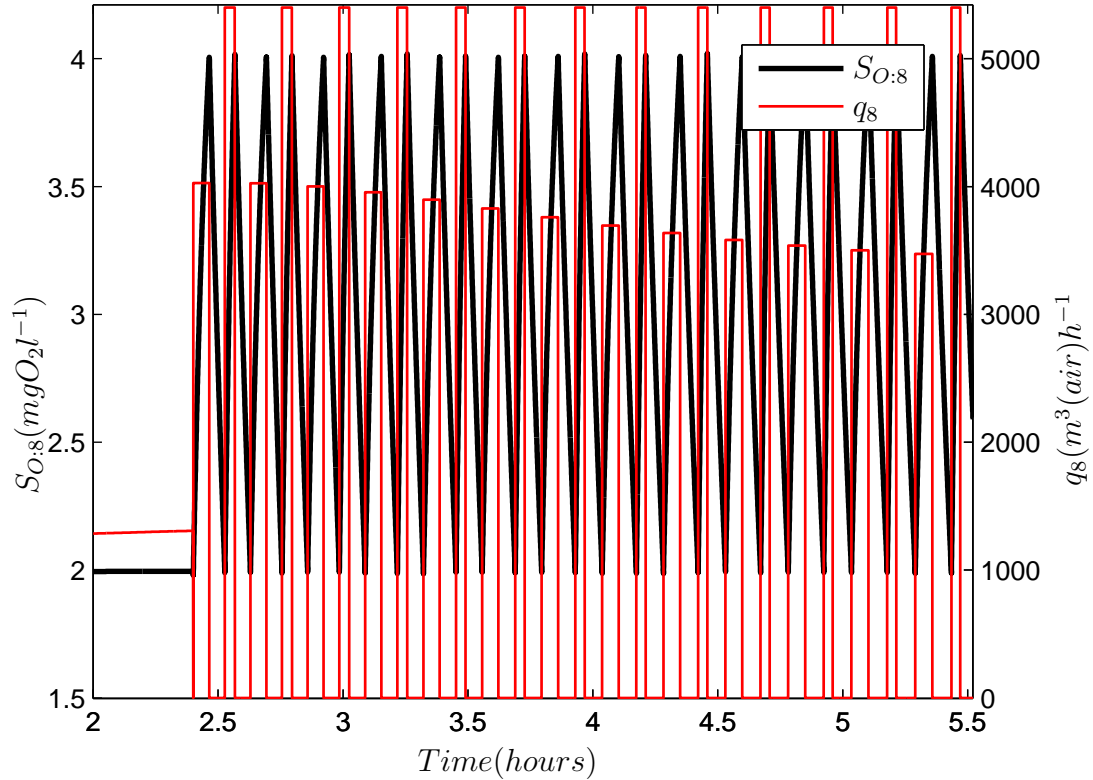


Figure 4.17. ON/OFF control.

was chosen to make  $OUR$  approximately independent of the variation in the DO concentration.  $q$  was  $q_{max}$  defined in Section 3.7 every other ON period, and  $q_{min}$  every other one.  $q_{min}$  is based on the desire to vary the concentrations reasonably fast and is the solution to

$$0 = \dot{S}_O = D(Q)(S_{O:in} - S_O) + K_La\left(\frac{q_{min}}{1.3}\right)(S_{O:sat} - S_O) - OUR, \quad \text{for } S_O = DO_{max}.$$

This is calculated, by using the exact values of  $OUR$  and the  $K_La$  parameters, which of course is not possible in reality. All calculations and the ON/OFF control were implemented with S-functions in Simulink. The sampling time  $h$  was chosen to be 1s. The optimization problems were solved in Matlab, using the function *lsqnonlin*. The error of the initial guesses were chosen to be 50 %. To let the the plant model settle, the experiment was started two and a half hours into the first day.

#### 4.5.2.4 Simulation results

The oxygen concentration  $S_{O:8}$  (not the measured one), and the air flow rate  $q_8$  during the experiment are shown in Figure 4.17. The DO data was run through the Filter (4.25) and then reconstructed with a Kalman filter based on the observer model (4.26) for  $h^* = h = 1s$ . The result is given in Figure 4.18. As seen the

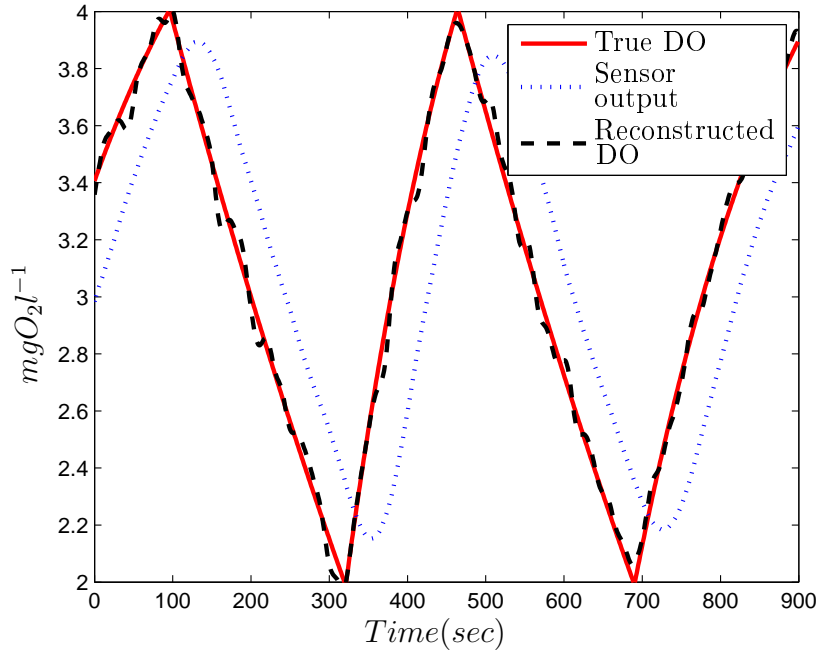
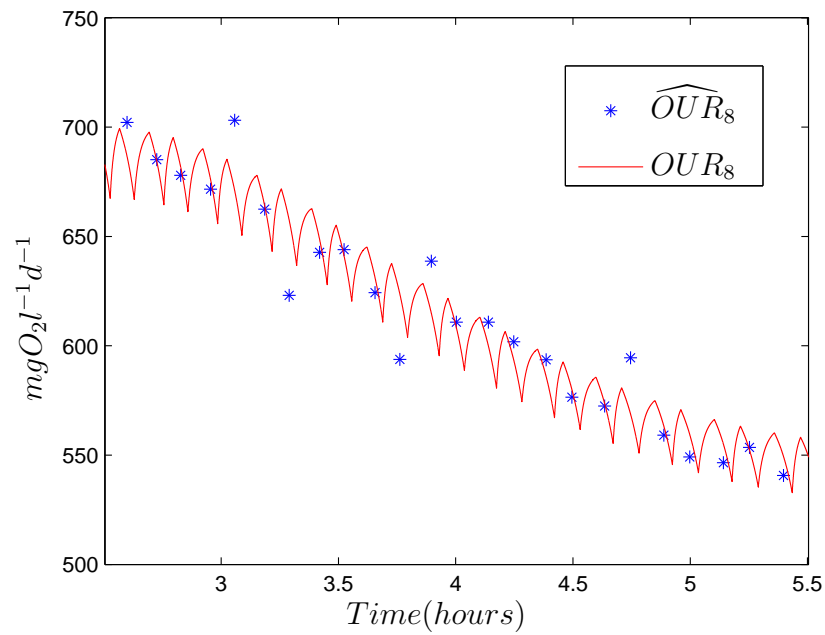


Figure 4.18. Reconstructed and measured DO data.

effect of forming the mean in the sensor is mainly a time delay for the considered variations. The reconstructed data was used and considered as the measurement  $S_{O_{m:s}}$  in the  $K_L a$  estimation algorithm. As time of estimation of  $OUR$  the mid of the OFF periods were chosen.  $\widehat{OUR}_8$  is illustrated in Figure 4.19. Convexity of the objective function  $O_2$  could not be confirmed, but the optimization algorithm converged for all investigated optimization problems. The estimated values of the  $K_L a$  parameters are given in Table 4.3 as a function of the number of ON periods that they are based on. The true parameter values are  $[k_1, k_2] = [1200, 6.6 \cdot 10^{-5}]$ . As seen, there is quite a large variation in the parameter estimates. Therefore, also the Criterion  $e_{K_L a}$  (see Equation (4.23)) is given in the table. Already after the first ON period, this is relatively small. The estimated function is so good that it is pointless to compare it with the real one in a figure.

### 4.5.3 A Kalman filter approach

Lindberg (1997) used a system identification method with excitation of the airflow to estimate the  $K_L a$  function, and also that an EKF can be used in the same manner. An observer model derived by extending the Model (4.13) with random walk models

Figure 4.19.  $\widehat{OUR}_8$ .Table 4.3. Estimated  $K_L a$  parameters and the criterim  $E$ .

Number of ON periods	$\hat{k}_1 \cdot 10^{-3}$	$\hat{k}_2 \cdot 10^5$	$e_{K_L a} \cdot 10^3$
2	0.89	9.61	22.7
4	1.13	7.09	2.5
6	0.98	8.44	11.0
8	1.15	6.87	4.1
10	1.11	7.24	3.2
12	1.08	7.43	4.2
14	1.14	7.01	2.3
16	1.27	6.19	2.3
18	1.29	6.07	2.8
20	1.20	6.60	2.3

for  $k_1$  and  $k_2$  is

$$\left\{ \begin{array}{l} \dot{x} = \underbrace{\begin{bmatrix} D(Q)(S_O - S_{O_{in}}) + k_1(1 - e^{-k_2 q})(S_{O_{sat}} - S_O) - OUR \\ 0 \\ 0 \\ 0 \end{bmatrix}}_{a(x,u,t)} + w \\ y = \underbrace{\begin{bmatrix} 1 & 0 & 0 & 0 \end{bmatrix}}_{c(x,u,t)} x + v \end{array} \right. . \quad (4.32)$$

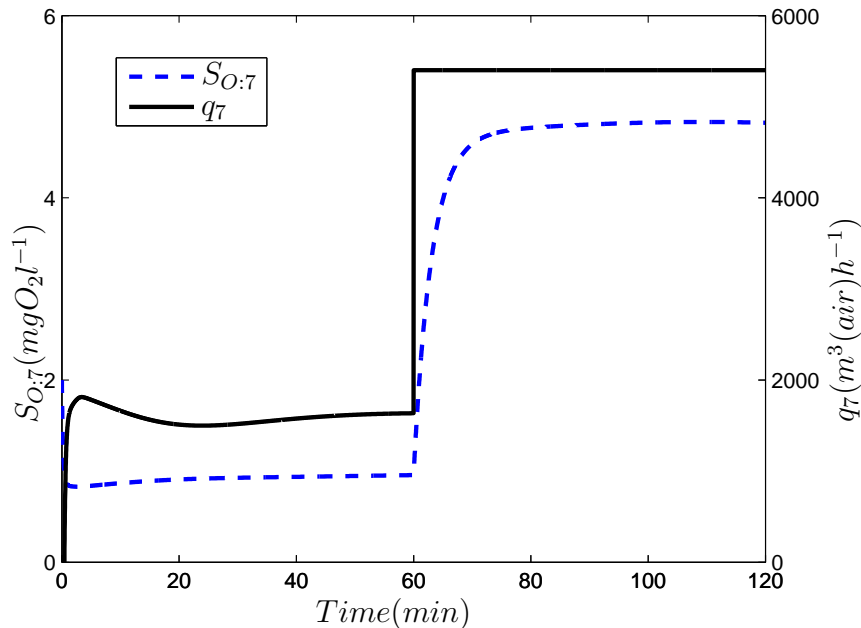
Here  $x = [S_O \quad OUR \quad k_1 \quad k_2]^T$  and  $u = [Q \quad q]^T$ . As in earlier designs the upper diagonal element of  $R_1 = E[ww^T]$  is  $D(Q)^2 R_{S_O}$ , where  $R_{S_O} = E[vv^T]$  is the variance of the oxygen measurements. The equations of the EKF can be directly applied to this model, but would become divergent without excitation of the air flow. Lindberg (1997) did not state the excitation signal but according to a figure, it is a discrete time signal with continuous amplitude. This kind of signal is not easily implemented at Ryaverket since the air flow need to be varied manually. A commonly used excitation signal for linear systems is binary white noise. This signal is called binary since it shifts between two discrete levels. It is called white since it has a flat spectrum within a frequency band  $[\omega_{min}, \omega_{max}]$ . Ljung and Glad (2002) stated that it is often necessary with more levels in the excitation signal when identifying a nonlinear system. Therefore, also a signal with three levels is tested. A continuous signal  $w_s(t)$  with frequencies equally distributed in  $[\omega_{min}, \omega_{max}]$  can be formed by applying an analog bandpass filter to white noise. A binary signal with frequencies approximately in the right band is then formed by

$$s(t) = \text{sign}(w_s(t)).$$

Taking the sign of the signal will however distort its spectrum. The excitation signal is finally formed by adjusting the level and interval to what is required in the application. The choice of  $\omega_{min}$  and  $\omega_{max}$  can be based on time domain properties of the system. It is unnecessary to have pulses so short that they are hardly visible in the response. It should be useful to have occasional pulses so long that the step response more or less settles. There is however no need for pulses longer than that.

#### 4.5.3.1 Simulation result

Tank 7 was chosen for simulation. To not disturb the process we need to guarantee a lowest DO concentration during the experiment. At startup the process was controlled to  $1\text{mgO}_2\text{l}^{-1}$ . After one hour the air flow was stationary and was  $1600\text{m}^3(\text{air})\text{h}^{-1}$ . This was taken as the lower level  $q_0$  in the excitation signal. To decide on the excitation frequencies a step was taken from this level to  $q_{max}$ , defined in Section 3.7. The response is illustrated in Figure 4.20. The time for the signal to reach 40% and 95% of the final value was  $T_{40} = 1.6$  and  $T_{95} = 11.2$  minutes respectively. It was decided to not allow shorter pulses than  $T_1$  and longer pulses than  $T_2$ . Based on this we get

Figure 4.20. Step response of  $S_{O:7}$ .

$$w_{min} = \frac{\pi}{T_{95}} \text{ and } w_{max} = \frac{\pi}{T_{40}}.$$

Note that this kind of reasoning for a nonlinear system only holds strictly if the process can be considered stationary during the experiment. A 12th order Butterworth band pass filter was used to form the signal  $w_s(t)$ . The estimated power spectral density of  $s(t)$  is shown in Figure 4.21, where the frequencies  $\omega_{min}$  and  $\omega_{max}$  has been included. This was calculated with the command *periodogram* in Matlab from samples of  $s(t)$ . The discrete normalized frequency has been recalculated to continuous frequency (*rad/min*). Taking the sign of the signal  $w_s(t)$  distorts the frequency content, and the spectrum of  $s(t)$  is not flat, but has its peak within the right band. Two excitation signals are tested. One pure binary white noise signal  $q_a(t)$  which is defined below

$$q_a(t) = \begin{cases} q_{max}, & s(t) = 1 \\ q_0, & s(t) = -1 \end{cases}.$$

The other signal  $q_b(t)$  is the same as  $q_a(t)$ , but the upper level is varied. It is  $q_{max}$  every other time that  $s(t)$  goes high and  $\frac{q_{max}+q_0}{2}$  every other.  $q_b(t)$  is illustrated in Figure 4.22 together with the DO response. The EKF based on the observer model (4.32) was implemented with an S-function in Simulink. Ideally, this should be merged with the DO Kalman filter described in Section 4.5.1, but that has not been employed here. The DO data was run through the sensor model (4.25) and then reconstructed with the DO observer. The reconstructed data was then used and considered to be the measurement in the EKF. The initial state was chosen to be 0.7 times the true variables, except for the DO concentration which was assumed to be known. The result for the excitation signal  $q_a(t)$  was that it was possible to

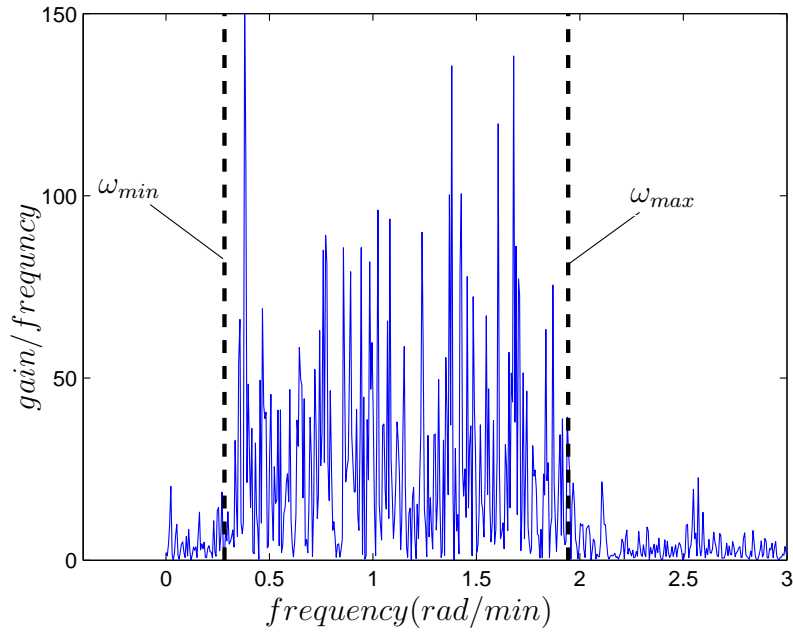


Figure 4.21. Spectrum of the signal  $s(t)$ .

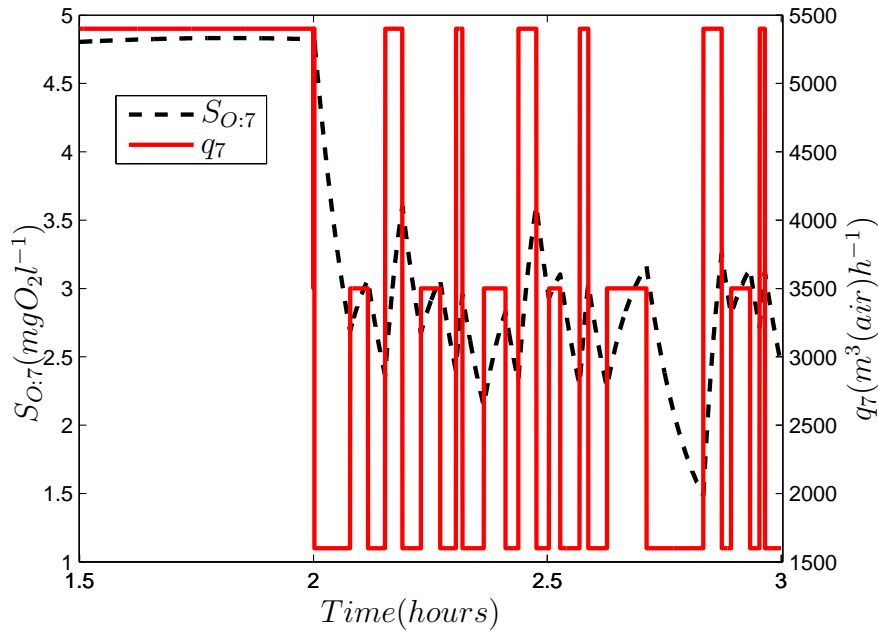


Figure 4.22. Excitation signal  $q_b(t)$  and the response in the DO concentration.

make the error  $e_{KLa}$  converge initially, but without a large variance in the estimated parameters, they started to diverge after a while.

The result for the excitation signal  $q_b(t)$  was better. The best result was for when the variance of the random walk models of  $k_1$  and  $k_2$  was set to zero, and they were given

a large initial error variance in  $P_0$ .  $\widehat{OUR}_7$  is illustrated in Figure 4.23. The variance

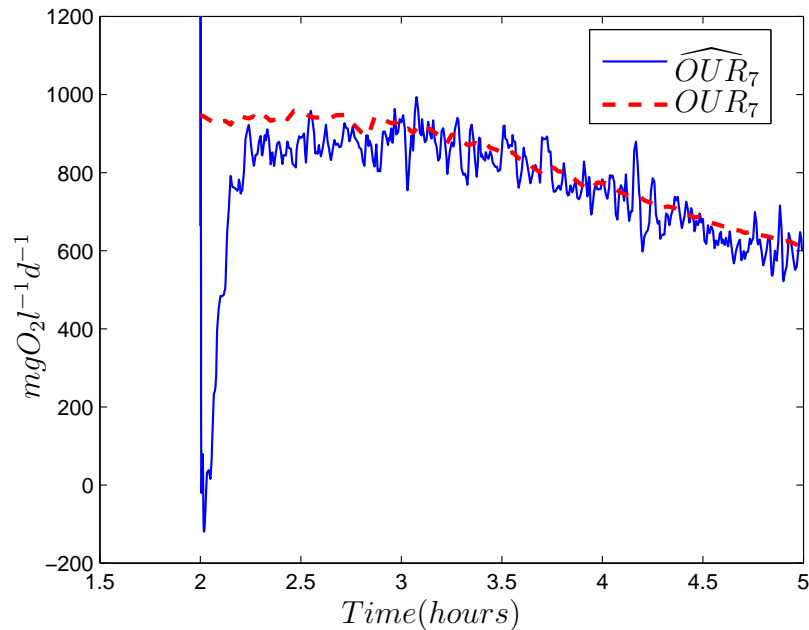


Figure 4.23.  $\widehat{OUR}_7$  for the excitation signal  $q_b(t)$ .

of the random walk model for this has been chosen large since this was positive for the convergence of the parameters. It has also been given a large initial covariance for fast convergence. There is an initial oscillation in the estimate. The criteria  $e_{K_L a}$  is illustrated in Figure 4.24. The convergence is fast, and the estimated function is too good to compare to the true function in a figure. For both the excitation signals it was, however, very difficult and time consuming to find good choices of the covariance  $R_1$  and the initial covariance  $P_0$ . This is of course much more difficult when applying the filter to real data when the actual variables are unknown.

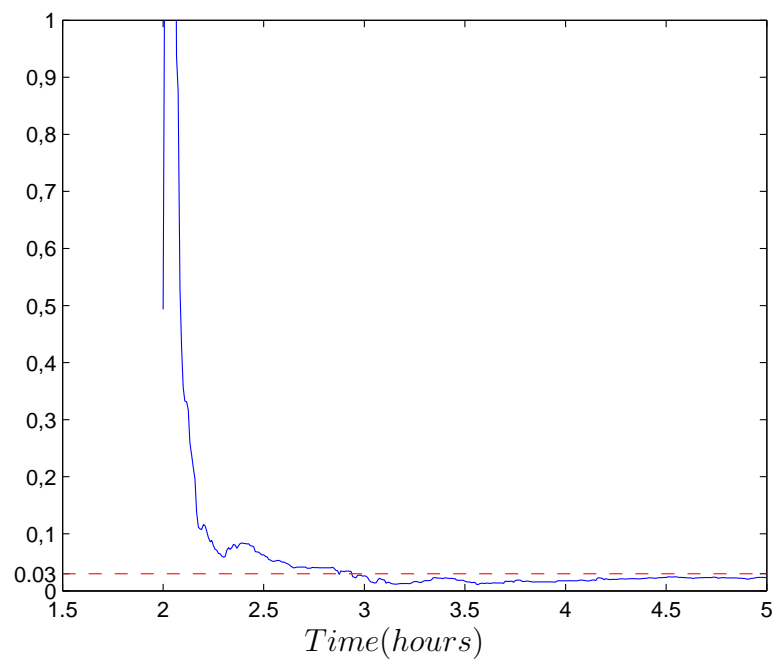


Figure 4.24. The error criteria  $e_{K_L a}$  for the excitation signal  $q_b(t)$ .

# 5 APPLIED ESTIMATION

Experiments to estimate the  $K_L a$  function have been performed at Ryaverket, and some of the observers presented in Chapter 4 have been evaluated for real data. For these purposes the model presented in Chapter 3 needs to be extended to include among others time dependency of parameters, and that the control of air flows in reality are based on the zone division of the basin and not the tank model. The model of the AS basin as a series of tanks is an approximation of reality, and this model is analyzed. All real data are from measurements in line 3, since the air flow sensors works best in that line. The solution for estimation of  $S_S$  and  $\gamma_{BH}$  described in Section 4.3 was not considered due to the placement of the nitrate sensors in the process.

## 5.1 Conventions

In Chapter 4, the variables were indexed based on which tank they belong to. This convention is used here too, except for the air flows that are indexed based on which zone they belong too. The  $K_L a$  functions are still indexed per tank. Diffuser is used to refer to the pipes in a zone with a corresponding air flow.

## 5.2 Tank approximation

In figure (5.1), an AS basin is illustrated. The flow  $Q$  is approximately the same in the influent as in the effluent. Within the basin, the flow consists of a flow in the direction of the effluent, but there are also back streams. In addition to this, the water is purposely mixed, either with mechanical stirrers, or as a consequence of the aeration. This makes it convenient to model the basin as a series of  $n$  *continuously stirred tank reactors* (CSTR:s). An unmixed flow without back streams is called a plug flow. To divide the basin into a series of tanks in model tracer tests are used.

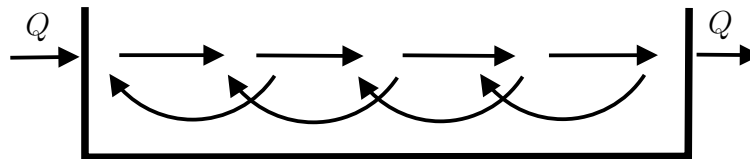


Figure 5.1. An AS basin.

A basic description of this is:

*approximately instantaneously, a large amount of a tracer substance, such as lithium chloride is poured into the water at some point of the basin. At some other down-*

stream point or points, the concentration of the tracer substance is measured. The response is then close to the hydraulic impulse responses of the system. The division of the basin is chosen such that the model gives approximately the same impulse response.

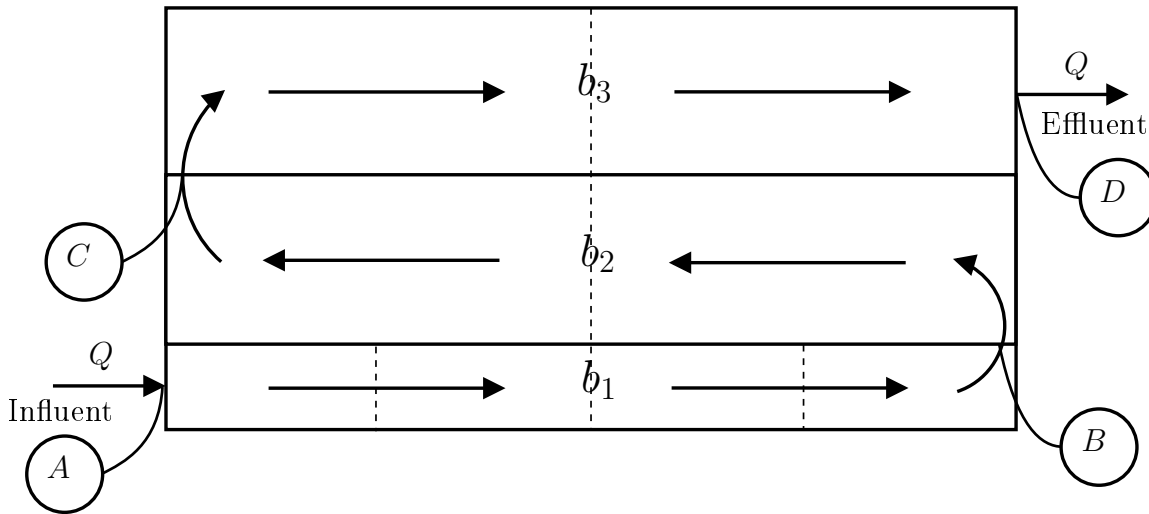


Figure 5.2. Activated sludge basin at Ryaverket.

The AS basin in line 3 at Ryaverket is illustrated in Figure 5.2. As seen, the basin actually consists of three sub basins, one small:  $b_1$ , and two equally large:  $b_2$  and  $b_3$ . At point  $B$  and  $C$ , the water flows through holes in the wall of the basin. These are thus natural boarder lines also in a model. The tank division within the sub basins are illustrated with dashed lines in the figure.

A tracer test has been performed at Ryaverket in another project (Kjellstrand 2006). The tracer substance lithium salt was poured into the water at the influent (point  $A$ ) and the response was measured at the points  $B$ ,  $C$ , and in the effluent (point  $D$ ). Based on this, each of the basins  $b_2$  and  $b_3$  were divided into two equally large tanks. The basin  $b_1$  is smaller but was modeled as 4 equally large tanks. The reason was that the flow through  $b_1$  had a plug flow character. The flow character in a model approaches that of a plug flow, as the number of tanks increases. For the exact volumes of the tanks in the model, refer to Table 3.1.

We are interested in how well the tank model describes the reality, especially regarding the basin  $b_3$ , since this is what is included in most of the estimators described in Chapter 4. The EKF in Section 4.4 also involves concentrations in Tank 6, but only as inputs to Tank 7. Also, as mentioned earlier, based on the physical description of the basin, the point  $C$  in Figure 5.2 is a natural border in the model. According to the model, an oxygen sensor should be representative for the whole volume of the tank it belongs to, while in reality concentrations vary within the tank. The DO concentration is even controlled separately for different volumes within the tank. We can also expect time delays not included in the model during fast changes because of distances within the tanks. For instance, the vertical distance between the diffusers at the bottom and the water surface where the DO sensors are located causes delays

in the sensor responses. The same goes for the horizontal distances between diffusers and sensors.

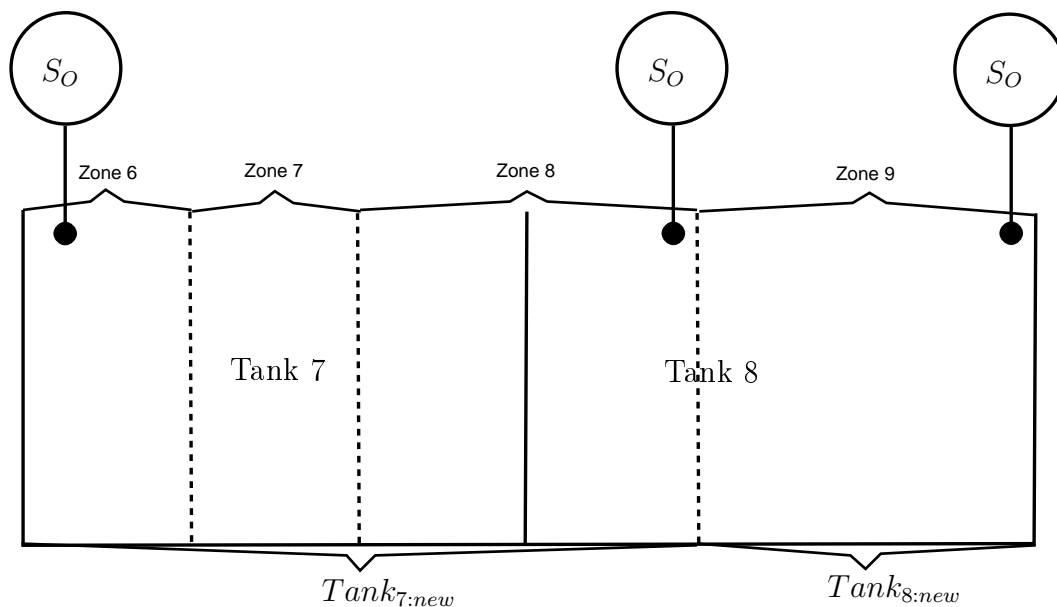


Figure 5.3. Model of the activated sludge process at Ryaverket.

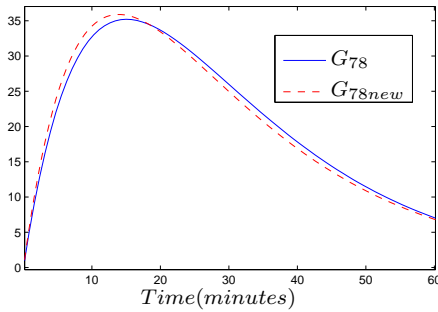
In Figure 5.3, the basin  $b_3$  is illustrated. The current tank division is inconvenient for two reasons. For one, the diffuser in Zone 8 is shared between the tanks which complicates model based control somewhat. Secondly, the only oxygen sensor in Tank 7 is placed close to the influent in Zone 6. One could question if this is representative for the whole volume. Therefore, a new tank division is considered. This is illustrated by  $Tank_{7:new}$  and  $Tank_{8:new}$  in Figure 5.3, where also the approximate positions of the DO sensors are given. The point of this change is that now the sensor in Zone 8 can be used as a measurement for Tank 8, and a downstream sensor may be more representative for the whole volume than an upstream one, although the volume of the new Tank 7 is larger than in the original model. Three transfer functions are defined in Table 5.1. Note that we do not consider reactions in the

Table 5.1. Transfer functions describing the system for a constant water flow.

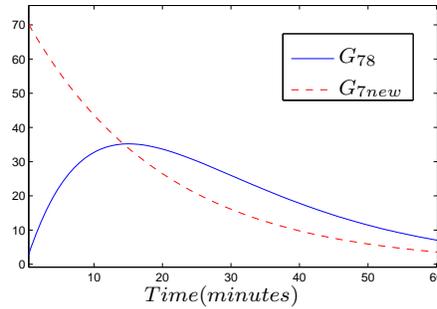
Transfer function	Describes
$G_{78}(s)$	The system from an input concentration of a substance to Tank 7 to the corresponding concentration in Tank 8 in the original model.
$G_{78new}(s)$	The system from an input concentration of a substance to Tank 7 to the corresponding concentration in Tank 8 in the redefined model.
$G_{7new}(s)$	The system from an input concentration of a substance to Tank 7 to the corresponding concentration in Tank 7 in the redefined model.

basin now, but only flows and mixing. The impulse responses of the systems have been simulated with the water flow  $\frac{11}{3}m^3s^{-1}$ , which is the same as was used in the simulation in Chapter 4. The impulse responses of  $G_{78}$  and  $G_{78new}$  are shown in Figure 5.4(a). As seen, these are close to the same, which indicates that the redefinition

of  $b_3$  is valid based on what we know since during the tracer tests, the response was only measured at the inlet and outlet of  $b_3$ , and not within the basin. This, however raises the question of what is the correct description of the system. In Figure 5.4(b) the impulse response of  $G_{78}$  and  $G_{7new}$  are shown. The former is a second order sys-



(a) Impulse responses of  $G_{78}$  and  $G_{78new}$ .



(b) Impulse responses of  $G_{78}$  and  $G_{7new}$ .

tem, and the latter is a first order system, and gives completely different responses. This says that we should have a different character of the response of the oxygen sensor in Zone8 from an input to Tank 7 in the two models.

Another way to model a basin that probably is more accurate is illustrated in Figure 5.4. Here a backflow  $R$  from the upstream tanks are included.

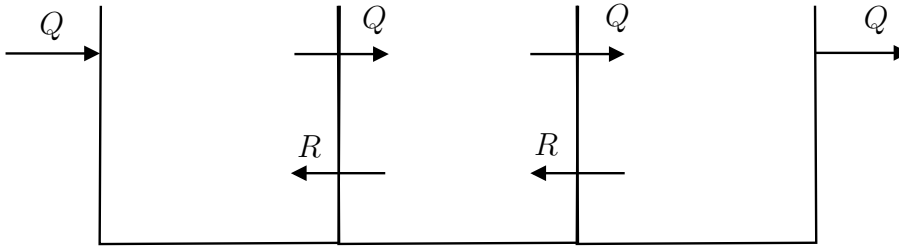


Figure 5.4. Tank model with a back flow  $R$ .

### 5.3 An applied model of the $K_L a$ function

The time variation of the  $K_L a$  function was mentioned in Sections 3.5.3 and 4.5. For evaluation and possible implementations of designs this concept becomes important. According to Lindberg (1997), the function varies with kind of wastewater and temperature. According to Stenstrom and Gilbert (1981) it also varies with TSS. The temperature dependency is described by

$$K_L a(T) = K_L a_{20} \theta^{T-20}, \quad (5.1)$$

where  $T$  is the temperature and  $K_L a_{20}$  is the value of  $K_L a$  at 20 °C. For stirred and only aerated tanks reported values of  $\theta$  are between 1.016 and 1.024 (Stenstrom

and Gilbert 1981). Here, the value 1.02 is chosen. The next equation describes the relationship between  $K_La$  for wastewater and freshwater

$$K_La_{wastewater} = \alpha K_La_{freshwater}.$$

(Stenstrom and Gilbert 1981). If the  $\alpha$  factor could be considered to be constant for a specific plant, it would be unnecessary to mention it, since the  $K_La$  parameters will be estimated for the same water as they are then used for. Unfortunately it is reported that the  $\alpha$  factor might be highly time variant. For a specific plant and constant air flow it is reported that the  $K_La$  function varied between  $59.6d^{-1}$  and  $125.7d^{-1}$  over a time period of two and a half month. It is suggested that this could mean a variation in  $\alpha$  between 0.47 and 1 (Stenstrom and Gilbert 1981). It is of course not possible to describe how the  $\alpha$  factor varies in a model. Any descriptions of how  $K_La$  varies with TSS has not been found. Therefore, only the temperature model is included in the  $K_La$  model. There are several diffusers in each tank. It would be very time consuming to estimate the function for each diffuser separately, and therefore we want to relate them in some way. Each diffuser consists of a set of pipes. We can assume that the all the pipes have approximately the same character. Let  $K_La_p(q_p)$ , be the  $K_La$  function for one pipe at 20 °C, with parameters  $k_{1p}$  and  $k_{2p}$ , refer to Equation (3.2).  $q_p$  is the air flow through the pipe and equals the total air flow in the corresponding zone divided by the number of pipes in that zone. The total  $K_La$  function in a tank can be described as a sum of the  $K_La$  functions for the pipes belonging to that tank. Including the temperature model (5.1), we get the following  $K_La$  functions for Tank 7 and 8 in the original tank model:

$$\begin{aligned} K_La_7(q_6, q_7, q_8, T) &= \theta^{T-20} \left( n_6 K_La_p \left( \frac{q_6}{n_6} \right) + n_7 K_La_p \left( \frac{q_7}{n_7} \right) + \frac{n_8}{2} K_La_p \left( \frac{q_8}{n_8} \right) \right) \quad (5.2) \\ K_La_8(q_6, q_7, q_8, T) &= \theta^{T-20} \left( \frac{n_8}{2} K_La_p \left( \frac{q_8}{n_8} \right) + (n_9 K_La_p \left( \frac{q_9}{n_9} \right)) \right). \end{aligned}$$

Here,  $n_i$  is the number of pipes in Zone  $i$ , and the values of these are given in Table 5.2. It has here been assumed that the airflow in Zone 8 is shared equally between the two tanks. Note that if the volumes of the tanks were not equal it would be necessary to include these in the equations.

Table 5.2. Number of pipes in the zones

Zone number ( $i$ )	Number of pipes in the zone ( $n_i$ )
3 – 8	320
9	240

## 5.4 Data treatment

At Ryaverket measurements are not stored in the data bank with a fixed sampling rate, but a new value is only stored when a sensor output has varied enough from the

last saved value, or after a relatively long period of time. The estimators described in Chapter 4 requires continuous signals or signals sampled at a fixed sampling rate, and the data is therefore linearly interpolated.

## 5.5 Estimation of the $K_La$ function

Although the unknown time variation of the  $K_La$  function, refer to Section 5.3, it is not considered to estimate the  $K_La$  function on a continuous basis. This is due to the economic reasons mentioned in Section 4.5. Instead, it was decided to estimate the function parameters at discrete occasions, and in evaluation or implementation of other designs use the Model (5.1) to update them. The choice of method was ON/OFF control, described in Section 4.5.2. Compared to the method described in Section 4.5.3, this method has better convergence properties, and it was also preferred by the staff at the plant.

Experiments were carried out on three occasions. It was found that even for fast changes in the air flow, the outputs of the DO sensors in Zone 8 and 9 were close to identical. This speaks for the validity of the original tank model, and it makes no sense to consider the suggested new tank division described in Section 5.2. This means that the oxygen sensor in Zone 6 needs to be used as a measurement for Tank 7. It was shown that this sensor varies with the variation in the air flow in zone 8. This is in accordance with the model, but there was a delay of several minutes in the response, and this dynamics is not included in the model. It was initially considered to estimate the function separately for the two tanks, although there is a model relating them.

A couple of changes of the estimation method described in Section 4.5.2 were made. In some experiments, only the air flow in one zone was varied, while the others belonging to the same tank was kept constant. In estimation, only this flow was included in the Model (5.2). This means that during the OFF periods, what was really estimated was  $OUR$  plus the "constant" contribution to the total function from the other zones belonging to the same tank. The system supplying air to the zones in all the lines consists of three compressors. This system is slow, and it is not possible to increase the air flows stepwise, it may take several minutes to reach a higher commanded air flow. It was therefore not possible to estimate  $K_La$  from step responses and it was instead estimated by solving the equation  $\dot{S}_O = 0$  for it, when the DO concentration had reached a stationary value for a constant air flow, refer to Equation 4.22. The response to a decrease in the commanded air flow was however quite fast, and the original method could be used to estimate  $OUR$ .

The DO Kalman filter described in Section 4.5.1 was applied to the data before any further estimations were performed. An example of the output for Zone 6 is shown in Figure 5.5, where the time delay of the Kalman filter has been removed. As seen, also for real data, the effect of mean value forming in the sensors and in the data storage system is mainly a time delay. The total time delay of the DO measurements

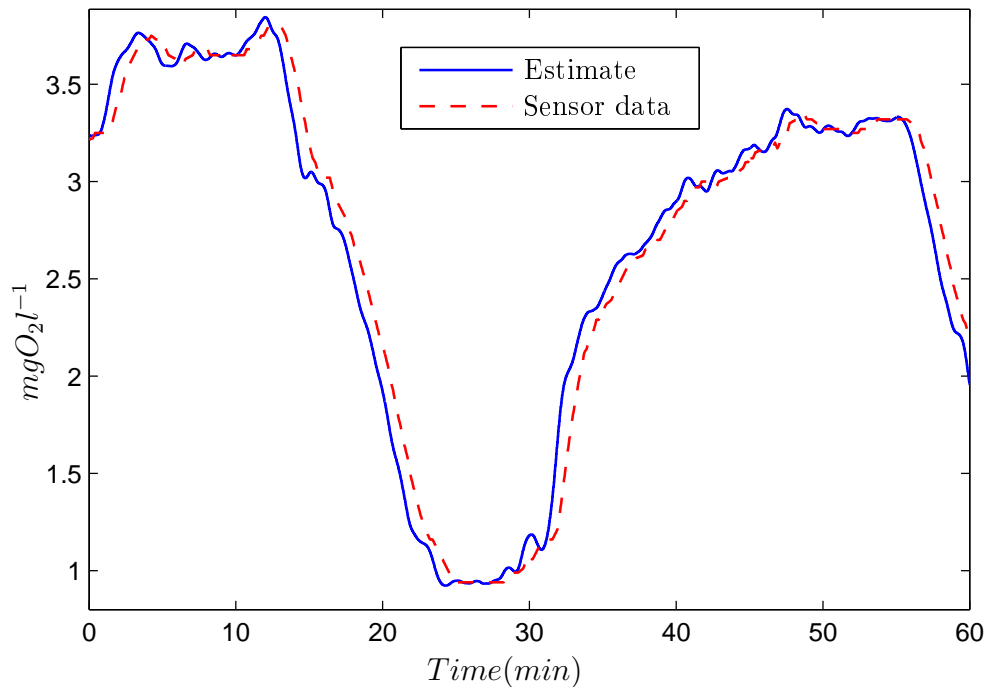


Figure 5.5. DO concentration in zone 6, measurement data and estimate.

compared to the measured air flow was found to be approximately 120 seconds. This includes time delays caused by distances in the basin. The smoothness of the measurement data may be surprising. This is caused by the mean value forming and that the data presented is formed by interpolating discrete time data points. The initial experiments were performed during two days. The temperature was then  $9.5\text{ }^{\circ}\text{C}$ .

### 5.5.1 Experiments in Tank 7

Only the air flow in zone 6 was varied consciously. The air flow in zone 7 was set to a constant value, since with reference control the control signal for this is the mean of the control signals for the flows in zone 6 and 8. Because of time delays it was not possible to time the exact times for when the air should be turned on again after an OFF period. This led to that the DO concentration sometimes approached as low values as  $1\text{ mg l}^{-1}$ , which can be seen in Figure 5.5. As stated in Section 4.5, we do not want to approach to low DO concentrations,  $1\text{ mg l}^{-1}$  is however not critically low.

The estimated pairs  $(\widehat{K_L a_i}, q_i)$ , are shown in Figure 5.6, refer to Section 4.5.2.2. The number of estimated pairs is small. This is due to that each ON and OFF period was way more time consuming compared to simulation. The reason is among others the necessary change of the estimation method stated earlier. As seen, there

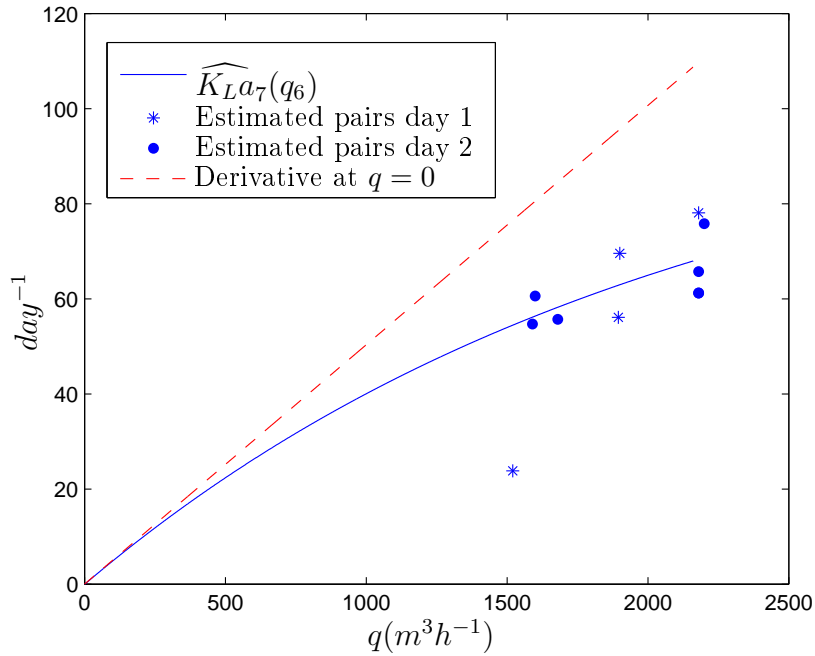


Figure 5.6. Estimated  $K_L a$  in Tank 7 as a function of  $q_6$ .

is one outlier among the estimated pairs. To compensate for the long periods, the estimated *OUR* values was interpolated in time before estimating  $K_L a$ . There is quite little variation in the air flow values in Figure 5.6. The reason for this is that high air flows were necessary to hold a high enough DO concentration. The estimated function  $\widehat{K_L a_7}(q_6)$  is also shown in the figure. This is  $K_L a$  in Tank 7 as a function of  $q_6$  for the temperature 9.5 °C. When estimating this, the outlier was removed. The estimated parameters  $k_{1:p}$  and  $k_{2:p}$ , recalculated for 20 °C are given in Table 5.3.

Table 5.3. Estimated  $K_L a$  parameters for the diffuser pipes.

$k_{1p}$ ( $day^{-1}$ )	$k_{2p}$ ( $m^{-3}hour$ )
0.4078	0.1521

## 5.5.2 Results from experiments in Tank 8

During the first day, the airflow was varied in Zone 8 and Zone 9 at the same time. During the second day it was only varied in Zone 9. The estimated triplet  $(q_8, q_9, \widehat{K_L a_8})$  values did not show a pattern that can be described with any strictly increasing function. The most likely reason for the bad result is that *OUR* in the tank was small, which makes mass balances have a relatively large effect, and as described in Section 5.2, we do not put much confidence in the model regarding

these. Because of this result it was decided to use the estimated  $K_{La}$  parameters for Tank 7 and the  $K_{La}$ -pipe model (5.2) as a model for  $K_{La}$  in both tanks.

### 5.5.3 A new experiment

To achieve a larger span in the airflows, and possibly shorter ON and OFF periods to achieve more data points, it was decided to carry out a new experiments for Tank 7 in which the airflow was varied in both Zone 6 and 7 at the same time. The large variation in the total air flow however led to problems with the system supplying the air, which in turn led to very few data series - ON and OFF periods. There were also disturbances in form of quite large variations in the water flow this day and it was decided to discard the collected data.

## 5.6 The aerobic EKF

Here, the result of the extended Kalman filter for two aerobic tanks presented in Section 4.4 when applied to real data from Tank 7 and 8 is presented. Lab analysis of BOD for filtered water samples in Tank 7 and 8 were taken during a couple of weeks to have to compare with the output of the filter. Filtered BOD is approximately the same as  $S_S$  (COD). The dependency of the parameters  $k$  in the ASM1 to temperature  $T$  is described by

$$k(T) = k(20^\circ\text{C})\theta_T^{T-20^\circ\text{C}},$$

where  $\theta_T$  is the temperature coefficient for the parameters. These have been gathered from the plant, and are given in Table 5.4 for the parameters included in the observer model (4.19). The EKF including the  $K_{La}$  model (5.2) with the parameters in Table 5.3, the temperature dependency of the ASM1 parameters, and the estimation of the sludge concentration  $X_X$  described in Section 4.2 was implemented in Simulink. No prefiltering of the oxygen sensor data was made, but due to the relative delay of the oxygen measurement data, described in Section 5.5, all other signals were delayed 120 seconds. The water flow within the basin was lowpass filtered, but measurements of the individual influent flows and TSS were not. These are namely naturally lowpass filtered in the estimation of  $X_X$ . The estimates of the EKF for some concentrations are given in Figure 5.6. As seen  $\hat{S}_{S:7}$  and  $\hat{S}_{S:8}$  tend to zero,

Table 5.4. Temperature coefficients for the ASM1 parameters.

Parameter	$\theta_T$
$\hat{\mu}_H$	1.05
$k_h$	1.072
$K_X$	1.116

$\hat{\gamma}_{X_{BH}}$  and  $\hat{X}_{BH}$  diverges, and  $\hat{X}_S$  goes even below zero. These estimations are of

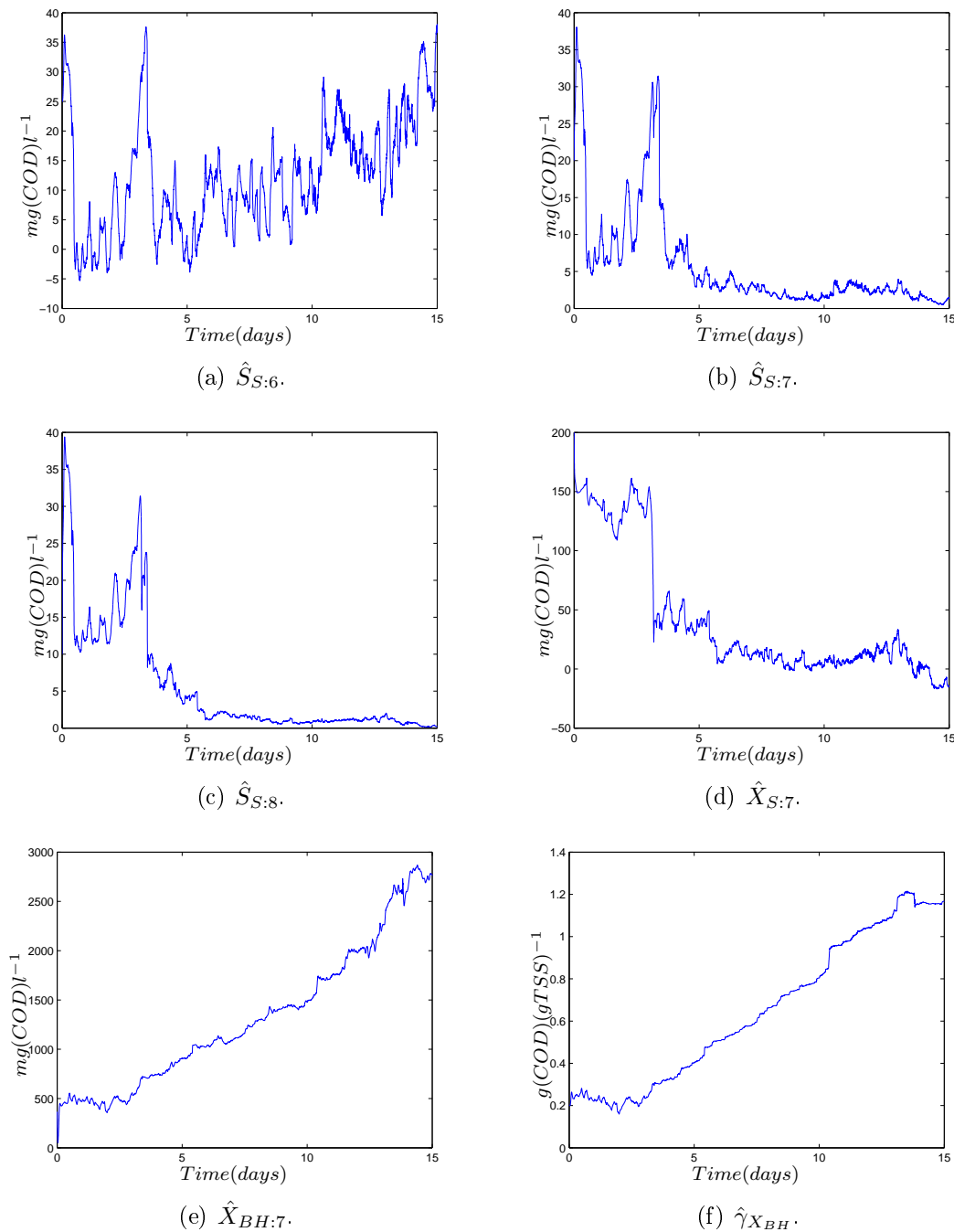


Figure 5.7. Estimates of the EKF.

course not valid. One possible reason for the bad performance of the filter is model errors. Some sources of errors they may have large impact are

- The approximation of the basin as a series of CSTR:s.
- The estimated  $K_L a$  functions. The real function may also be timevarying in a way not included in the model.

- The ASM1 parameters.

In Section 4.4.3 it was also found that the filter diverges without enough variation in the real concentrations, which is another possible reason. The parameters in the filter has been varied to make the estimates more reasonable, but the result has still been equivalent to that presented in Figure 5.6.

## 5.7 Estimation of $OUR$

The observer for  $OUR$  described in Section 4.3.4 has been simulated for real data using the same necessary temperature models and pretreatment of signals as in Section 5.6. The result for Tank 7 is shown in Figure 5.8(a). There is another way

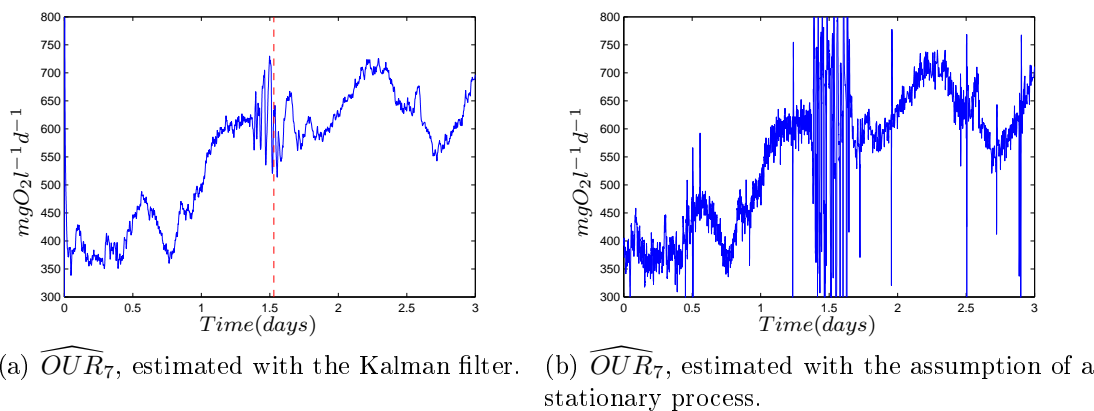


Figure 5.8. Estimated  $OUR$  in Tank 7.

of estimating rate expressions, that is by solving Equation 4.11 under the assumption that the process is stationary ( $\dot{S}_O = 0$ ). This solution is illustrated in Figure 5.8(b). The time period for when this varies as most is for the first day of  $K_La$  experiments. Naturally, it is not possible to use this method for such extreme conditions. The two estimates have the same mean, but the Kalman estimate has much smaller variance.

When the process is stationary, it is not possible to detect any errors in the observer model, these will be compensated for by an erroneous  $\widehat{OUR}$  such that the equations adds up to the oxygen measurements. During large perturbations it is however possible to detect model errors. In Figure 5.9, the measured DO concentration -  $S_{O_m}$ , and the Kalman filter DO concentration estimate  $\hat{S}_O$  in Tank 7 is shown for the period of the first day of  $K_La$  experiments. During the time interval  $T_1$ , the airflow was varied in Zone 8 and 9, and during the interval  $T_2$ , it was varied in Zone 6 only. The division into these periods is illustrated in Figure 5.8(a) with the dashed vertical line. During the period  $T_1$ ,  $\widehat{OUR}$  in Figure 5.8(a) varies heavily, and  $\hat{S}_O$  is not in phase with  $S_{O_m}$  in Figure 5.9. The amplitude of  $\hat{S}_O$  is also smaller than  $S_{O_m}$ . The reason for this is that for these fast processes the filter cannot compensate fast enough for errors by varying  $\widehat{OUR}$ . In the filter, we account for that the DO sensor

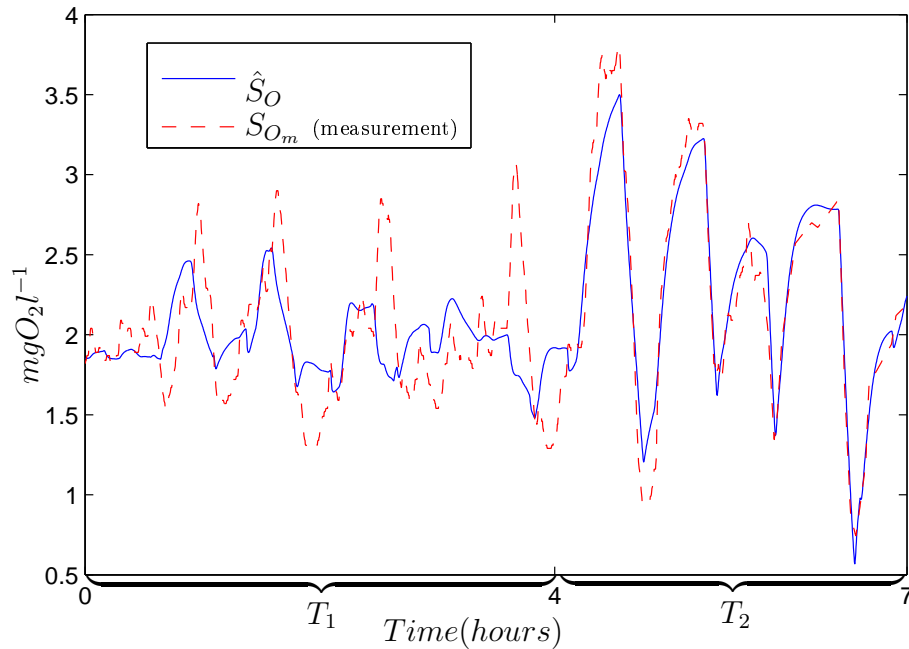


Figure 5.9. Measured and estimated DO concentration in Tank 7 during the  $K_La$  experiments.

should react as fast for variations in the air flow in Zone 8 as in Zone 6, and from the delay in  $S_{O_m}$  compared to  $\hat{S}_O$ , we can draw the conclusion that this is not the case. During the period  $T_2$  when the air flow is varied in Zone 6, the DO signals in Figure 5.9 are in phase, and  $\widehat{OUR}$  varies less, which says that the model works better for this flow. It should be noted that the  $K_La$  function has been estimated for the same data and for Zone 6 as considered here. The observed phenomenon may in general not be a problem, since, normally the air flow is not varied this heavily, and the stationary tank model may still be a good approximation. But the oxygen concentration in Zone 7 and 8 as a function of the air flow in Zone 6 must be described by the same kind of dynamics, and the assumption when the  $K_La$  parameters were estimated was that the tank was perfectly stirred, i.e. it was assumed that the DO concentration did not differ w.r.t. distance in the tank.

## 6 PROCESS OPTIMIZATION

The aim of the aerobic process is to assure a low concentration of soluble biodegradable substrate in the effluent by taking care of the waste that cannot be cleaned in the anoxic process. The only costs are for the total air flow rate and possible effluent discharges. The optimization problem can be formulated as

*Minimize the cost for aeration, while preserving a good effluent quality*

Optimization of the influent flows is so complicated that it is left out from the discussion. It is initially considered how the aerobic process could be optimized if all control variables could be varied independently for these. Control variables to consider are the aerobic volume, the air flows, the oxygen setpoints, and the TSS concentration in  $Q_X$ . To unravel the possibilities for optimization, simplified versions of the equations describing an aerobic tank are given below.

$$\begin{aligned}\dot{S}_O &= K_L a(q)(S_{O_{sat}} - S_O) + D(Q)(S_{O:in} - S_O) \\ &\quad - \hat{\mu}_H \frac{1-Y_H}{Y_H} \frac{S_O}{K_{OH}+S_O} \frac{S_S}{K_S+S_S} X_X \gamma_{X_{BH}} \\ \dot{S}_S &= D(Q)(S_{S:in} - S_S) - \hat{\mu}_H \frac{1-Y_H}{Y_H} \frac{S_O}{K_{OH}+S_O} \frac{S_S}{K_S+S_S} X_X \gamma_{X_{BH}} \\ &\quad + k_h \frac{X_S}{K_X + X_X \gamma_{X_{BH}}} \frac{S_O}{K_{OH}+S_O}\end{aligned}\quad (6.1)$$

Nitrification, denitrification and decay of biomass have been neglected. The equations for heterophic biomass has been removed since this concentration in reality on a short term basis only is controllable via the sludge concentration  $X_X$ , which in turn is controllable via TSS in  $Q_X$  (and the influent flows). Also  $X_S$  is in reality only controllable via the inputs and we consider only its effect on  $S_S$ . If effluent restrictions are not violated, the only cost is for aeration. As practiced at the plant it is here assumed that the cost is equivalent to and linear in the air flows. Reducing the oxygen setpoint has the following effects

- The expression  $(S_{O_{sat}} - S_O)$  increases and makes a smaller  $K_L a$  necessary and thus a smaller flow rate.
- The monod expression  $M_{S_O} = \frac{S_O}{K_{OH}+S_O}$  is decreased, which decreases both hydrolysis and the reaction rates of  $S_S$  and  $S_O$ .

$M_{S_O}$  is illustrated in Figure 6.1, and we can see that changes of the DO concentration above  $1mgO_2l^{-1}$ , has minor effects on the reaction rates. One could thus suggest that the DO concentration could identically be set to for example  $1.5mgO_2l^{-1}$ . Only during high load it may be beneficial with a higher concentration, but it is during high load that there is the most to gain. During low load, little oxygen is consumed. There is a reason for this not being done. At the plant, one are working with reducing the oxygen reference. Currently, it varies between 2 and 4  $mgO_2l^{-1}$ . The reason why a constant reference of  $2mgO_2l^{-1}$  is not used is that one wants to see the effect of

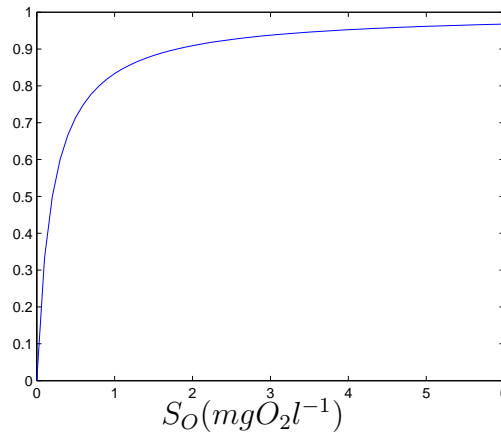


Figure 6.1. The Monod expression  $M_{S_O}$ .

reducing it. It is namely so that the oxygen concentration has more effects than can be seen in the ASM1. A too low concentration benefits certain microorganisms with harmful or unfavorable properties. Since the model suggests that it is reasonable to identically decrease the setpoint, while this is really based on properties outside the model, it is motivated that the DO setpoint should not be varied on a short term basis based on the model.

$X_S$  is degraded by hydrolysis into  $S_S$ , which then must be further degraded. This is an unnecessary cost since particulate substrate can be removed in the secondary clarifier and the disc filters. By reducing the aerobic volume during low load, it is possible to reduce hydrolysis effects.

The  $K_L a$  function is nonlinear with strictly decreasing increase w.r.t. the air flow, and it would therefore be positive to allocate the reactions as even as possible over several tanks. To make this possible, we need to be able to control the reaction rates. As stated earlier, these are not controllable via the DO concentrations within reasonable intervals in these. They are, however, controllable via the sludge concentration  $X_X$ . For this kind of optimization, it is necessary that at least three tanks are aerated. This is since the reaction rate must be identically small in the last aerobic tank since this is bounded in  $S_S$ , which must be small to fulfill the restriction on the effluent. If the flow in reality has more of a plugflow character, this can be considered even for a smaller volume.

Except for the DO concentration, none of the control variables considered so far can actually be optimized independently for the aerobic compartments. Both the aerobic volume and the sludge concentration affect the denitrification capacity, and it may even be necessary to consider processes outside the basins. Under the assumption that the tank model is valid, there is however one set of variables that can be optimized independently for the aerobic tanks. We can consider reference controllers in which the control variable is a prescribed  $K_L a$  function, see for instance Olsson and Newell (1999). From this, the necessary air flows can be calculated. At Ryaverket, there are several air flows in each tank, and there is no unique choice of these. But because

of the  $K_{La}$  functions nonlinear characteristics, there is a cost optimal choice. We consider here the  $K_{La}$  model described in Section 5.3. In Tank 6 there are equally as many pipes in each zone and no zone is shared with another tank. The optimization problem is in this case therefore trivial, all flows should be equal. By the same argument, one finds that it is optimal to let the flows  $q_6$  and  $q_7$  in Tank 7 to be identical. With the Model (5.2), the optimization problem becomes

$$\begin{aligned} & \text{minimize } f(q_6, q_8, q_9) = 2q_6 + q_8 + q_9 \quad \text{w.r.t. } q_6, q_7, q_9 \\ & g_1(q_6, q_8) = \theta^{T-20}(2n_6 K_{La_p}(q_6/n_6) + \frac{1}{2}n_9 K_{La_p}(q_8/n_6) - K_{La_{7_{sp}}}) = 0 \\ & g_2(q_8, q_9) = \theta^{T-20}(\frac{1}{2}n_6 K_{La_p}(q_8/n_6) + n_9 K_{La_p}(q_9/n_9) - K_{La_{8_{sp}}}) = 0 \\ & (q_6, q_8, q_9) \in D = \{200 \leq q_6, q_8 \leq 2160m^3h^{-1} \quad 400 \leq q_9 \leq 2160\} \quad (m^3h^{-1}) \end{aligned} \quad (6.2)$$

Here,  $n_8$  and  $n_9$  has been substituted with  $n_6$  since they are equal, refer to Table 5.2.  $K_{La_{7_{sp}}}$  and  $K_{La_{8_{sp}}}$  are the by the reference controller specified necessary values of  $K_{La}$  in the tanks. The boundary  $D$  are restrictions on the flows. The lower boundaries are used at the plant to assure enough mixing of the water at all times. The optimal solution are either globally optimal or lies on the boundary of the domain  $D$ . At a globally optimal point we have that the gradients of  $f$ ,  $g_1$  and  $g_2$  w.r.t the  $q$ :s are parallel (Persson and Böiers 1988). Another way to express this is that

$$\det \begin{bmatrix} \text{grad}(f) \\ \text{grad}(g_1) \\ \text{grad}(g_2) \end{bmatrix} = 0.$$

This together with the equations for  $g_1$  and  $g_2$  gives the possible globally optimal points. This has been simplified in a symbolic math program, and there were two such points. The solutions on the boundary can be calculated from the equations for  $g_1$  and  $g_2$  by inserting that for example  $q_9 = 400$ . Totally, there are 8 possible optimal solutions that needs to be calculated. This optimization method has been evaluated for real data.

## 6.1 Optimization based on real data

Here, the estimated  $K_{La}$  parameters in Table 5.3 were used. Air flow and temperature measurement data with the sampling time 10 minutes for half a year was collected from the plant for Zone 6 to 9 and for line 3. Using the Model (5.2), the  $K_{La}$  function in the tanks was calculated for each time instant. The calculated values were taken as the specified values in the Optimization problem (6.2). The optimal individual flows were quite different compared to the measurement data, while the change in the total air flow were not as significant. For the whole period 4.5 % less air was needed with the optimal solution. There is one subperiod of 30 (day 100 to 130) days for which the benefit of the solution is more significant. The total supplied air could for this be reduced by 12 %. The optimized total air flow

for the subperiod is illustrated in Figure 6.2 and the optimized individual air flows are illustrated in Figure 6.3 for the same period.

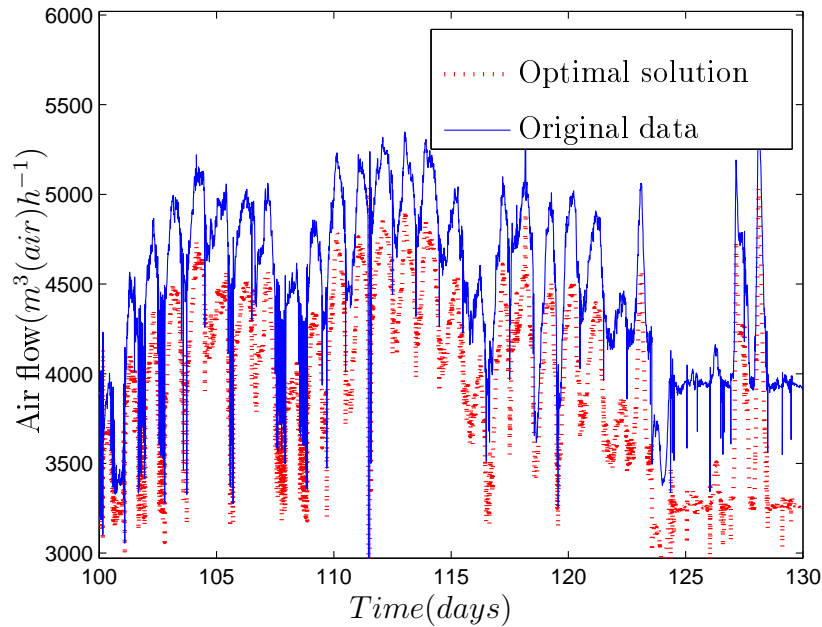


Figure 6.2. Total airflow ( $f$ ).

The measurement data for this period is extreme, it is saturated for Zone 8 while the flow in Zone 9 is minimal, and the flow in Zone 6 is much smaller than that in Zone 7, which gives a high potential for the solution. Compared to the developed estimators in Chapter 4, we can expect this solution to be more robust, and less sensitive to errors in the estimated  $K_La$  parameters. This due to that what we really want to achieve are air flows more evenly allocated over the diffusers. How much that can be saved is of course highly dependent on the characteristics of the real  $K_La$  function. This property has not been considered in more detail.

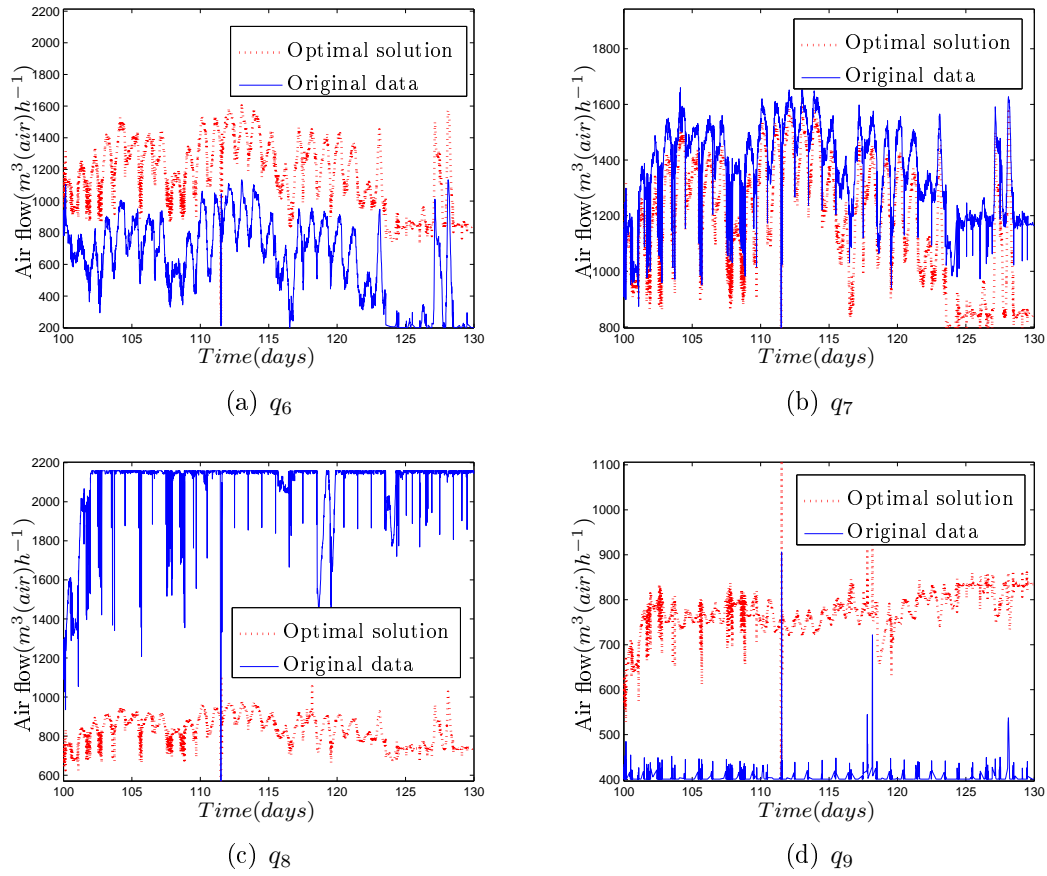


Figure 6.3. Optimized air flows.

# 7 REVIEW OF RESULTS AND DISCUSSION

A case study based on plant data was formed to evaluate designs by simulation. One limitation in this is that only zero mean sensor noises with Gaussian distributions are considered.

## 7.1 Estimation via rate expressions

In Section 4.3 a method was presented in where the parameter  $\gamma_{X_{BH}}$  is determined from  $NUR$ , estimated by a linear Kalman filter in an early upstream tank assuming that the Monod expression in  $S_S$  is often saturated there. This method can be used in several ways to estimate substrate concentrations in the downstream aerobic tanks. It was illustrated for estimation of  $S_S$  via estimation of the rate expressions  $OUR$ . Limitations in this method are:

- $OUR$  includes nitrification which was neglected in the calculations of  $S_S$ , which leads to errors.
- The estimation of  $S_S$  is quite sensitive to errors in  $\gamma_{X_{BH}}$ . This is due to the nonlinear Monod expression in  $S_S$ .
- Compared to the aerobic tanks, measurement noise in the measured input of the nutrient has a relatively large effect in the anoxic tanks. This is in particular true for the considered plant, since the early tanks in this are relatively small. Measurement noise is limiting since there is a compromise between noise reduction and convergence speed for the estimates of a filter.
- Secondary calculations for  $\gamma_{X_{BH}}$  based on estimated variables amplifies disturbances. This can be resolved by using an EKF to estimate the parameter directly.
- The assumption of zero mean measurement noise in the case study may in this case be severe. The experience at the plant is namely that the nitrate sensors sometimes are drifting.
- Parts of the variable  $S_{NO}$  in the ASM1 consists of nitrite which is not measured. This have been neglected in simulation.

To decrease noise effects due to the measured input in the estimation of  $\gamma_{X_{BH}}$ , different alternative observer models were considered. The possibility to approximate two tanks as one for a larger volume and smaller noise effects was investigated with the

result that the optimal approximation was dependent on the concentrations in the tank. It was illustrated that the inverse of the Monod expression is too sensitive to noise and disturbances to be used for direct estimation of substrate concentrations in the anoxic tanks.

## 7.2 An EKF for the aerobic compartments

The second estimation method was estimation of biomass and soluble- and particulate substrate concentrations with an extended Kalman filter (EKF) for a series of  $n$  aerobic tanks. For one tank, the estimates were divergent but for two tanks the filter was convergent for the simulation data in the case study, and performed well. This result was over expectation with fast convergence from an initial guess and accurate estimates. One could expect that it is necessary with one oxygen measurement per unknown input. One reason for the positive result is the modeling of  $X_{BH}$  as a product of the fast varying sludge concentration which is an input to the filter and a slowly varying parameter  $\gamma_{X_{BH}}$  which is estimated. The possibility to introduce more process noise and implement the filter using the Runge Kutta 4 method was investigated with a result which was equivalent to previous simulations with the EKF. The EKF for two tanks has some negative properties though:

- As in the previous method, the estimates are somewhat biased which is mainly due to the neglect of nitrification in the derivation of the observer model. If the real effect of nitrification in the process is quantified, this effect can be reduced.
- The estimation of  $X_S$  may be slow, but by describing a correlation between measured TSS in  $Q_{in}$  and  $X_S$ , this estimation could be made faster. There certainly is a correlation between these concentrations also in reality, but it is a bit hypothetical how strong this is.
- A sensitivity analysis showed little sensitivity for the estimates to errors in most of the parameters in the internal model of the observer describing the process. On the other hand, the sensitivity to errors in the  $K_L a$  functions were quite large. The problems with  $K_L a$  parameter errors were smaller if the relative error was the same for both tanks. This is positive since in an application, the diffusers are likely to be equal and described by the same model.
- The convergence of the filter for two tanks is dependent on certain variations in the concentrations. Although the influent concentrations to an ASP often follows a daily rhythm and often with a large peak each day, restrictions on variations in estimated concentrations are too restrictive in an observer design.

For better convergence properties, and possibly less sensitivity to parameter errors a redefined model involving three tanks was evaluated. The result was a filter with

convergence independent of variations in the concentrations. The convergence of  $\hat{X}_S$  was in general also somewhat faster. The sensitivity property was however not improved significantly. To explain the properties of the filter, observability conditions were investigated for sampled points of the simulation data. *Locally weakly observability* roughly means that it is possible to distinguish states from their neighbors without going to far. This could be investigated using the observability rank condition. The EKF is based on a linearization of the observer model around the current estimated state, one could therefore expect observability/detectability of these linearizations to be an important property. This property was investigated using several methods. The results for the sampled points were:

- EKF based on measurements in one tank: Locally weakly observability could not be confirmed and the linearizations of the model were neither observable nor detectable. This is in accordance with the poor simulation results with the filter.
- EKF based on measurements in two tanks: Locally weakly observability was confirmed for all points. This shows on some observability properties, but is not a contradiction to the dependency of variations of the filter since the EKF is not an optimal filter. The linearizations around the points were neither observable nor detectable. By transformations into stair case form, it was shown that the eigenvalue of the unobservable mode was 0 for all points.
- EKF based on measurement in three tanks: For this case both observability conditions could be confirmed. This result can be related to the independency of variations for this filter.

The relative dependencies of the states in the observer model to the non detectable modes in the linearized models were investigated for the filter based on two tanks. The aim of this was to show that this dependency was small for all variables for relevant periods of each day in the simulation case. This could explain the convergence of the filter for this data. The result was different than expected.  $X_S$  showed high dependency to the non detectable mode for almost all times. It was concluded that observability of linearizations of the observer model is not necessary for the EKF, but still a positive and important property.  $X_S$ 's relatively high dependency of the non detectable mode was especially large which possibly can explain its slower convergence. The process model considered in this project is simpler than in previous formulated extensive observers for the ASM1 since nitrification in this case is separated from the AS basin. The extension of the developed EKF to a process with a mixed aerobic process should however be straightforward. For that more concentrations need to be included in the observer model, such as autotrophs, ammonium and nitrate, but it also introduces possibilities of more sensors, since both nitrate and ammonium can be measured online.

## 7.3 Estimation of the $K_La$ function

The methods for  $K_La$  estimation found in the literature are unsuitable for Ryaverket, and needed to be further developed. The *ON/OFF* control method described in Section 4.5.2 is an extension of a method described by Suescun *et al.* (1998). Mass balances were included in the equations because of the relatively high flow rate at the plant and the parameters were estimated by solving a set of optimization problems. One would expect the method to give accurate estimates in simulations with zero mean measurement noise and a perfect model, which was also the result.

The other evaluated  $K_La$  estimation method uses an EKF and excitation of the air flow, which was inspired by the work by Lindberg (1997). Implied by the control system at the plant, only excitation signals with discrete levels were considered. The result was that the convergence of the filter was highly dependent on choice of variances and initial covariance. Lindberg (1997) used an excitation signal with continuous amplitude, which can explain the better convergence achieved.

The DO measurement data at the plant is formed by moving average. Compared to sensor dynamics of traditional DO sensors the effect of this filtering is relatively small, but for completeness a Kalman filter to reconstruct the actual concentration was designed with good simulation results.

It is reported that the  $K_La$  function may be varying in a way that it is not possible to include in a model. Therefore it is desirable to estimate the function on a continuous basis, but the evaluated  $K_La$  estimation methods rely on excitation of the air flow rates, which is too costly to be economically justified. It was therefore decided to estimate the function on discrete occasions with the *ON/OFF* control method, and then use a model for it only including its temperature dependency.

A possibly less costly method for continuous estimation of the  $K_La$  function would be a respirometer. A respirometer is a separate chamber without aeration in which *OUR* is estimated (Olsson and Newell 1999). Respirometer measurements are, however, not available online at the considered plant.

Experiments to estimate the function were performed on three occasions at the plant. These experiments were very time consuming, which led to that only a few measurement series could be collected. One reason for this was the necessary modification of the method. The experiments on Tank 8 was unsuccessful due to a small oxygen uptake rate, which led to that water flow had a relatively large effect, and the model of this is a weak part of the total model. By introducing the model of the  $K_La$  function for one pipe, the  $K_La$  function for Tank 8 could be based on estimations for Tank 7. The results of the experiments in this tank were quite successful, although a larger difference in the flow rate values, and more measurement series would have been desired. A larger difference could have been achieved if the air flow was varied in more than one zone at a time. This would also give faster variation in the DO concentration and therefore more measurement series. It could probably make the concentration to be more consistent throughout

the tank, i.e. make the process behave more like a perfectly stirred tank model. This approach was tested on a later occasion, but unfortunately disturbances and problems in the central air flow control system when varying the air flow made this experiment unsuccessful.

## 7.4 Evaluation of the EKF based on real data

The EKF approach was evaluated for real data for two tanks, and unfortunately the filter was divergent for this. Possible reasons are:

- Concentrations may have varied too little in reality, and the result from simulation is that the filter needs variations in the concentrations to be convergent.
- Errors in the estimation of the  $K_La$  parameters, and unmodel time variations of the real  $K_La$ . It is known from simulation that the EKF is especially sensitive for variations in the  $K_La$  functions.
- Errors in the ASM1 parameters. It is, however, known from simulation that the EKF has relatively low sensitivity to errors in these.
- Neglect of nitrification/denitrification in the observer model, especially nitrification.

Model errors were further analyzed by considering the model of the AS basin as a series of continuously stirred tank reactors. It was illustrated that the performed tracer tests do not give a unique division of the basins, while this is an important concept in the observer model. Depending on the division, sensor responses have totally different characters from an input to the basin holding the two tanks in the model. Naturally, there are also higher order dynamics due to vertical and horizontal distances within the basin, and this is not accounted for in the model. This property was illustrated using measurement data, and it was stated that this dynamics have especially large effect when estimating the  $K_La$  function. Figure 7.1 illustrates the sources of errors in the observer model of the EKF.

## 7.5 Optimization of the aerobic process

It was concluded that few of the control variables can be optimized independently for the aerobic compartments and that the oxygen set point should not be optimized continuously based on the ASM1 since it affects properties not included in the model. Optimization of the individual air flows were considered and solved. Results for real data was presented that showed that 5 % of the total cost could be saved with the solution, but also this method relies on that the tank model and the estimated  $K_La$  parameters are valid.

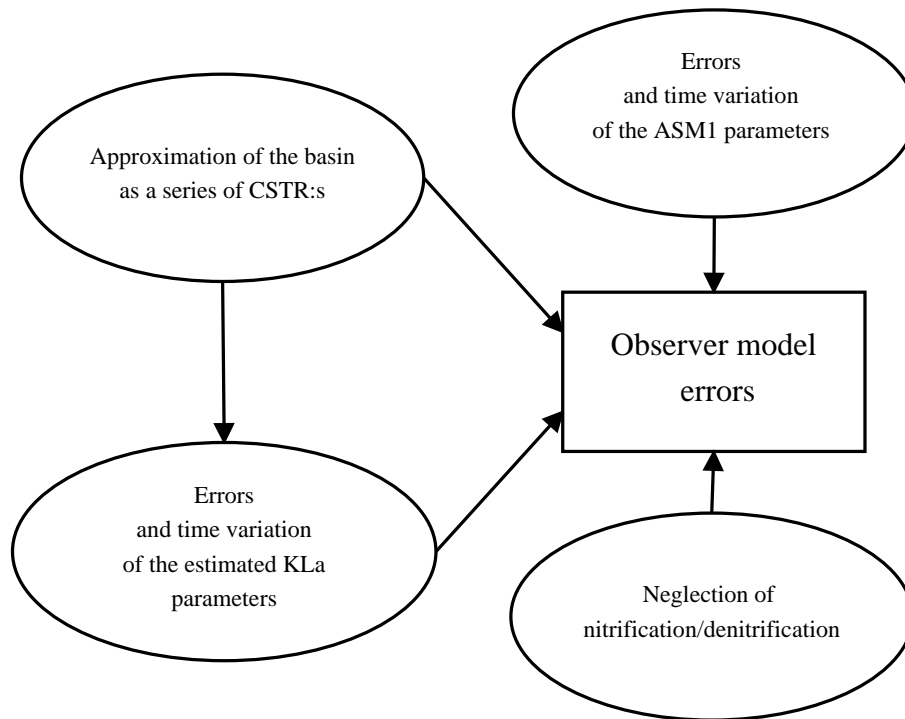


Figure 7.1. Sources of errors in the observer model.

## 7.6 Possibilities for Ryaverket

A solution for substrate estimation discussed for Ryaverket is to assume that the parameter  $\gamma_{X_{BH}}$  is constant, and estimate a value of it from lab analysis of soluble substrate. From the lab analysis we get an estimate of the Monod expression in  $S_S$ , which can be used to estimate  $\gamma_{X_{BH}}$  from estimates of  $OUR$  in the aerobic tanks. This can then be used to estimate  $S_S$  online. With this method, we can also compensate somewhat for errors in the estimated  $K_La$  function. The possibility of this method relies on that  $\gamma_{X_{BH}}$  varies little, and that the  $K_La$  parameters do not vary much in an unmodeled way. The method should be used on Tank 8, since the concentration in  $S_S$  is smallest there, and this gives the smallest sensitivity to parameter errors. There is, however, a negative effect of the small concentration. The relatively small  $OUR$  in this tank makes the effects of water flows to be more significant in the process, and as stated earlier we do not rely much on the model of the water flow. Problems with this model and a small  $OUR$  was seen when estimating the  $K_La$  parameters.

## 8 CONCLUSIONS

Optimization of the activated sludge process is limited by the lack of measurements of concentrations in the commonly used models for it, such as the activated sludge model NO.1. This is in particular true for some of the main variables, such as the concentration of dissolved and particulate substrate, and bacterial biomass. A general remedy for absence of online measurements is to find an observer to estimate unmeasured variables based on a dynamic model and online measurements of other variables. Observers for substrate and biomass have earlier been formulated for the ASM1, but with unrealistic assumptions of measurements and parameters, and without considering sensitivity to errors in its internal model.

The goal of this work was an independent solution ready for implementation for estimation of all relevant concentrations in the ASM1 in the aerobic compartments of an ASP. The lesson from previous work is that it is necessary to include more measurements in the algorithms. This has been solved by including more tanks in the model, and also taking measurements of totally suspended solids in the influents into account for faster estimation. Two methods have been developed:

- Separate estimation of bacterial biomass in the anoxic compartments, and substrate in the aerobic compartments.
- An extended Kalman filter (EKF) for  $n$  aerobic tanks for estimation of all concentrations of interest.

The latter one is the more interesting since it consists of only one observer, and it would be more realistic. Possible unrealistic assumptions about the nitrate sensors in the first one have namely been made in simulation. The EKF performs well in simulation, but showed to be especially sensitive to errors in the  $K_L a$  function. Methods to estimate the function have been further developed and evaluated in simulation with good results. The evaluation of the EKF based on real data was unsuccessful, a result which can be explained by errors in the observer model, and the dependency of variations in concentrations implied by the EKF for two tanks. The  $K_L a$  function may also be time varying in a way which was not possible to include in the model.

The developed methods are far more realistic than earlier formulated since no assumptions of measurements of in reality immeasurable quantities have been made. Some of their negative properties are process dependent and positive for a possible future implementation would be a process with more and smaller aerobic tanks with better defined borders. Cheaper methods for continuous estimation of the  $K_L a$  function than available today may also be necessary.

Optimization of the aeration was also considered, and it was concluded that the DO set points should not be continuously optimized based on the ASM1. Optimization

of the individual air flows were solved, and results for winnings of the method based on real data was presented. The magnitude of the possible winnings is, again, dependent on the estimated  $K_La$  parameters and that the tank model is valid. It was also concluded that the DO set point should not be varied on a continuous basis.

cleardoublepage

# Bibliography

- Alex, J., Beteau, J.F., Copp, J.B., Hellinga, C., Jeppsson, U., Marsili-Libelli, S., Pons, M.N., Spanjers, H. and Vanhooren, H. (1999). Benchmark for evaluating control strategies in wastewater treatment plants. In: *European Control Conference*. Karlsruhe, Germany.
- Andréasson, N., Evgrafov, A. and Patriksson, M. (2005). *An introduction to continuous optimization*. Studentlitteratur. Lund.
- Benazzi, F., Gernaey, K.V., Jeppsson, U. and Katebi, R. (2007). On-line estimation and detection of abnormal substrate concentrations in wwtp:s using a software sensor: a benchmark study. *Environmental Technology*, **28**, 871–882.
- Besaçon, G. (2007). *Nonlinear Observers and Applications*. Springer. New York.
- Boukroune, B., Darouach, M., Zasadzinski, M., Gill, S. and Fiorelli, D. (2009). A nonlinear observer design for an activated sludge wastewater treatment process. *Journal of Process Control*, **19**, 1558–1565.
- Cecil, D. and Kozłowska, M. (2009). Software sensors are a real alternative to true sensors. *Environ. Model. Softw.* doi:10.1016/j.envsoft.2009.05.004.
- Chachuata, B., Rocheb, N. and Latifia, M.A. (2005). Optimal aeration control of industrial alternating activated sludge plants. *Biochemical Engineering Journal*, **23**, 277–289.
- Copp, J. B. (2001). *The COST Simulation Benchmark: Description and Simulator Manual*. COST Action 624 and COST Action 682. <http://www.ensic.inpl-nancy.fr/COSTWWTP/>.
- Henze, M., Gujer, W., Mino, T. and van Loosdrecht, M. (2000). *Activated Sludge Models ASM1, ASM2, ASM2d and ASM3*. IWA Publishing. UK.
- Kjellstrand, R. (2006). Hydraulic behaviour in an activated sludge tank -from tracer test through hydraulic modelling to full-scale implementation. PhD thesis. Chalmers University of Technology. SE-412 96 Göteborg, Sweden. ISSN 1652-943X, <http://hdl.handle.net/2320/1737>.
- Lennartson, B. (2002). *Reglerteknikens grunder*. Studentlitteratur. Lund.
- Lewis, F.L. (1986). *Optimal estimation with an introduction to stochastic control theory*. Wiley Interscience. Atlanta.
- Lindberg, C.F. (1997). Control and estimation strategies applied to the activated sludge process. PhD thesis. Uppsala University. Department of Materials Science.

- Ljung, L. and Glad, T. (2002). *Modeling of dynamic systems*. Prentice Hall. Upper Saddle River.
- Miller, S.L. and Childers, D.G. (2004). *Probability and random processes with applications to signal processing and communications*. Elsevier academic press. Burlington.
- Olsson, G. and Newell, B. (1999). *Wastewater Treatment Systems, Modeling, Diagnosis and Control*. IWA publishing. London.
- Persson, A. and Böiers, L-C. (1988). *Analys i flera variabler*. Studentlitteratur. Lund.
- Åstrom, K.J. and Wittenmark, B. (1997). *Computer controlled systems, theory and design*. Prentice Hall. Saddle river.
- Samuelsson, P., Halvarsson, B. and Carlsson, B. (2007). Cost-efficient operation of a denitrifying activated sludge process. *Water research*, **41**, 2325–2332.
- Soons, Z.I.T.A., Shi, J., Stigter, J.D., van der Pol, L.A., van Straten, G. and van Boxtel, A.J.B. (2008). Observer design and tuning for biomass growth and kla using online and offline measurements. *Journal of Process Control*, **18**, 621–631.
- Stenstrom, M.K. and Gilbert, R.G. (1981). Effects of alpha, beta and theta factor upon the design, specification and operation of aeration systems. *Water research*, **15**, 643–654.
- Suescun, J., Irizar, I., Ostolaza, X. and Ayesa, E. (1998). Dissolved oxygen control and simultaneous estimation of oxygen uptake rate in activated-sludge plants. *Water Environment Research*, **70**, 316–322.
- Wik, T. (1999). On modeling the dynamics of fixed biofilm reactors - with focus on nitrifying trickling filters. PhD thesis. Chalmers University of Technology. SE-412 96 Göteborg, Sweden. ISBN 91-7197-797-X.
- Xin-She, Y. (2008). *Introduction to computational mathematics*. World Scientific Pub. New Jersey.

